



CoCo2

Prototype system for a
Copernicus CO₂ service

Second synthesis of CO₂ and CH₄ observation-based emission estimates

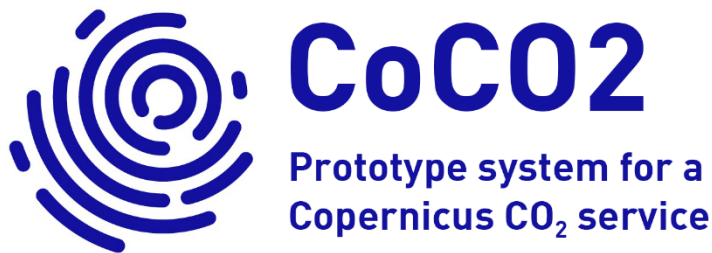
WP8

coco2-project.eu



Co-ordinated by
 **ECMWF**





D8.2: Second synthesis of CO₂ and CH₄ observation-based emission estimates

Dissemination Level:	Public
Author(s):	Glen P. Peters, A. M. Roxana Petrescu, Robbie M. Andrew, Ragnhild Børke, Gregoire Broquet, Frédéric Chevallier, Audrey Fortems-Cheiney, Aki Tsuruta, Arjo Segers, Matthew McGrath, Chunjing Qiu, Espen Sollum, Richard Engelen.
Date:	7/02/2023
Version:	v1
Contractual Delivery Date:	31/12/2022
Work Package/ Task:	WP8 / T8.2
Document Owner:	Vrije Universiteit Amsterdam
Contributors:	CICERO
Status:	Final

CoCO₂: Prototype system for a Copernicus CO₂ service

**Coordination and Support Action (CSA)
H2020-IBA-SPACE-CHE2-2019 Copernicus evolution –
Research activities in support of a European operational
monitoring support capacity for fossil CO₂ emissions**

Project Coordinator: Dr Richard Engelen (ECMWF)
Project Start Date: 01/01/2021
Project Duration: 36 months

Published by the CoCO₂ Consortium

Contact:
ECMWF, Shinfield Park, Reading, RG2 9AX,
richard.engelen@ecmwf.int



The CoCO₂ project has received funding from the European Union's Horizon 2020 research and innovation programme under grant agreement No 958927.

Table of Contents

List of Figures	6
List of Tables	8
List of Acronyms	9
Executive Summary	10
1 Introduction	10
1.1 Background	10
1.2 Scope of this deliverable	12
2 Methodologies	12
2.1 Anthropogenic CO ₂ and CH ₄ emissions and removals from UNFCCC.....	12
2.2 Fossil CO ₂ emissions.....	12
2.3 Net land CO ₂ flux.....	13
2.4 Anthropogenic CH ₄ emissions	16
2.5 Other methodological issues	19
2.5.1 System boundary issues	19
3 Fossil CO ₂ emissions.....	20
3.1 Inventory-based estimates.....	20
3.2 Atmospheric inversions	23
4 Net land CO ₂ fluxes	26
4.1 Bookkeeping and inventory-based estimates.....	27
4.2 Inventory-based land-surface models	28
4.3 Inversion-based estimates	32
4.4 Summary discussion of net land	34
5 Anthropogenic CH ₄ emissions.....	35
5.1 Inventory-based estimates.....	36
5.1.1 EU27	36
5.1.2 Australia.....	37
5.1.3 Nordic countries.....	38
5.2 Atmospheric inversions	39
5.2.1 USA	39
5.2.2 EU27	40
5.3 Uncertainties from inverse systems	41
5.4 Priors.....	43
6 Deviations and counter measures	44
7 Conclusion	44
8 References	45
9 Annex 1: Fossil CO ₂ figures.....	53
10 Annex 2: Additional fossil CO ₂ inversion figure	63

11	Annex 3: Net land CO ₂ fluxes figures.....	64
12	Annex 4: Methane figures.....	65

List of Figures

Figure 1: Comparison of unharmonized global fossil CO ₂ emissions from multiple inventory datasets.	20
Figure 2: Comparison of global fossil CO ₂ emissions from multiple inventory datasets with system boundaries harmonised as much as possible. Harmonisation is limited by the disaggregated information presented by each dataset.	21
Figure 3: Comparison of EU fossil CO ₂ emissions from multiple inventory datasets. CDIAC does not report emissions for countries that did not exist prior to 1992. The uncertainty whiskers in the top-right indicate the approximate uncertainty for EDGAR and UNFCCC.	21
Figure 4: Comparison of EU fossil CO ₂ emissions from multiple inventory datasets with system boundaries harmonised as much as possible. Harmonisation is limited by the disaggregated information presented by each dataset. CDIAC does not report emissions for countries that did not exist prior to 1992.	22
Figure 5: Comparison of China (top) and USA (bottom) fossil CO ₂ emissions from multiple inventory datasets with system boundaries harmonised as much as published data detail allows.	23
Figure 6: EU27+UK total CO ₂ fossil emissions, as reported by nine global inventory data sources: BP, EIA, CEDS, EDGAR, GCP, IEA, CDIAC, PRIMAP-hist and UNFCCC NGHGs with a top-down, fast-track CIF-CHIMERE atmospheric inversion (black dot) (Fortems-Cheiney and Broquet, 2021b). The data represent EU27+UK for the year 2019 split per fuel type. 'Others' are emissions not categorised by fuel, and international bunker fuels are not usually included in total emissions at sub-global level. Neither EDGAR nor PRIMAP-hist publishes a break-down by fuel type, so only the totals are shown.	24
Figure 7: Comparison of inversion results for the EU with prior FFCO ₂ emissions estimated by the TNO-GHGco-v3 inventory (Fortems-Cheiney and Broquet, 2021b). Note that the proximity of the inversion results to the prior estimates is not a direct indicator of verification, without additional information on the prior and posterior uncertainty and supporting statistical analysis (see discussion in the text).	25
Figure 8: A comparison of inventories and inversions land CO ₂ fluxes for the EU28 (EU27+UK). Shaded areas show maxima and minima of the TRENDY (grey) and GCP inversion (yellow) collections.	26
Figure 9: Net land CO ₂ flux for bookkeeping type models for the EU27. Romania has been removed from the EU27 total due to carbon stock data.	28
Figure 10: Net land CO ₂ flux for bookkeeping type models for Brazil.	28
Figure 11: A comparison of the global LULUCF from the bookkeeping models, the TRENDY DGVM individual results and median, and the Grassi et al (2022) inventory estimates. Note that the TRENDY results are from Friedlingstein et al 2022a, but the bookkeeping models from Friedlingstein et al 2022b.	29
Figure 12: The global net land CO ₂ flux for the TRENDY DGVM individual results and median compared with the inventory estimate from Grassi et al. (2022a).	30
Figure 13: A comparison of UNFCCC NGHGs for the EU27 and the TRENDY DGVM individual results and median with bookkeeping models and S3-S3 (top) and S3 (bottom).	31
Figure 14: A comparison of UNFCCC NGHGs for Brazil and the TRENDY DGVM individual results and median with bookkeeping models and S3-S3 (top) and S3 (bottom).	32
Figure 15: The net land CO ₂ flux from six inversions (thin lines) and median and inventory estimates for the EU27 (top) and Brazil (bottom).	33
Figure 16: The CAMS inversions without (green) and with (orange) adjustments for lateral carbon fluxes and a managed land mask for Brazil and the EU28. The uncertainty band for one standard deviation is shown for the adjusted inversion.	34

Figure 17: Total global CH ₄ anthropogenic emissions from seven inventories, updated from Minx et al., 2021. The FAO independently estimates CH ₄ from agricultural, but uses EDGARv6 and PRIMAP-hist for the remaining sectors.	35
Figure 18: EU27 total anthropogenic sectoral emissions as: a) total, b) Energy, c) Industry and Products in Use (IPPU), d) Agriculture and e) Waste from UNFCCC (2022) submissions and all sectors excl. LULUCF (EDGAR v4.3.2, v6.0 and v7.0, GAINS and FAOSTAT) and CAPRI for Agriculture only. The means represent the common overlapping period 1990-2015. Last reported year in this study refers to 2020 (UNFCCC and FAOSTAT), 2015 (GAINS), 2012 (EDGARv4.3.2), 2018 (EDGARv6.0) and 2021 (EDGARv7.0).	37
Figure 19: Australia total anthropogenic sectoral emissions as: a) total, b) Energy, c) Industry and Products in Use (IPPU), d) Agriculture and e) Waste from UNFCCC (2022) submissions and all sectors excl. LULUCF (EDGAR v4.3.2, v6.0 and v7.0, GAINS and FAOSTAT). The means represent the common overlapping period 1990-2015. Last reported year in this study refers to 2020 (UNFCCC and FAOSTAT), 2015 (GAINS), 2012 (EDGARv4.3.2), 2018 (EDGARv6.0) and 2021 (EDGARv7.0).....	38
Figure 20: A comparison of CO ₂ , CH ₄ , and N ₂ O in the Nordic countries for UNFCCC, EDGARv6 (shown as EGR2021), and EDGARv7. For CH ₄ the differences are significant.....	39
Figure 21: Total anthropogenic CH ₄ emissions (Tg CH ₄ yr ⁻¹) for USA from inventories (EDGARv4.3.2, v6, v7 and GAINS) plotted against UNFCCC national reports (CRFs and BURs) and global inversion ensembles a) CH ₄ emissions based on satellite concentration observations (GOSAT) and b) from global model surface stations (SURF). The inversion ensembles are presented for the 4 methods (1, 2, 3.1 and 3.2) as described in section 1.4 of Deng et al. (2022).	40
Figure 22: Total anthropogenic CH ₄ emissions (Tg CH ₄ yr ⁻¹) for EU27 from UNFCCC national reports (CRFs) compared to GOSAT obs-based global and regional inversion ensembles from a) CTE-CH ₄ b) Deng et al. (2022) methods (m1, m2, m3.1 and m3.2), and c) CAMSv19 and v21.	40
Figure 23: Total anthropogenic CH ₄ emissions (Tg CH ₄ yr ⁻¹) for EU27 from UNFCCC national reports (CRFs) compared to VERIFY simulations (CIF) and SURF observation-based global and regional inversion ensembles from a) CTE-CH ₄ b) Deng et al. (2022) methods (m1, m2, m3.1 and m3.2), c) FELXPART-CIF and FLEXkF and d) CAMSv19r and v21r.....	41
Figure 24: VERIFY_inclusive (S4) inversion run, uncertainty reduction maps computed as $(1 - \Delta_{\text{post}}/\Delta_{\text{prior}})$ for 2006 and 2018 with different sets of observation stations.....	42
Figure 25: VERIFY_core (S5) inversion run, uncertainty reduction maps computed as $(1 - \Delta_{\text{post}}/\Delta_{\text{prior}})$ for 2006 and 2018 with different sets of observation stations.....	42
Figure 26: CTE-CH ₄ GOSAT inversion run, uncertainty reduction maps computed as $(1 - \Delta_{\text{post}}/\Delta_{\text{prior}})$ for 2010 and 2017.	43
Figure 27: Anthropogenic CH ₄ prior and posterior emissions with their uncertainties from CTE-CH ₄ - GOSAT, CTE-VERIFY inclusive (S4) and core (S5) runs compared to UNFCCC (2022) inventories and with prior anthropogenic datasets (EDGARv4.3.2 and v6.0).....	44
Figure 28: Comparison of inversion results (red lines) for each EU country with FFCO ₂ prior emissions estimated by the TNO-GHGco-v3 inventory (blue lines), Mt CO ₂ (Fortems-Cheiney and Broquet, 2021b). Note that the proximity of the inversion results to the prior estimates is not a direct indicator of verification, without additional information on the prior and posterior uncertainty and supporting statistical analysis (see discussion in the text).....	63

List of Tables

Table 1: Data sources for the fossil CO ₂ emissions included in this study	14
Table 2: Data sources for the land CO ₂ emissions included in this study.....	15
Table 3: Data sources for the CH ₄ emissions included in this study	17
Table 4: Ranking of top world emitter countries by inventory and sectors and their contribution (%) to the total CH ₄ country emissions. The numbers were calculated based on the average from 2010 to the last available inventory year. EDGARv4.3.2 data is not shown in this table since it ends in 2012.....	36
Table 5: Contribution from BU and TD of top 10 emitters (Tg CH ₄) to the global anthropogenic budget (average of 2010-last available year).....	65
Table 6: Uncertainties estimated for CH ₄ sources at the global scale: based on ensembles of inventories and inversion estimates, national reports, and specific uncertainty assessments of EDGAR. Note that this table provides uncertainty estimates from some of the key literature based on different methodological approaches. It is not intended to be an exhaustive treatment of the literature.	65
Table 7: A description of the priors used in different inversions	66

List of Acronyms

Acronyms used throughout the report are listed here, except for the names of models or datasets:

AD: Activity Data

BU: Bottom-Up

BUR: UNFCCC Biennial Update Reports

CO2MVS: CO₂ Monitoring and Verification Support

CoCO₂: Prototype system for a Copernicus CO₂ service (EU Horizon 2020 project)

CRF: UNFCCC Common Report Format

DGVM: Dynamic Global Vegetation Model

FCO₂: Fossil CO₂ emissions

FFCO₂: Fossil fuel CO₂ emissions

EF: Emission Factor

GHG: Greenhouse Gas

GST: Global Stocktake

IPCC: Intergovernmental Panel on Climate Change

LULUCF: Land Use, Land-Use Change, and Forestry

NGHGI: National Greenhouse Gas Inventory

TD: Top-Down

UNFCCC: United Nations Framework Convention on Climate Change

VERIFY: Observation-based system for monitoring and verification of greenhouse gases (EU Horizon 2020 project)

Executive Summary

This is the second of three versions of this deliverable. In this version, the section on net land CO₂ fluxes has been rewritten, the section on CH₄ has had extensive updates and expansion, and the section on fossil CO₂ emissions has been revised with the latest data available.

The aim of the deliverable is to identify, quantify and explain divergences between global inventories, atmospheric inversions, process models and national inventories submitted to the UNFCCC. We present consistent comparisons of CO₂ and CH₄ emission estimates based on inventories and observations for various countries to highlight interesting aspects. We cover fossil CO₂ emissions, net land CO₂ fluxes, and anthropogenic CH₄ emissions. Most of the data products are from the VERIFY project, with a gradual inclusion of CoCO₂ products as the project evolves. The first edition of this deliverable was December 2021, this is the second version (December 2022), with a third and final version due in December 2022. Each version of the deliverable is planned to be an evolution of the previous, with better discussions of the comparisons between the datasets.

Progress has been made on making comparisons across datasets, but significant gaps remaining in harmonising system boundaries and providing relevant information on uncertainty. For fossil CO₂ emissions, the importance of adjusting for harmonised system boundaries was demonstrated and that describing differences requires detailed comparison of components (e.g., fossil fuel category or sectors). The fossil CO₂ inversions show proof of concept, but so far lack uncertainty information for a full analysis. For net land CO₂ fluxes, comparisons were made with inventories in three groups: 1) bookkeeping models, 2) process-based models, 3) inversions. System boundary issues remain highly problematic in the land-sector, even when comparing similar models together, and this is an area that requires significantly more research. For CH₄ emissions, divergences between inventories can be linked back to differences in activity data or emission factors, but this data can be difficult to obtain. For the inversions, the general magnitudes and trends agree, but uncertainties remain large. More effort is needed on providing relevant uncertainty information, particularly more detail on the priors, and the extent to which observations are constraining results leading to statistically significant differences with inventories.

A consistent conclusion across all components analysed is the difficulty of harmonising datasets into a comparable format. The tradition of comparing datasets as published is easy, but problematic. To reconcile differences between alternative datasets requires a much deeper understanding of each dataset, such as the methods and input data sources, and particularly providing considerably more information on uncertainties to help understand when differences are statistically significant. Often the necessary data is not available or time consuming to access. A systematic reconciliation and comparison often require a close dialogue with data providers. Throughout this document we discuss some of the key challenges in making comparisons and lay the foundation for the final report in December 2023.

1 Introduction

1.1 Background

Emissions and removals of greenhouse gases (GHGs), including both anthropogenic and natural fluxes, require reliable quantification, including estimates of uncertainties, to support credible mitigation action under the Paris Agreement. Reported inventory-based emissions and removals are generally estimated using 'bottom-up' inventory estimates. 'Top-down', observation-based estimates can provide complimentary monitoring and verification of the bottom-up emission estimates. These independent estimates can be performed at multiple scales and for a variety of applications: the global and continental scale for science purposes,

country scale for reporting to the UNFCCC, sub-country scale for urban planning, and point sources like large power plants for verification (Pinty et al., 2019), to name just a few examples.

In this report, bottom-up inventory estimates are generally assumed to follow the IPCC reporting guidelines, and we contrast them with top-down inventory estimates from inversion models. Bottom-up inventory estimates are in general a combination of activity data (e.g., fuel use) and associated emission factors (e.g., emissions per fuel use). However, in many cases, bottom-up inventory estimates can be a complex combination of different approaches, including the use of actual continuous gas measurements at specific point sources or modelling based on numerous data sources (e.g., transport emissions modelling using traffic data and fleet databases). The development of bottom-up inventory estimates with higher spatial (gridded) and temporal (daily, hourly) resolution may also rely on different observational datasets. The term 'bottom-up' can therefore connote several different things.

Top-down observational estimates combine prior inventory estimates with a variety of observations to provide valuable constraints on the inventories (Deng et al., 2022). The main distinction is that top-down estimates generally use an inversion, or some other sort of model, together with a variety of observations, to provide estimates of emissions that can then be compared with the bottom-up inventory estimates. Since atmospheric concentrations respond to the sum of all emissions and removals, inversion-based estimates are less suited to provide information on individual sectors (unless they are geographically separated), though due to high resolution, observation-based approaches are particularly suited to identify point sources or small geographical areas like cities.

Bottom-up inventories and top-down observational estimates are complementary and should be used together to improve and build trust in National Greenhouse Gas Inventories (NGHGs) reported to the UNFCCC. With dense observation networks and measurements of auxiliary parameters such as isotopic composition of GHG or concentrations of co-emitted gases, additional source-specific information can be gained to support the validation of national emission inventories at smaller spatial scales. Observation-based estimates can be particularly valuable for trace gases with large uncertainties in their emissions (Maksyutov et al., 2019).

In the context of providing recommendations for the implementation of an observation-based operational anthropogenic CO₂ emissions Monitoring and Verification Support (CO2MVS) capacity within the Copernicus programme, one objective of CoCO₂ is to provide inputs to the Global Stocktake (GST) process, in the form of anthropogenic CO₂ and CH₄ emission products for the first GST (2023), at a spatial scale consistent with GST requirements. CoCO₂ identified the relevant needs for the periodic GST through the development of a User Requirement Document (URD). The work described in this document represents the starting point for future syntheses to serve future GSTs.

This document is an extension of reconciliation reports and country analysis produced under the VERIFY project (Andrew, 2020; Petrescu et al., 2020; Petrescu et al., 2021a; Petrescu et al., 2021b; Petrescu et al., 2022), but this document has a more global focus. We identify and analyse CO₂ and CH₄ emissions from a selection of countries to identify differences with UNFCCC National GHG Inventories (NGHGI), and thereby identify countries or sectors where observation-based estimates can complement NGHGs. We choose countries that show interesting or relevant differences. This document is the second in a series of three, due at the end of each year of the project (December 2021, December 2022, December 2023). This report is structured as follows: Chapter 1 presents the background, scope and objectives of this work, Chapter 2 the methodologies, Chapter 3 focuses on the fossil and net land CO₂ fluxes, Chapter 4 presents the CH₄ results both total and sectoral, and the report ends with discussions, conclusions and outlines future needs for research.

1.2 Scope of this deliverable

The scope of this deliverable is to compare annual GHG estimates from inventory-based, model-based, and observation-based inventories and compare them with UNFCCC NGHGI for a selection of countries. We use data products from VERIFY and CoCO₂ and focus on fossil CO₂ emissions, net land CO₂ fluxes, and anthropogenic CH₄ emissions. For space requirements we only show for a few select countries, with figures for additional countries presented in the annex.

Changes compared to the first version of the deliverable (D8.1, due December 2021)

- Fossil CO₂ emissions
 - Updated to most recent data
 - Reduced discussion on inversions and no updates available
- Land CO₂ flux
 - Updated to most recent data
 - Separated figures into data types (inventories, land surface models, inversions)
- Anthropogenic CH₄ emissions
 - Updated to most recent data
 - Added uncertainty reduction maps for one inversion (CTE-CH₄)
 - Started the discussion on priors to explain differences between results from different datasets.

Changes for the third and final version of the deliverable (D8.3, due December 2023)

- Fossil CO₂ emissions
 - Update to most recent data
 - Include uncertainty bounds on figures
 - Include inversions
 - Include some regional datasets: Asia (MEIC and REAS), Africa (CoCO₂)
- Land CO₂ flux
 - Update to most recent data
 - Try and make system boundaries more consistent in each figure
 - Provide deeper explanation of differences
- Anthropogenic CH₄ emissions
 - Update to most recent data and include new datasets
 - Compare priors between all datasets (activity data and emission factors)
 - Plot natural CH₄ emissions for all top emitters (thought to be the culprit for increased global emissions during the past decades)
 -

2 Methodologies

2.1 Anthropogenic CO₂ and CH₄ emissions and removals from UNFCCC

UNFCCC National Greenhouse Gas Inventories (NGHGI, 2022) emissions (CO₂ and CH₄) and removals (CO₂) are compiled by individual countries, with Annex I Parties to the UNFCCC required to report emissions inventories annually using the Common Reporting Format (CRF). The reported data is generally for the period 1990 to N-2 (two years before the current year), but some countries provide data for earlier or later periods. The non-Annex I Parties report their estimates in Biennial Update Reports (BURs) submissions to the UNFCCC, but since these reports are in irregular formats and require manual compilation to obtain a cross-country dataset, we use a precompiled dataset¹ (Deng et al., 2022).

2.2 Fossil CO₂ emissions

The different fossil CO₂ emission data and methods are summarised in Table 1.

¹downloaded from <https://zenodo.org/record/5089799#.YdRTzGjMJJaR>

The bottom-up inventory-based fossil CO₂ estimates are presented and split per fuel type and reported for the last year when all data products are available, an update to Andrew (2020).

The top-down atmospheric inversions fossil CO₂ estimates for the year 2019 are from an inversion assimilating satellite observations. To overcome the current lack of CO₂ observation networks suitable for the monitoring of fossil fuel CO₂ emissions at national scale, this inversion is based on atmospheric concentrations of co-emitted species: CO and NO₂. While the spatial and temporal coverage of these CO and NO₂ observations is large, the conversion of the information on these co-emitted species into fossil fuel CO₂ emission estimates is complex and carries large uncertainties. We have not been able to fully characterise the uncertainty in the inversions, therefore limiting our ability to compare to inventories. In this second version of the report, we use the same inversion data as from the first version of the report. The fossil CO₂ inversions are a CoCO₂ product.

2.3 Net land CO₂ flux

The net land CO₂ fluxes include CO₂ emissions and removals from LULUCF activities, based on inventories, process models and inversion estimates (Table 2). We considerably rewrite the net land CO₂ flux section in the second version of the report. We split the figures into three sets, based on bottom-up inventory-based estimates, land-surface models, and inversions.

For the bottom-up inventory-based estimates, we present the net land CO₂ flux (emissions and removals) from the LULUCF sector reported to UNFCCC (2022), three bookkeeping models (BLUE, H&N, OSCAR based on (Friedlingstein et al., 2022b)), global inventories (FAO), and a newly published dataset (Grassi et al., 2022a).

For the land-surface models, we use an ensemble of dynamic global vegetation models (DGVMs) TRENDYv10 from GCP2021 (Friedlingstein et al., 2022a). The TRENDYv10 results do not have a managed land mask applied.

For the top-down observational-based estimates, we use inverse model results from GCP2021 (Friedlingstein et al., 2022a), and an improved CAMS inversion including lateral fluxes and managed land masks (Chevallier et al., 2005; Chevallier, 2021) which is a CoCO₂ product. The GCP2021 inversions do not have a managed land mask applied.

Table 1: Data sources for the fossil CO₂ emissions included in this study

CO ₂ anthropogenic				
	Data/model name	Contact / lab	Species / Period	Reference/Metadata
	UNFCCC NGHGI (2022)	UNFCCC	Anthropogenic fossil CO ₂ 1990-2020	IPCC Guidelines for National Greenhouse Gas Inventories (IPCC, 2006) UNFCCC NIRs/CRFs (UNFCCC, 2022)
BU	Compilation of multiple CO₂ fossil emission data sources (Andrew, 2020): EDGAR, BP, EIA, CDIAC, IEA, GCP, CEDS, PRIMAP	CICERO	CO ₂ fossil country totals and split by fuel type 1990-2020 (or last available year)	EDGAR v7.0_GHG (Crippa et al., 2022) BP 2022 report (BP, 2022) EIA (EIA, <i>no date</i>) CDIAC https://energy.appstate.edu/CDIAC updated from (Gilfillan and Marland, 2021) IEA (IEA, 2022) CEDS (O'Rourke et al., 2021) GCP (Friedlingstein et al., 2022a) PRIMAP-hist (Gütschow and Pflüger, 2022)
TD	Fossil fuel CO₂ inversions	LSCE	Inverse fossil fuel CO ₂ emissions 2005-2020	VERIFY Deliverable D2.12 (Fortems-Cheiney and Broquet, 2021a), an as-yet unpublished update of Deliverable D2.11 (Fortems-Cheiney and Broquet, 2021b)

Table 2: Data sources for the land CO₂ emissions included in this study

Product Type / file or directory name	Contact / lab	Variables / Period	References
Inventories			
UNFCCC NGHGI (2022)	UNFCCC	LULUCF Net CO ₂ emissions/removals	IPCC, 2006 Guidelines for National Greenhouse Gas Inventories, Prepared by the National Greenhouse Gas Inventories Programme. IGES, Japan, https://www.ipcc-nggip.iges.or.jp/public/2006gl/ , 2006.(IPCC, 2006) UNFCCC Annex 1 CRFs https://unfccc.int/ghg-inventories-annex-i-parties/2022 (UNFCCC, n.d.-b) UNFCCC BURs: https://unfccc.int/BURs (UNFCCC, n.d.-a) via (Deng et al., 2022)
Bookkeeping models			
BLUE	MPI/LMU Munich	Net C flux from land use change, split into the contributions of different types of land use (cropland vs pasture expansion, afforestation, wood harvest)	(Hansis et al., 2015) as updated in (Friedlingstein et al., 2022b)
H&N	Woodwell Climate Research Center	C flux from land use and land cover	(Houghton and Nassikas, 2017) as updated in (Friedlingstein et al., 2022b)
OSCAR	IIASA	C flux from land use and land cover	(Gasser et al., 2020) as updated in (Friedlingstein et al., 2022b)
FAO	FAOSTAT	CO ₂ emissions/removal from LULUCF sectors	(Federici et al., 2015; Tubiello et al., 2021)
Grassi	JRC	CO ₂ emissions/removal from LULUCF sectors	(Grassi et al., 2022a)
Process-based models			
TRENDY v10 (2020)	MetOffice UK	Land related C emissions (NBP) from	(Friedlingstein et al., 2022a) and references therein.
Inversion models			
GCP 2021 Global inversions (CTE, CAMS, CarboScope, UoE, CMS-Flux, NISMON-CO2)	GCP	Total CO ₂ inverse flux (NBP) 6 inversions	(Friedlingstein et al., 2022a) and references therein.
CAMS via CoCO₂	LSCE	CO ₂ fluxes, includes lateral fluxes and a managed-land mask	(Chevallier, 2021)

2.4 Anthropogenic CH₄ emissions

The bottom-up inventory-based estimates for CH₄ anthropogenic emissions come from three global inventories: EDGAR (v4.3.2, v6.0 and v7.0), FAOSTAT and GAINS (Table 3). These estimates are not completely independent from NGHGs (see Figure 4 in (Petrescu et al., 2020)) as they integrate their own sectorial modelling with the UNFCCC data (e.g. common activity data (AD) and IPCC emission factors (EFs)) when no other source of information is available.

We do not report data for the natural CH₄ emissions, but they are available from the VERIFY project as wetlands and “other natural emissions”, the latter including geological sources, inland waters (lakes, rivers and reservoirs) and biomass burning (Saunio et al., 2020). The natural emissions were subtracted from inversions (see section 4, following the methodology described by Deng et al. (2022)).

The top-down observational-based estimates from atmospheric inversions combine atmospheric observations, transport and chemistry models and estimates of GHG sources with their uncertainties, to estimate emissions. Emission estimates from inversions depend on the data set of atmospheric measurements and the choice of the atmospheric model, as well as on other settings (e.g., prior emissions and their uncertainties). For CH₄, we use data from both regional (EU27) and global inversions developed in the VERIFY project, the CIF intercomparison (Berchet et al., 2021), CoCO2 CH₄ results from CAMS v19r and v21r, and from the GCP (Saunio et al., 2020). Inversion priors are based on both GOSAT and SURF observations, as well as EDGAR v4.3.2 and v6 (Table 3).

Table 3: Data sources for the CH₄ emissions included in this study

Product name	Variables / Period	Contact / lab	References
Inventories (anthropogenic)			
UNFCCC CRFs and BURs	CH ₄ totals and sectoral emissions with uncertainties 1990-2020	MS inventory agencies	UNFCCC CRFs https://unfccc.int/ghg-inventories-annex-i-parties/2022 UNFCCC BURs : https://unfccc.int/BURs via (Deng et al., 2022)
EDGARv4.3.2	CH ₄ totals and sectoral emissions 1990-2012	EC-JRC/PBL	(Janssens-Maenhout et al., 2019)
EDGAR v6.0	CH ₄ totals and sectoral emissions 1990-2018	EC-JRC/PBL	(Crippa et al., 2021) (Crippa et al., 2019) (Janssens-Maenhout et al., 2019) (Solazzo et al., 2021)
EDGARv7.0	CH ₄ totals and sectoral emissions 1990-2020	EC-JRC/PBL	(Crippa et al., 2021; Crippa et al., 2022)
GAINS	CH ₄ sectoral emissions 1990-2015	IIASA	(Höglund-Isaksson, 2012; Höglund-Isaksson, 2017; Höglund-Isaksson et al., 2020) (Gómez-Sanabria et al., 2018)
FAOSTAT	CH ₄ agriculture emissions, and Energy, IPPU & Waste 1990-2020	FAO	(FAOSTAT, 2022) (Tubiello, 2019; Tubiello et al., 2021)
CAPRI	CH ₄ agricultural emissions 1990-2014 and 2016, 2018	EC-JRC	(Britz and Witzke, 2014)

			(Weiss and Leip, 2012)
Atmospheric inversions			
GCP CTE-CH ₄	Prior and posterior CH ₄ fluxes with uncertainties from SURF (2005-2018) and GOSAT (2010-2017)	FMI	(Saunois et al., 2020) and model specific references in Appendix B, Table B4, (Petrescu et al., 2021b) (Tsuruta et al., 2017)
CTE-CH ₄ VERIFY S4, S5	Prior and posterior CH ₄ fluxes with uncertainties(2005-2018)	FMI	(Tsuruta et al., 2017) (Thompson et al., 2022)
CAMS v19r CAMS v21r	Prior (1999-2019) and posterior NOAA based CH ₄ fluxes (1999-2019) and NOAA-GOSAT based (2009-2019) Prior (1979-2021) and posterior NOAA based CH ₄ fluxes (1979-2021) and NOAA-GOSAT based (2009-2021)	TNO	https://confluence.ecmwf.int/display/CKB/CAMS%3A+Reanalysis+data+documentation
FLEXPART – CIF FLExKFv2021 VERIFY	Prior and posterior CH ₄ fluxes from VERIFY and VERIFY-CIF intercomparison	NILU, EMPA	(Brunner et al., 2012) (Brunner et al., 2017) (Berchet et al., 2021)

2.5 Other methodological issues

In the figures presented in this report, we essentially plot the various inversions and inventory methods on the same figure, to allow a visual comparison. There has not been a full uncertainty analysis, that would for example, quantify if one dataset has a statistically significant difference to another. Very few datasets provide uncertainty information. Methods to present the results, including uncertainties, need to be improved. Additionally, methods are needed to assess the statistical significance of any differences, given reported uncertainties.

2.5.1 System boundary issues

System boundary issues are a challenge for all comparisons made here. Independent estimates often have different system boundaries. These can sometimes be minor, but at other times (e.g., land) be significant. Relevant system boundary issues are discussed in each section below, but here we discuss some key issues.

2.5.1.1 Country gridding

A general system boundary issue is masking of gridded results to the country level, where it is important that it is known how modelling groups have defined emissions in each grid cell and to ensure the mask correctly captures country and economic zone effects, in line with how official NGHGs are reported.

2.5.1.2 Land masks

In a UNFCCC context, the net uptake on land (LULUCF) is defined based on a ‘managed land proxy’. This proxy was originally intended to represent anthropogenic activities, and is defined to cover land “where human interventions and practices have been applied to perform production, ecological or social functions” (IPCC, 2006). Countries do not report spatial grids of their managed land definitions, but “intact” and “non-intact” forest area has been found to be a good proxy for unmanaged and managed land (Grassi et al., 2021). Applying a non-intact forest area mask to the net land CO₂ flux in an inversion model or DGVM is one way to approximate the system boundary of LULUCF in NGHGs.

2.5.1.3 International shipping and aviation

For a careful comparison of inversions (gridded) results with UNFCCC NGHGs (country) several factors needed to be considered.

International transport is not included in country totals in NGHGs, but it is reported as a “memo” based on the sale of bunker fuels in each country (not the use of bunker fuels). A flight starting in France and landing in Poland would be classed as international, even though all the emissions occurred over EU territory. An inversion using satellite information, might see the emissions over each country in the flight path, but that would not appear in the NGHG. The same problem applies to flights with a landing or take-off in the EU but landing a country outside of the EU. International shipping has the same issues, whether a shipping leaving Europe to cross the Atlantic or a ship along the Rhine crossing country borders.

Despite this potential system boundary issue, it is unclear whether it is important yet. Inversions currently relying on in-situ observations would not be affected by this, as the observations would not detect the emissions emitted at cruising altitude. For this reason, the TNO emission inventories (from CoCO₂ WP2), include landing and take-off of all flights, domestic and international, but not the emissions at cruising altitude. This could nevertheless be an issue for shipping, but the size of the source is probably below the detection limit of current inversion methodologies. As methods improve, and as satellite data are increasingly used, these second-order effects will need a more detailed assessment.

3 Fossil CO₂ emissions

Fossil CO₂ emissions (FCO₂) can be separated into emissions from the oxidation of fossil fuels (FFCO₂) and chemical transformation of fossil carbonates into CO₂. Care needs to be taken to ensure consistency in comparisons, as some methods compare FCO₂ and others FFCO₂. This is discussed further in the relevant sections.

3.1 Inventory-based estimates

Figures 1, 2, 3, and 4 show fossil CO₂ emissions (FCO₂) from global datasets, both globally and for the EU27. 'Raw' totals from these datasets have differing system boundaries, meaning they don't all include the same set of emissions sources. Harmonising is an attempt to remove these differences in coverage to provide more comparable estimates, partly to prevent the false inference of uncertainty relating to the spread of raw estimates. Further details are provided by Andrew (2020). Figures 1 and 3 show unharmonized inventories, while Figures 2 and 4 show harmonised inventories. Importantly, our harmonization process is constrained by the level of detail published in individual datasets, and the harmonization is necessarily partial, not ending up exactly with apples-for-apples comparisons, but closer than comparing unharmonized data.

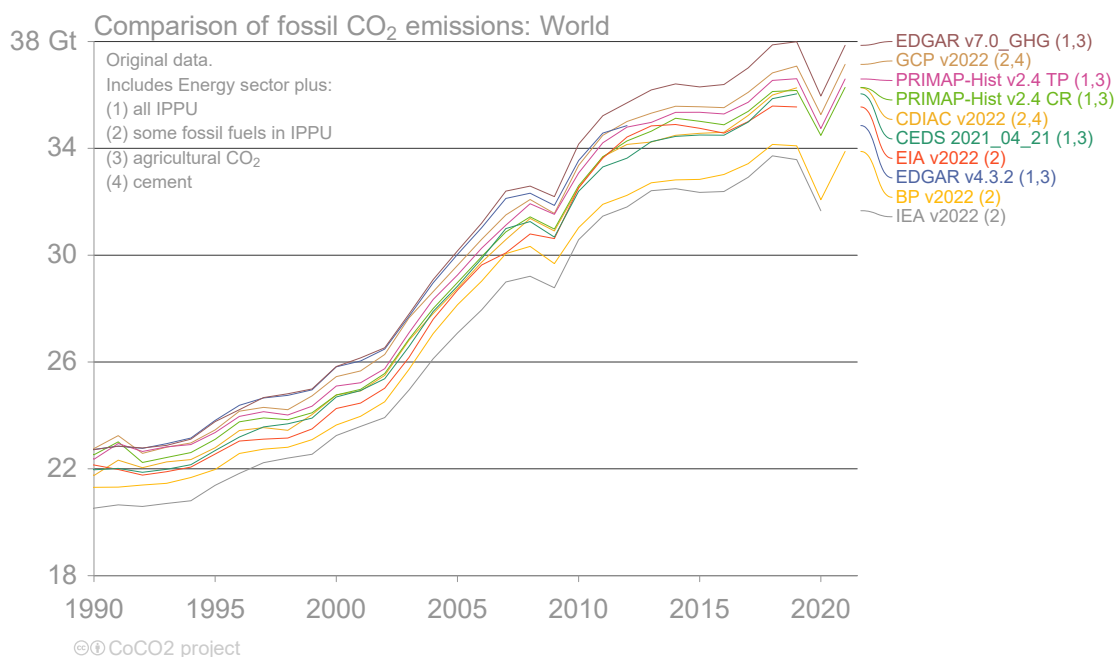


Figure 1: Comparison of unharmonized global fossil CO₂ emissions from multiple inventory datasets.

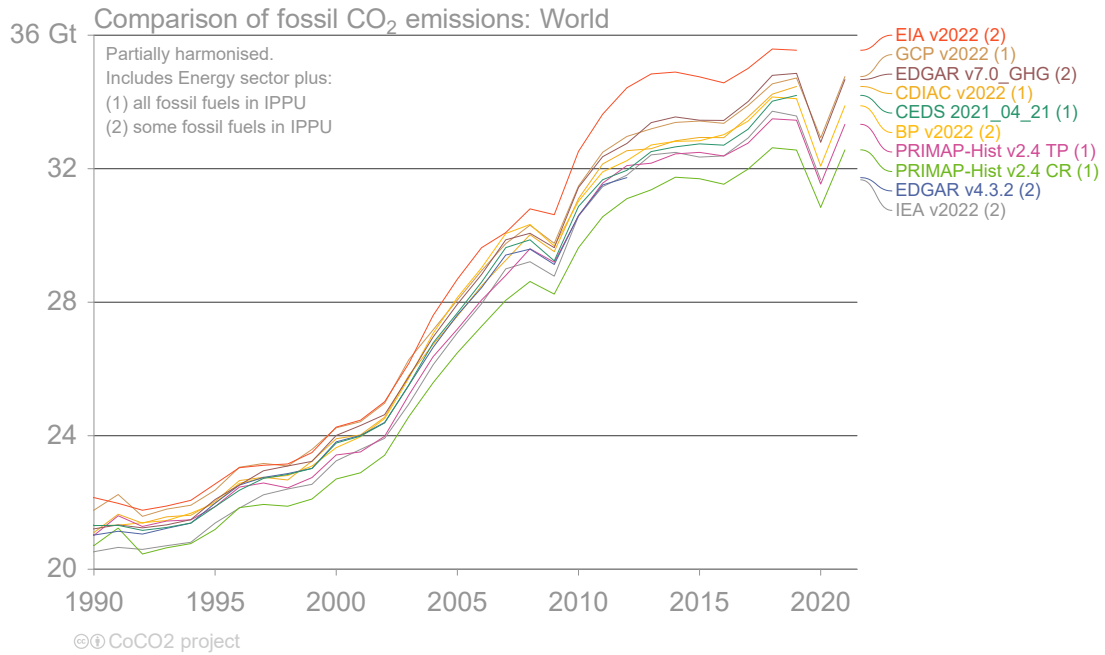


Figure 2: Comparison of global fossil CO₂ emissions from multiple inventory datasets with system boundaries harmonised as much as possible. Harmonisation is limited by the disaggregated information presented by each dataset.

Most datasets agree well within expected system boundary differences (Andrew, 2020). As reported in the previous version of this report (December 2021), we discovered that EIA’s estimates were high, and investigation showed that the emissions estimates had grown twice despite the underlying energy data remaining virtually unchanged. Contact with the EIA revealed they had introduced two separate errors leading to double-counting, and their correction led to a drop in EIA’s estimates of global fossil CO₂ emissions by about 1 Gt CO₂.

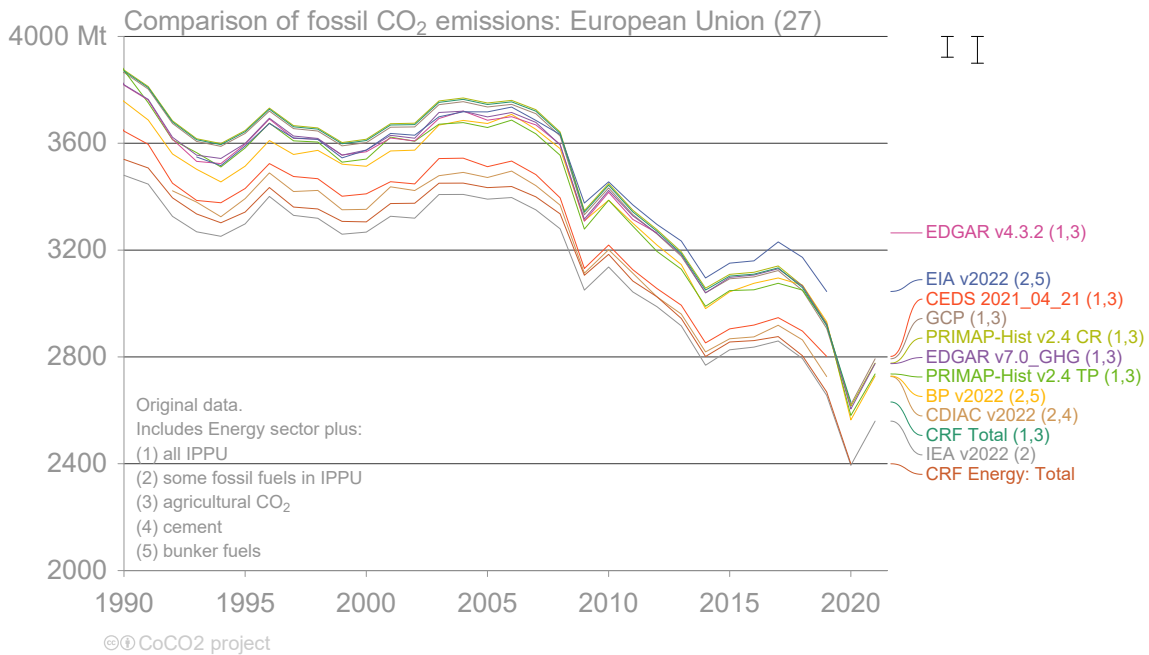


Figure 3: Comparison of EU fossil CO₂ emissions from multiple inventory datasets. CDIAC does not report emissions for countries that did not exist prior to 1992. The uncertainty whiskers in the top-right indicate the approximate uncertainty for EDGAR and UNFCCC.

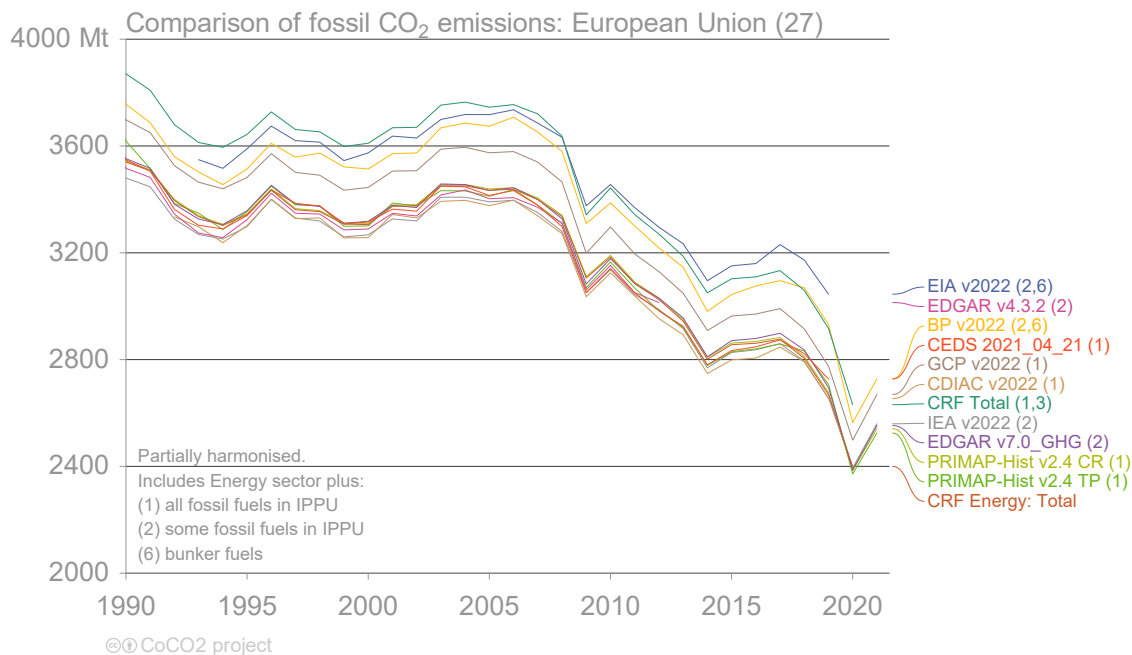
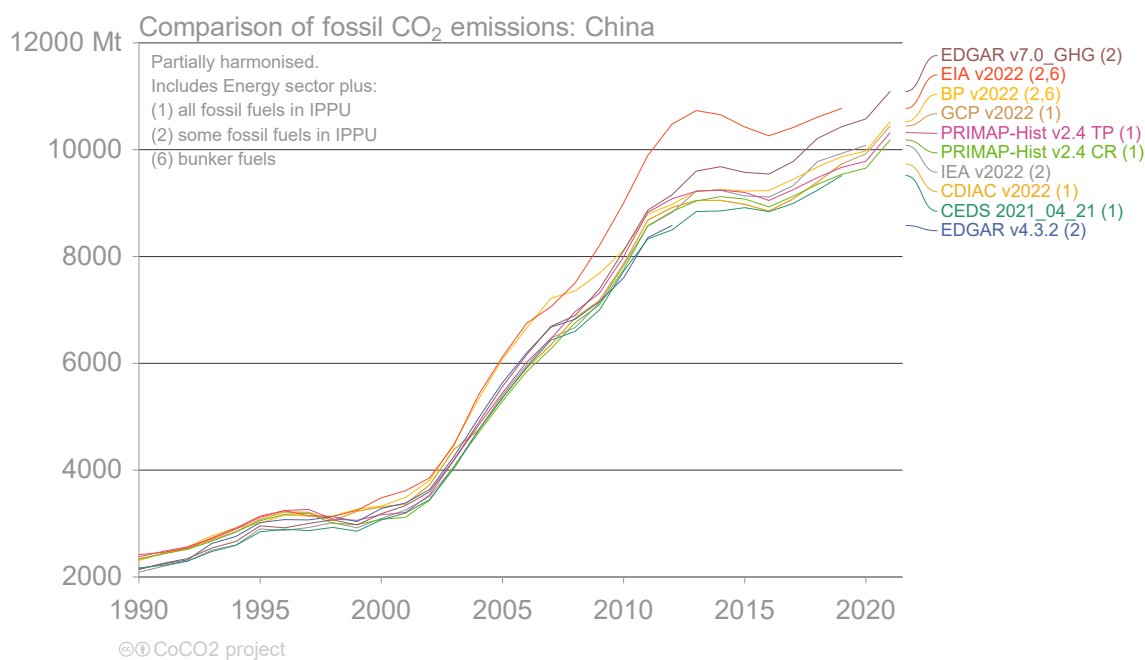


Figure 4: Comparison of EU fossil CO₂ emissions from multiple inventory datasets with system boundaries harmonised as much as possible. Harmonisation is limited by the disaggregated information presented by each dataset. CDIAC does not report emissions for countries that did not exist prior to 1992.

For the bottom-up inventory-based estimates, it is possible to produce the figures for all countries. Figure 5 repeats the figures for two-largest emitters, China and USA, and figures for the next-largest emitters can be found in the Annex: India, Russia, Japan, Iran, Germany, Saudi Arabia, South Korea, and Indonesia. For China, the EIA estimates are significantly higher than others, and Andrew (2020) offers some explanation for this. Otherwise, the datasets are similar in most instances, but further work is ongoing to uncover the reasons for remaining divergences between these datasets.



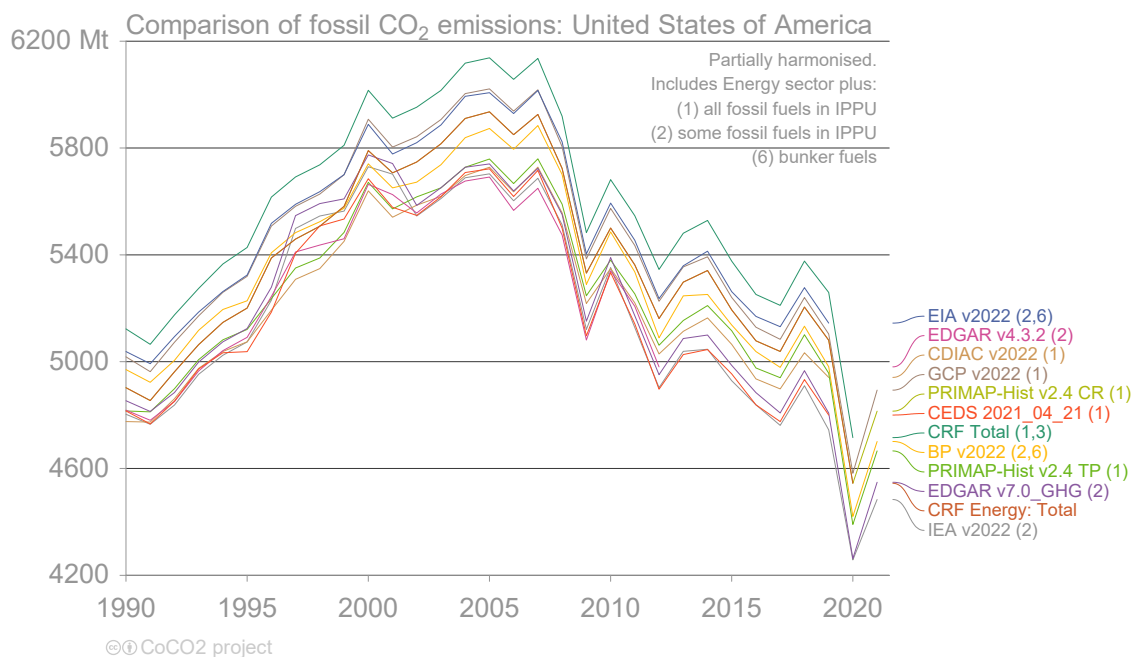


Figure 5: Comparison of China (top) and USA (bottom) fossil CO₂ emissions from multiple inventory datasets with system boundaries harmonised as much as published data detail allows.

3.2 Atmospheric inversions

The best top-down observation-based constraint on national scale estimates of anthropogenic CO₂ emissions in Europe over more than the past decade are satellite measurements of NO₂ and CO, which are “proxy” species co-emitted with CO₂ by fossil fuel combustion (FFCO₂). Results from the first atmospheric inversions of the European FFCO₂ emissions in VERIFY (Konovalov and Lvova (2018); Petrescu et al. (2021a)), indicated that there were much larger uncertainties associated with the assimilation of CO data than to that of NO₂ data for such a purpose.

In the first and second (current) version of this report we present selected results from outputs from the VERIFY project (deliverable D2.11 and deliverable D2.12), which developed an atmospheric inversion workflow quantifying monthly and annual budgets of the national emissions of FFCO₂ in Europe (Fortems-Cheiney and Broquet, 2021b; Fortems-Cheiney et al., 2021). This workflow, implemented in the Community Inversion Framework (CIF; Berchet et al., 2021), estimates the NO_x emissions that when fed into a regional chemical transport model (CHIMERE; Menut et al., 2013) best match satellite-measured NO₂ concentrations, while simultaneously minimising the difference between these estimated NO_x emissions and those from the prior inventory dataset, TNO-GHGco-v2 or TNO-GHGco-v3 (Denier van der Gon et al., 2020). This is a minimisation of least-squares optimisation process, solved iteratively (Rodgers, 2000; Chevallier et al., 2005). This workflow is applied over the period 2005-2020, on a 0.5°×0.5° grid. Ratios of FFCO₂ emissions to NO_x emissions directly derived from TNO-GHGco-v3 for five sectors (energy, industry, residential, road transport and the rest of the sectors), for each country and each month are then used to estimate fossil CO₂ emissions from the NO_x estimates produced by the inversion modelling. Several critical aspects of this workflow need to be highlighted: (i) Fortems-Cheiney and Broquet (2021a) have not reported estimates of the uncertainty in the final FFCO₂ emissions yet (ii) the FFCO₂ emission budgets provided by the TNO-GHGco-v3 inventory are based on the emissions reported by countries to UNFCCC, which are assumed to be accurate in Europe, therefore the inversion prior estimate (which is also its first guess in the variational inversion framework) is consistent with the inventory estimates.

For the EU27+UK, inversion products (emissions provided by the TNO-GHGco-v2 inventory and the maps of total Nox anthropogenic Emissions) yield credible numbers compared to nine inventory estimates from datasets with global coverage (Figure 6). After modelling was complete it was discovered that the prior fossil emissions estimates provided by TNO included non-combustion emissions (prior estimates were FCO₂, and not FFCO₂), the effect of which has not yet been determined.

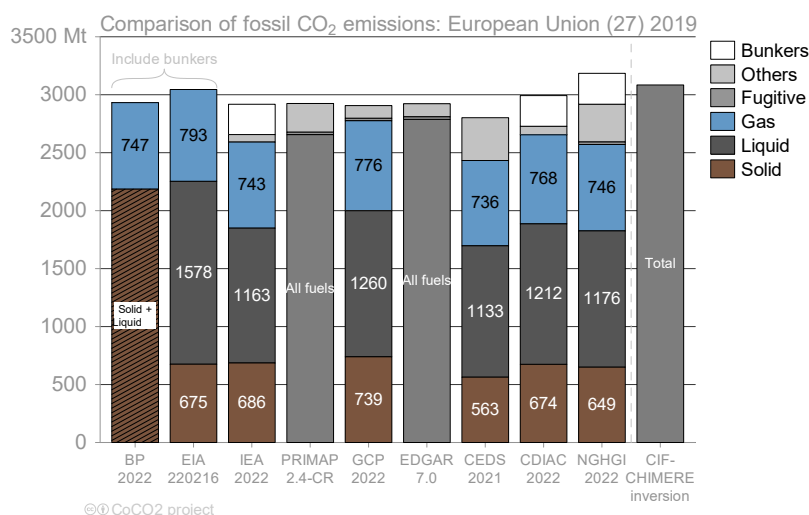


Figure 6: EU27+UK total CO₂ fossil emissions, as reported by nine global inventory data sources: BP, EIA, CEDS, EDGAR, GCP, IEA, CDIAC, PRIMAP-hist and UNFCCC NGHGI with a top-down, fast-track CIF-CHIMERE atmospheric inversion (black dot) (Fortems-Cheiney and Broquet, 2021b). The data represent EU27+UK for the year 2019 split per fuel type. ‘Others’ are emissions not categorised by fuel, and international bunker fuels are not usually included in total emissions at sub-global level. Neither EDGAR nor PRIMAP-hist publishes a break-down by fuel type, so only the totals are shown.

Figure 7 shows the annual posterior fossil-CO₂ estimate from Fortems-Cheiney and Broquet (2021b) compared with the prior estimates for the EU27. As discussed above, the similarity of the inversion estimates with the inventory estimates here does not indicate a verification of the inventory estimates, but rather suggests that the workflow functions well and that the inversion was not pulled away from its prior estimate by major lack of fit to the satellite NO₂ data. Further work will be needed to make the inversion outputs more independent and less reliant on (prior) inventory estimates before they can be used for verification, and to derive robust estimates of the posterior uncertainties. Despite the agreement with the inventory estimates, Fortems-Cheiney and Broquet (2021b) indicate that the relative uncertainty in their estimates is likely very high (probably similar to that reported by Konovalov and Lvova (2018)) due to high uncertainties in both the NO_x inversions and the conversion into FFCO₂ emission estimates. This work is continuing.

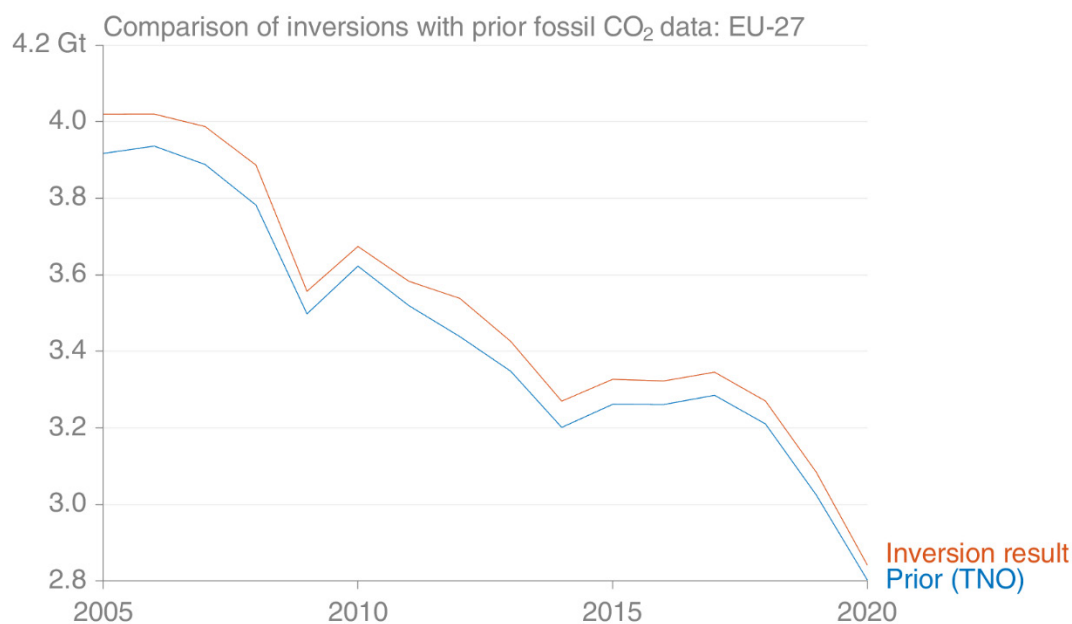


Figure 7: Comparison of inversion results for the EU with prior FFCO₂ emissions estimated by the TNO-GHGco-v3 inventory (Fortems-Cheiney and Broquet, 2021b). Note that the proximity of the inversion results to the prior estimates is not a direct indicator of verification, without additional information on the prior and posterior uncertainty and supporting statistical analysis (see discussion in the text).

While we still lack quantified posterior uncertainty estimates, they are currently thought to be high. Therefore, the agreement of the inversion result with inventory estimates is encouraging but is insufficient to confirm either of the estimates. The close agreement tells us that the inversion approach has not found sufficient evidence that the inventories are incorrect. Some reasons for this are lack of spatial coverage, sensitivity to the surface in the data, and the relatively high level of observation uncertainties. Country-level results show in some cases near-perfect agreement between the inversion modelling output and inventory estimates (Figure 28). However, this generally results from insufficient satellite data (because of cloud cover) for these countries, and/or that emissions of NO₂ are low (e.g., rural areas), such that minimal ‘correction’ is obtained to adjust the prior (inventories). Thus far the work involved has been aimed at proving the concepts and building the required modelling infrastructure and workflow. One of the main constraints to reducing uncertainty in this approach is the current lack of observation networks dedicated to the monitoring of FFCO₂ emissions, such as the planned constellations of satellite CO₂ spectro-imagers (Fortems-Cheiney and Broquet, 2021b): “the uncertainties in the FFCO₂ inversions presented here are still too high to attempt at using these inversions to improve the current knowledge on the FFCO₂ national scale emission budgets in Europe, although further progresses are expected”. Focusing on national-scale inversion configurations for European countries and on recent years during which the availability and resolution of CO₂ and pollutant data has significantly increased, CoCO₂’s WP4 (T4.4) should make a step forward towards an assessment of national scale FFCO₂ emission budgets in Europe.

Inversion results for countries outside of Europe are not yet available from the combined projects VERIFY, CHE, and CoCO₂. Some progress has been made in CoCO₂ (Task 4.4) for the USA. Given CoCO₂’s additional focus on the global top-10 emitters, effort will need to be invested in sourcing inversion results, potentially from collaborators outside of Europe (e.g., Basu et al., 2020).

4 Net land CO₂ fluxes

The net land CO₂ fluxes are based on inventories, process models, and atmospheric inversions estimates from VERIFY, extended to include a CoCO₂ inversion (using CAMS). In the first version of this report, the inventory datasets (UNFCCC, FAOSTAT, BLUE, Houghton & Nassikas), the TRENDYv10 ensemble (min, median, max), the atmospheric inversions (min, mean, max), plus a CAMS inversion including lateral fluxes (CoCO₂ activity) and a managed land mask (Chevallier, 2021) were all included on the same figure (Figure 8). The problem with this figure is that it mixes too many datasets with many different system boundaries. In this version of the deliverable, we will break this figure into three separate figures depending on the key methodology used.

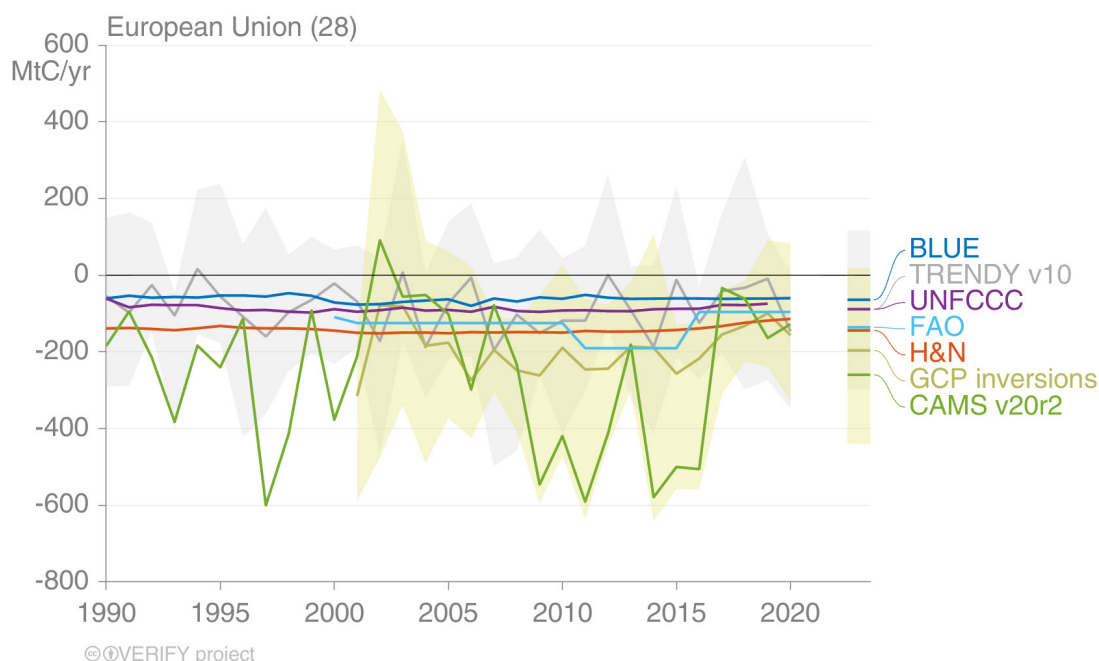


Figure 8: A comparison of inventories and inversions land CO₂ fluxes for the EU28 (EU27+UK). Shaded areas show maxima and minima of the TRENDY (grey) and GCP inversion (yellow) collections.

System boundary issues plague comparisons of net land CO₂ fluxes. The question of how to define whether these carbon fluxes are anthropogenic is at the core of this issue (Grassi et al., 2018). The carbon cycle and land surface modelling communities (e.g., IPCC assessment reports) define anthropogenic carbon fluxes on land differently to the inventory community (e.g., IPCC guidelines), though methods are being developed to bridge the differences (Grassi et al., 2021). There are two dimensions to this complex problem: 1) what land areas have anthropogenic changes (what is 'managed land'), and 2) are environmental factors (CO₂ fertilisation, climate, etc) or disturbances anthropogenic? The IPCC Guidelines (used in UNFCCC NGHGI) have country determined 'managed land' areas and include direct and indirect (environmental) factors. Bookkeeping approaches (BLUE, H&N, OSCAR) consider direct effects on land reported as having a land use transition, but exclude indirect effects. Land surface models (TRENDY) and inversions consider all land and all effects, but therefore need to disaggregate results to the appropriate level to facilitate comparisons with other datasets. Depending on the share of land managed versus transitioning, and the size of the direct and indirect effects, the differences can be substantial (Grassi et al., 2018; Petrescu et al., 2020). Therefore, comparison of independent estimates of net land CO₂ fluxes need to consider the effect of these system boundary issues. The CoCO₂ CAMS inversion includes a managed land mask and therefore provides additional knowledge to aid in comparisons.

To reduce the effect of these system boundary issues and facilitate a more meaningful discussion of system boundary issues, this second version of the deliverable splits the comparisons into three figures: 1) Bookkeeping and inventory-based estimates, 2) inventory-based land-surface models, and 3) inversion-based estimates. In each of these figures, the comparisons are made relative to the UNFCCC NGHGI estimates (Annex I countries) or the estimates of Grassi et al. (2022a) (non-Annex I countries). Each of these figure types will be discussed in turn.

4.1 Bookkeeping and inventory-based estimates

Figure 9 (EU27) and Figure 10 (Brazil) show the inventory estimates for the bookkeeping models – OSCAR, BLUE, Houghton & Nassikas – together with the inventory-based estimates (FAO and Grassi et al. (2022a)), compared with the UNFCCC NGHGI. These countries are selected to facilitate a discussion on the comparisons. The three bookkeeping models consider direct effects only, for identified land-use transitions. They, therefore, exclude indirect effects and emissions from land that does not transition (e.g., forests remaining forests). The three inventory estimates (FAO, Grassi et al 2022a, NGHGI) are based on the IPCC Reporting Guidelines, though with different level of Tiers, but are otherwise expected to give similar results. Grassi et al (2022a) is based on the UNFCCC NGHGI data reported in 2021 (Annex I countries), which differ slightly to the UNFCCC NGHGI data reported in 2022. Overall, FAO uses a simpler approach and the forest land areas based on country statistics from the FAO/FRA process which may differ to NGHGIs. However, within uncertainties, the agreement is reasonable between FAO, Grassi et al. (2022a), and UNFCCC NGHGI.

There are often large differences between the bookkeeping models and the inventory-based estimates. First and foremost, the bookkeeping models and the inventory-based methods are estimating different things: the bookkeeping models include direct effects of land-use transitions, the inventories include direct and indirect effects of the larger managed land (Grassi et al., 2018). Thus, any alignment between bookkeeping models and inventory estimates should be coincidental. However, in some cases, there may be physical rational behind similarities. Since most of the EU land area is managed and the Houghton and Nassikas bookkeeping model takes a country level approach using FAO data, then the similarity in estimates for the EU could imply the indirect effects are relatively small (Petrescu et al., 2020). BLUE and OSCAR use an alternative grid-based land-use product (LUH2), which may explain their higher estimates, through processes such as shifting cultivation. However, since most of the Brazilian forest area is unmanaged, then the similarities in the estimates would require different drivers. While each country requires a deeper analysis of the underlying areas and implied emission factors (carbon densities) to reconcile the differences between estimates, any agreement between these datasets should be considered coincidental. Work is ongoing to better map between these estimates (Grassi et al., 2022b).

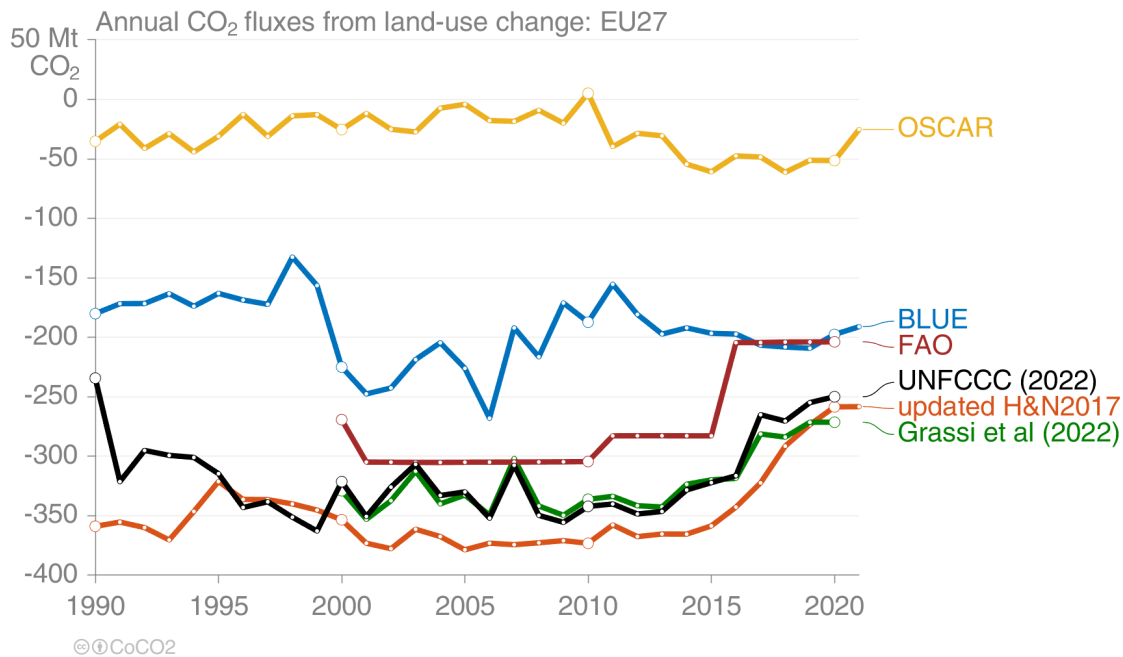


Figure 9: Net land CO₂ flux for bookkeeping type models for the EU27. Romania has been removed from the EU27 total due to carbon stock data.

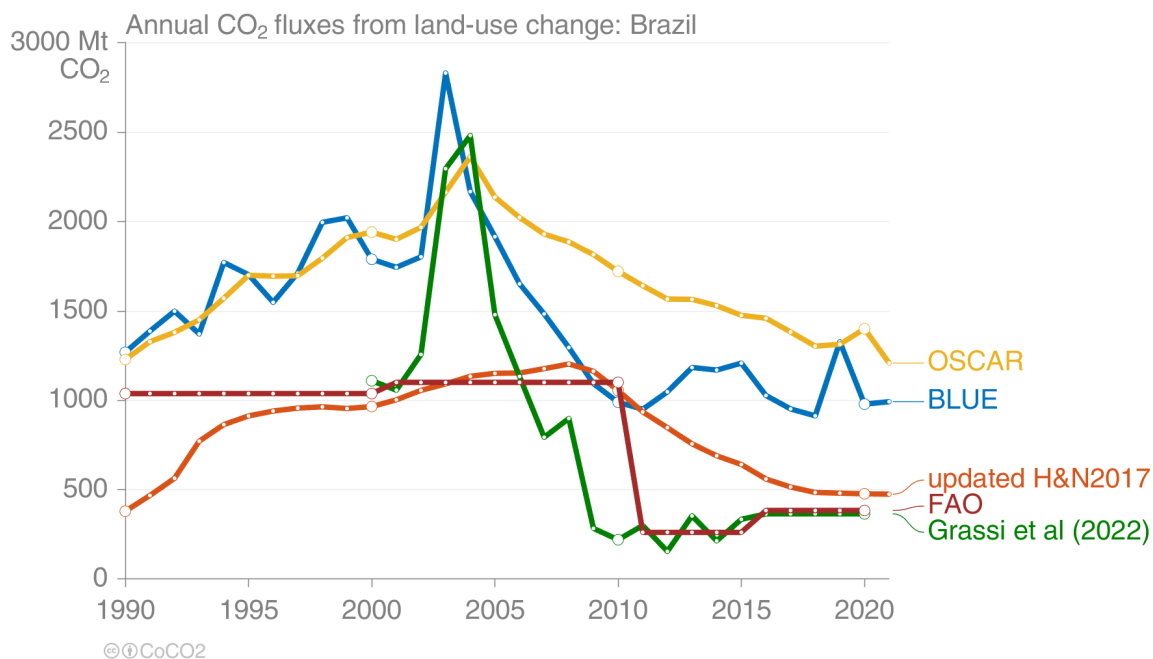


Figure 10: Net land CO₂ flux for bookkeeping type models for Brazil.

4.2 Inventory-based land-surface models

As process-based land surface models, the Dynamic Global Vegetation Models (DGVMs), can provide additional details to inventories, and allow modelling of future evolution of the net land CO₂ flux. The process-based models are forced by climate and therefore have interannual variability, while bookkeeping models and inventories are based on data or methods that essentially smooth out variability. This makes comparisons more complicated.

A total of 17 DGVMs follow a consistent protocol to allow model comparisons (Friedlingstein et al., 2022b). The different simulations in the TRENDY protocol are:

- S0 is a control simulation using fixed pre-industrial (1700) atmospheric CO₂ and a time-invariant pre-industrial land cover distribution,
- S1 applies historical changes in atmospheric CO₂ and Nitrogen inputs,
- S2 applies S1 and climate,
- S3 applies S2 and changing land cover distribution and wood harvest rates.

The 'natural' land sink is given by S2 and the net land CO₂ flux is given by S3, the difference (S3-S2) is directly comparable to the estimated land use flux from the bookkeeping models (Friedlingstein et al., 2022b). There are two main choices on how to compare the TRENDY results with the UNFCCC NGHGs:

1. Compare with inventories and the TRENDY estimated net CO₂ land flux (S3)
2. Compare with bookkeeping models and the TRENDY LUC estimate (S3-S2).

Neither of these comparisons with the UNFCCC NGHGs has a consistent system boundary, with a mapping required to make consistent comparisons (Friedlingstein et al., 2022b; Grassi et al., 2022b). We nevertheless make the comparisons here to facilitate a discussion of the system boundary issues.

Figure 11 shows a comparison of the bookkeeping models, DGVMs, and the Grassi et al (2022) inventory. There is a good agreement between the DGVMs and bookkeeping models, as has been discussed in the Global Carbon Budget (Friedlingstein et al., 2022b). However, there is a large discrepancy with the global inventory estimates due to the different definitions used by the science community and the inventory community (Grassi et al., 2018). Though this figure is global, it is a good illustration of why the bookkeeping models, DGVMs, and inventories are not suitable for meaningful comparisons. While bookkeeping models and DGVMs can produce similar estimates, bookkeeping models only account for land-use change and harvest (but without any forest demography structure) at constant CO₂ and climate, whereas DGVMs account for all fluxes but generally not for forest disturbances and their impact on forest sinks. The inventory estimates include a large share of managed forests, where CO₂ fertilisation and other environmental factors over a significantly larger land area, turn an emission source into a sink.

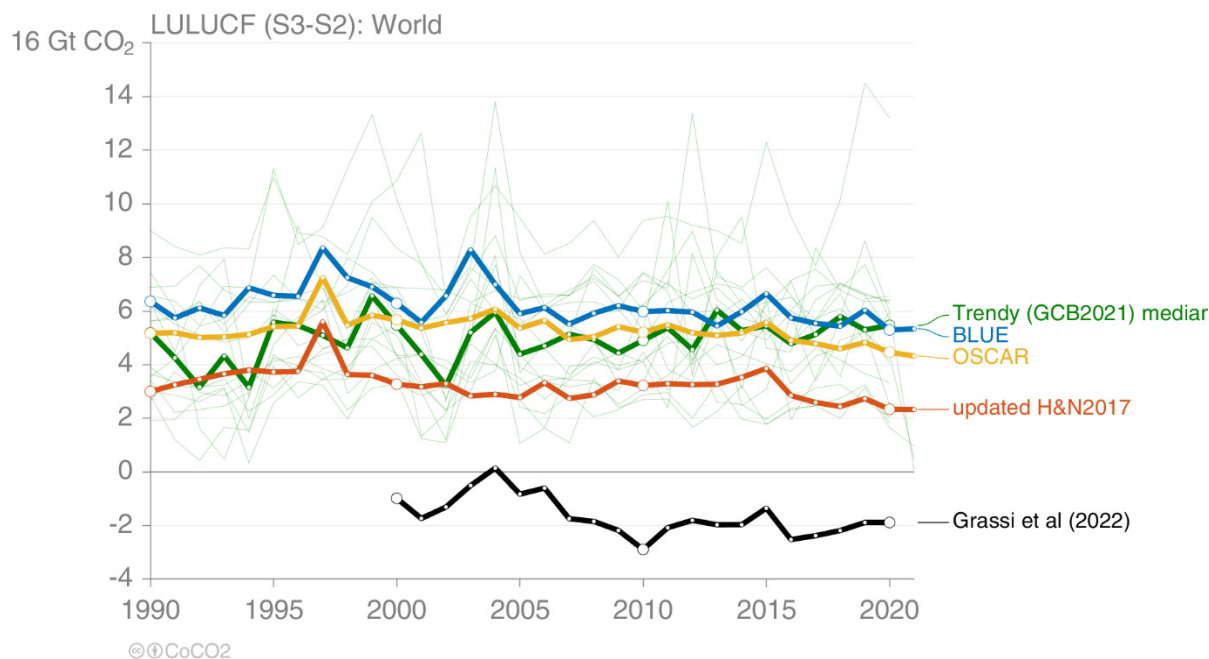


Figure 11: A comparison of the global LULUCF from the bookkeeping models, the TRENDY DGVM individual results and median, and the Grassi et al (2022) inventory estimates. Note that the TRENDY results are from Friedlingstein et al 2022a, but the bookkeeping models from Friedlingstein et al 2022b.

Figure 12 compares the total net land CO₂ flux with the Grassi et al (2022) global inventory. The rationale behind this choice is that the NGHGs countries generally report larger areas as managed, though, not all areas. If all areas were assumed managed, then the TRENDY net land CO₂ flux would presumably be more similar to the Grassi et al. (2022a) inventory estimate. In Friedlingstein et al. (2022b), a reconciliation is made between the bookkeeping models and the inventory-based estimates, by combining the bookkeeping model estimates (analogous to S3-S2) with the non-intact forest share (α) of the total land sink (S2), which could be expressed as $(S3-S2)+\alpha S2=(\alpha-1)S2+S3$. A study still under review at the time of writing provides a more detailed discussion of reconciling bookkeeping models and inventory estimates using the TRENDY ensemble (Grassi et al., 2022b), by estimating country level values of α to make the adjustment between the different datasets (they use the bookkeeping models directly, not the TRENDY S3-S2). The outcome of this analysis can be included in the next version of the deliverable (December 2023).

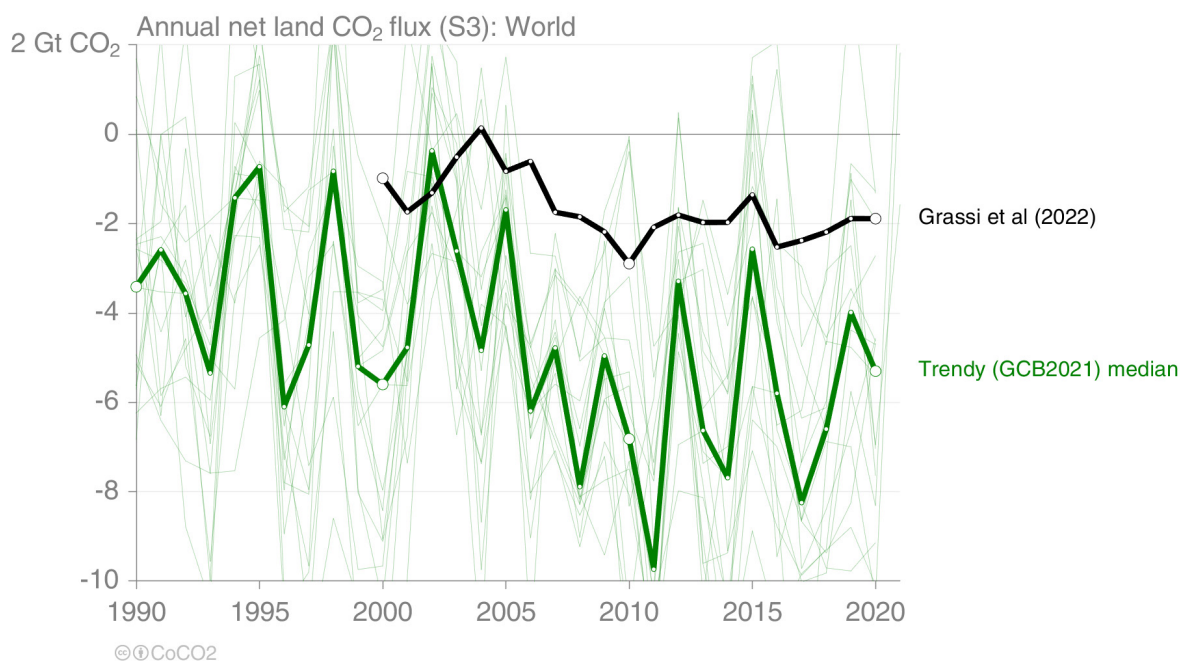


Figure 12: The global net land CO₂ flux for the TRENDY DGVM individual results and median compared with the inventory estimate from Grassi et al. (2022a).

Figure 13 (EU27) and Figure 14 (Brazil) show some sample country level results to illustrate the challenges and differences.

For the EU27, the UNFCCC NGHGI is very similar to the S3 simulation (bottom), which could be expected if all EU27 land is managed and direct and indirect effects are considered: essentially, the NGHGI and the net land CO₂ flux from DGVMs have very similar system boundaries in the case of the EU. The differences between the bookkeeping models, DGVMs, and the UNFCCC NGHGI are larger (top), as indicated earlier, and this is since different models and methods separate out the contributions to the total emissions using different assumptions.

For Brazil, the results contrast with the EU. A large part of Brazil is not defined as managed land, thus the Grassi et al. (2022a) inventory and the DGVM (S3) have different system boundaries: the DGVMs suggest that Brazil is a sink (larger area), while the inventory suggests otherwise (smaller area). On the other hand, the bookkeeping models, DGVMs, and inventories are more comparable in Brazil, likely indicating they use similar system boundaries (areas).

These examples indicate that it is easy to overinterpret comparisons between inventories, bookkeeping models, and DGVMs, as they all capture different components and land areas.

While some estimates may match in one country, they can diverge in another, purely because of system boundary issues. Differences in methods and data give additional uncertainties. The key system boundaries to consider are the land area under consideration, and whether direct or direct and indirect effects are included.

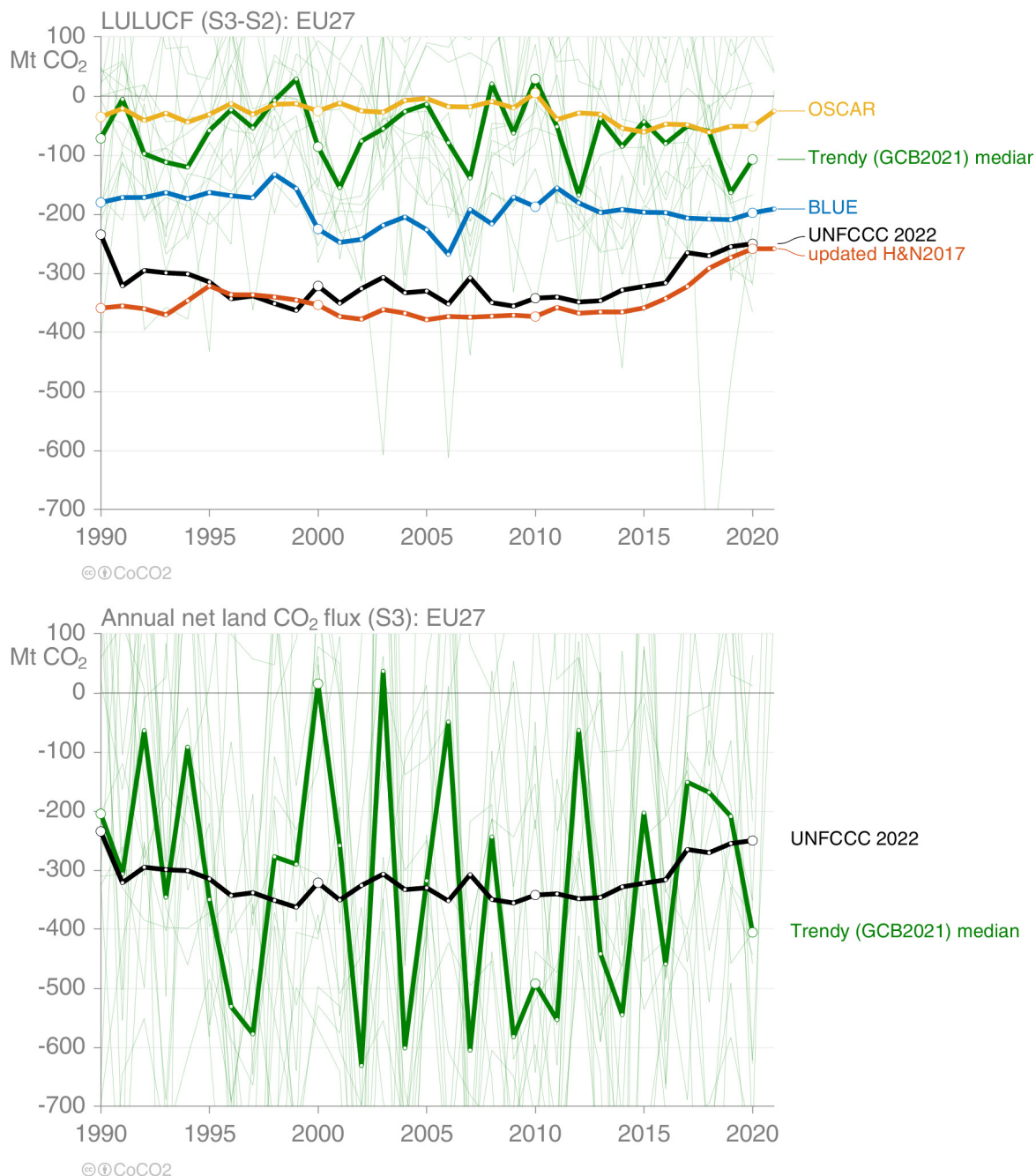


Figure 13: A comparison of UNFCCC NGHGs for the EU27 and the TRENDY DGVM individual results and median with bookkeeping models and S3-S3 (top) and S3 (bottom).

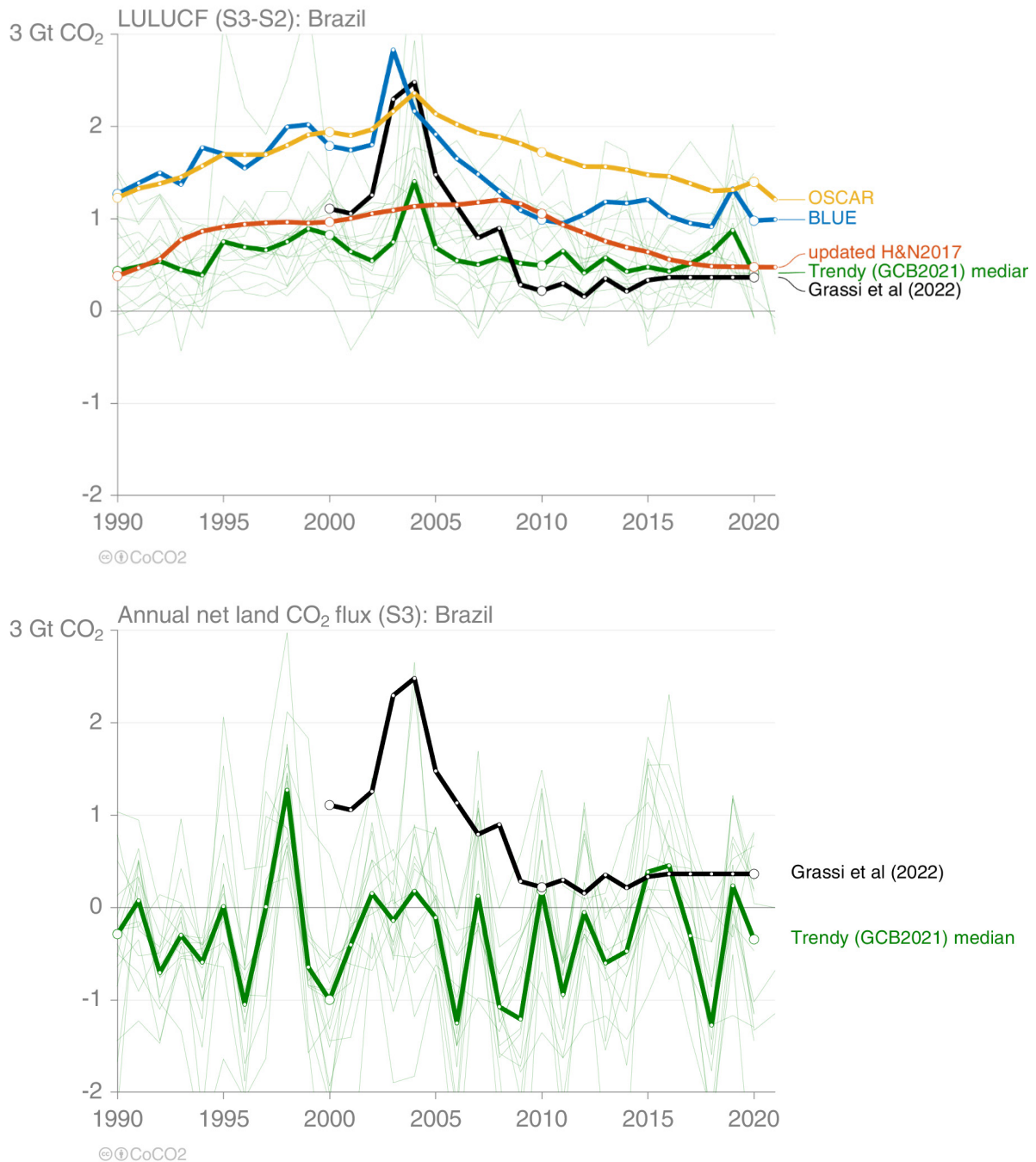


Figure 14: A comparison of UNFCCC NGHGs for Brazil and the TRENDY DGVM individual results and median with bookkeeping models and S3-S3 (top) and S3 (bottom).

4.3 Inversion-based estimates

A comparison of inversions with inventories gives yet another method to compare the net land CO₂ flux. Here, the six inversions from the Global Carbon Budget 2021 are used (Friedlingstein et al., 2022a), initially without a managed land mask or lateral transport adjustments. Figure 15 shows the inversions and their mean compared to inventory estimates for the EU27 and Brazil. The mean of the inversions is much lower than the inventory for the EU27, in contrast to what was found for the TRENDY DGVM results (S3). For Brazil, the results are similar, but this is not expected since the inversions should capture a much larger land area than the inventory alone. These inversions have not been adjusted for lateral fluxes, nor a managed

land mask. The next version of this report (December 2023) will include the lateral fluxes for the individual inversions; however, we now look at the potential size of this effect.

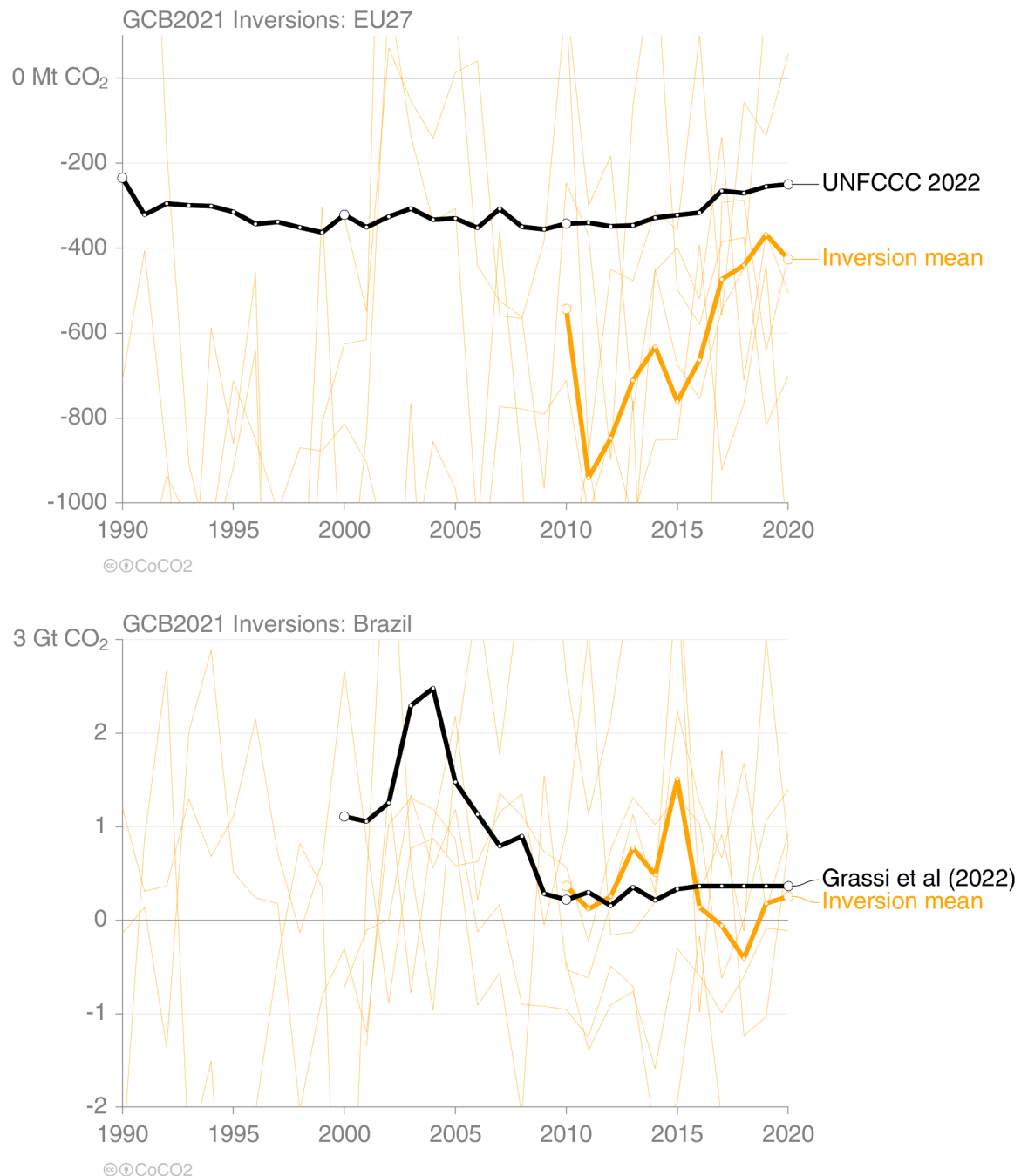


Figure 15: The net land CO₂ flux from six inversions (thin lines) and median and inventory estimates for the EU27 (top) and Brazil (bottom).

The CAMS inversion has been repeated to include lateral carbon fluxes and a managed land mask. These inversions are shown for the EU28 (not available for the EU27) and Brazil, in Figure 16. While this is only available for one set of inversions (CAMS), the results give a clear indication of the trend. In both cases shown, the use of a managed land mask and adjusting for lateral fluxes brings the inversions much closer to the inventory-based estimate. Similar results are found for other regions, depending on the area of managed land and the size of the lateral fluxes. The findings of Chevallier (2021) suggest that the land mask has a small effect on the results, suggesting that the lateral flux corrections are the dominant driver of the

differences. This needs more confirmation as these results are further analysed in the CoCO₂ project.

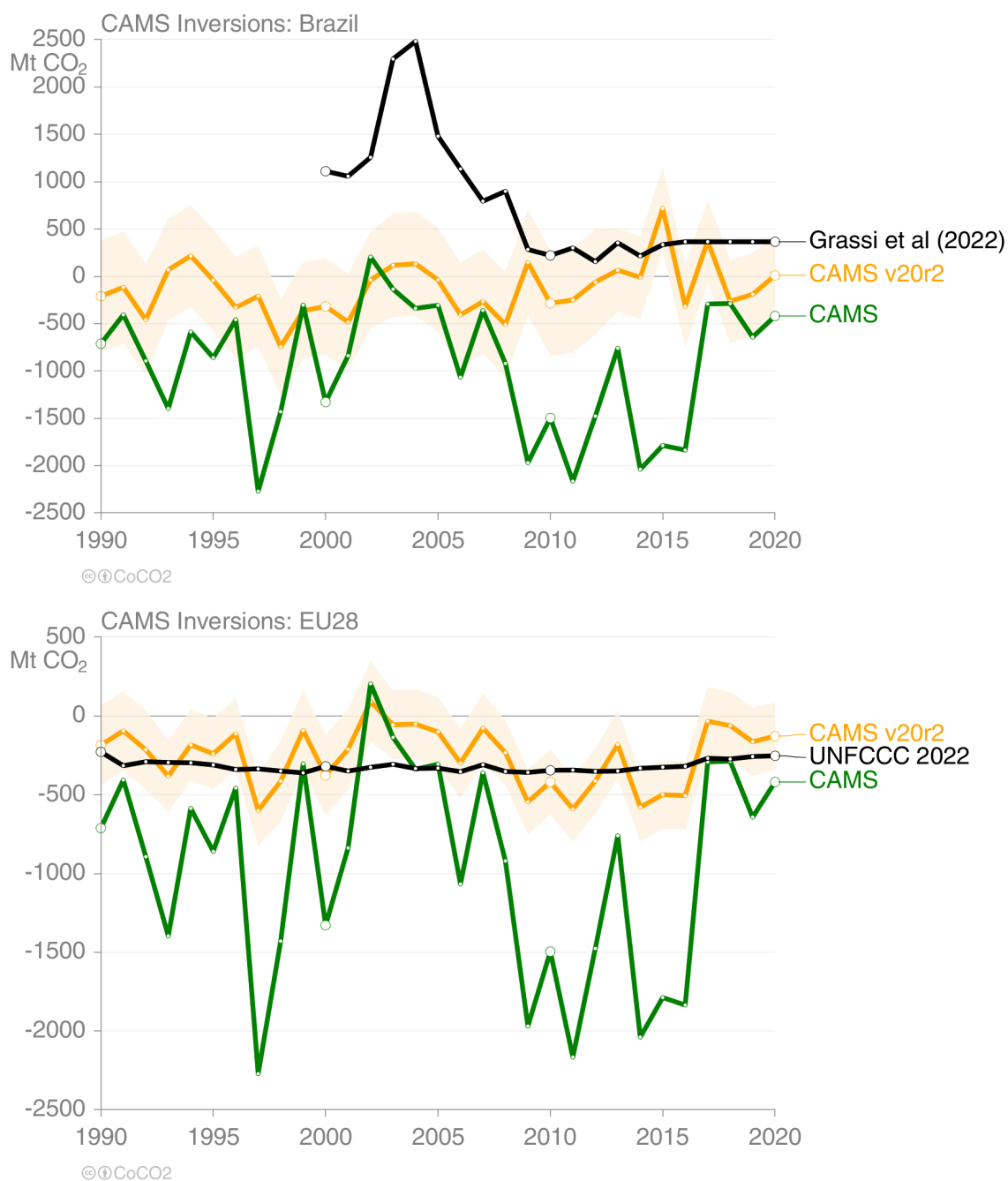


Figure 16: The CAMS inversions without (green) and with (orange) adjustments for lateral carbon fluxes and a managed land mask for Brazil and the EU28. The uncertainty band for one standard deviation is shown for the adjusted inversion.

4.4 Summary discussion of net land

In this revised section on net land CO₂ fluxes, the issues in comparing estimates on land were highlighted. Without adjusting datasets for consistent system boundaries, one could argue that there is little to be gained in comparing different land use data products. A key driver of the results is likely to be the land areas covered, which are not routinely provided by different datasets. If land areas are available, then back calculation of implied carbon densities and their changes over time can be compared to provide additional interpretation of different data products. This can be used to estimate the potential size of direct and indirect effects, or even

potential sizes of lateral carbon fluxes. ^{CO₂}There are some recent studies that develop methods to reconcile different bookkeeping and inventory estimates using DGVMs as a bridge between estimates (e.g., Grassi et al 2022b), but much further work is needed to move more in the direction of verification.

5 Anthropogenic CH₄ emissions

Methane is the second most important GHG after CO₂ but more potent because of its higher radiative efficiency. CH₄ contributes to ~17% of the total global GHGs emissions using a Global Warming Potential (GWP, CO₂-eq), but around 50% of current observed warming (IPCC AR6) due to its potent but short-lived nature. Sector wise, the primary sources of anthropogenic CH₄ emissions are agriculture, fossil fuel production, and waste management. In this report, we compare and analyse data for top CH₄ emitter countries, from observation-based bottom-up and top-down sources and compare them to national inventories reported to UNFCCC, from the Common Reporting Format tables (CRFs) for Annex I parties or from the Biannual Updated Reports (BURs) for the non-Annex I parties.

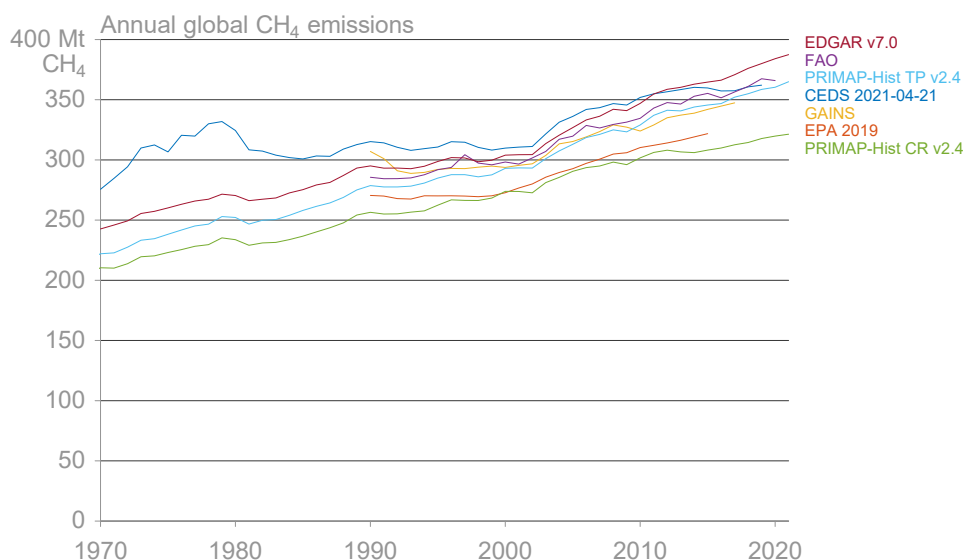


Figure 17: Total global CH₄ anthropogenic emissions from seven inventories, updated from Minx et al., 2021. The FAO independently estimates CH₄ from agricultural, but uses EDGARv6 and PRIMAP-hist for the remaining sectors.

Figure 17 presents the total global anthropogenic CH₄ emissions from seven inventories. All the datasets Figure 17 agree in terms of increasing trends during the last two decades, with differences in absolute emissions values. The differences between inventories are mainly caused by methodologies of producing or using AD, EFs or technological abatement (Minx et al., 2021). For example, the EPA inventory uses the reported emissions by the countries to the UNFCCC (often Tier 3) while other inventories produce their own estimates using a consistent approach for all countries and country-specific AD and EFs. FAOSTAT and EDGAR mostly apply a Tier-1 approach to estimate CH₄ emissions, while GAINS uses a Tier-2 approach. CEDS is based on pre-existing emissions estimates from FAOSTAT and EDGAR, which are then scaled to match country-specific inventories, largely those reported to the UNFCCC (Minx et al., 2021). For EU27 the use of AD and EFs and linkages between data sources has been summarized in Figure 4 in Petrescu et al., 2020.

Table 4 presents the ranking of top world emitter countries by inventory and sectors and their contribution (%) to the total country emissions. The ranking of most of the countries across the three inventories agree well, except for Indonesia, where EDGARv6.0, v7.0 and GAINS report a very large contribution from the Energy sector while UNFCCC (BUR) reports three

times lower emissions. Indonesia reports that the waste sector has the highest contribution to the country's emissions. For Argentina, the largest contribution is from agriculture, while the inventories rank the contributions from energy and waste differently.

The contribution (2010-2020/2021) of the 10 largest emitters (China, India, USA, EU27, Brazil, Indonesia, Russia, Mexico, Australia, and Argentina) to the total global anthropogenic CH₄ emissions is 58% for EDGARv6.0, 56% for EDGARv7.0, and 62% for GAINS (2010-2015).

Table 4: Ranking of top world emitter countries by inventory and sectors and their contribution (%) to the total CH₄ country emissions. The numbers were calculated based on the average from 2010 to the last available inventory year. EDGARv4.3.2 data is not shown in this table since it ends in 2012.

	Countries	Inventory estimates														
		Energy					Agriculture					Waste				
1		UNFCCC	EDGARv6	EDGARv7	FAOSTAT	GAINS	UNFCCC	EDGARv6	EDGARv7	FAOSTAT	GAINS	UNFCCC	EDGARv6	EDGARv7	FAOSTAT	GAINS
2	China	49%	42%	43%	51%	49%	41%	35%	35%	24%	33%	10%	21%	22%	25%	18%
3	USA	44%	44%	43%	47%	46%	36%	36%	37%	33%	32%	20%	20%	20%	20%	22%
	India	12%	9%	9%	15%	15%	74%	67%	67%	64%	67%	14%	23%	24%	21%	18%
	EU27	20%	21%	22%	24%	17%	52%	47%	47%	45%	54%	28%	31%	31%	31%	29%
	Brazil	6%	4%	4%	8%	3%	78%	71%	71%	66%	81%	16%	24%	25%	26%	15%
	Russia	57%	61%	63%	63%	76%	15%	15%	14%	13%	9%	27%	23%	23%	24%	15%
	Indonesia	14%	43%	50%	51%	51%	30%	38%	31%	29%	34%	56%	19%	19%	20%	15%
	Mexico	12%	20%	19%	21%	18%	59%	43%	43%	38%	50%	29%	37%	38%	41%	33%
	Australia	33%	30%	30%	27%	33%	55%	59%	59%	64%	53%	12%	11%	11%	9%	14%
	Argentina	8%	17%	18%	18%	13%	73%	72%	71%	70%	74%	19%	11%	11%	12%	13%
	average 2010-last year															

5.1 Inventory-based estimates

For total and sectoral anthropogenic CH₄ emissions from the inventory data we compare emissions time series from 1990-last available reported year from three EDGAR versions (v4.3.2, v6 and v7) which cover all sectors (Energy, Industry Processes and Products (IPPU), Agriculture and Waste), GAINS model which covers all sectors but IPPU which is nevertheless a small flux (~1%) compared to other sectors and from the UNFCCC CRFs and BURs. We include EDGARv4.3.2 as it is still used as a prior in some inversion models. For the sectoral emissions we also analyse the data from FAOSTAT (2022) and CAPRI model (only for EU27). We identified in most inventories, in this or similar order, the following top emitters: China, India, USA, Brazil, EU27, Russia, Indonesia, Mexico, Argentina and Australia.

For the total and sectoral CH₄ emissions we chose to exemplify EU27 and Australia due to interesting discrepancies we found between the data sources, both in terms of values and trends. All other country figures are found in the Annex.

5.1.1 EU27

For EU27 the total CH₄ anthropogenic emissions from all three EDGAR versions are consistently higher than the UNFCCC CRFs, while GAINS is lower. The datasets generally agree on reduction trends (1990-2015): 31% for UNFCCC, 34% GAINS, 34% EDGARv6.0, and 28% for EDGARv7.0. This also holds for Agriculture and Waste which, together, have the highest share of the total emissions (88%, Table 4). For Energy, all datasets have similar reduction trends (41% - 56% 1990-2015) and this is due to the updates and use of Tier 1

default EFs reported in the NGHGs.

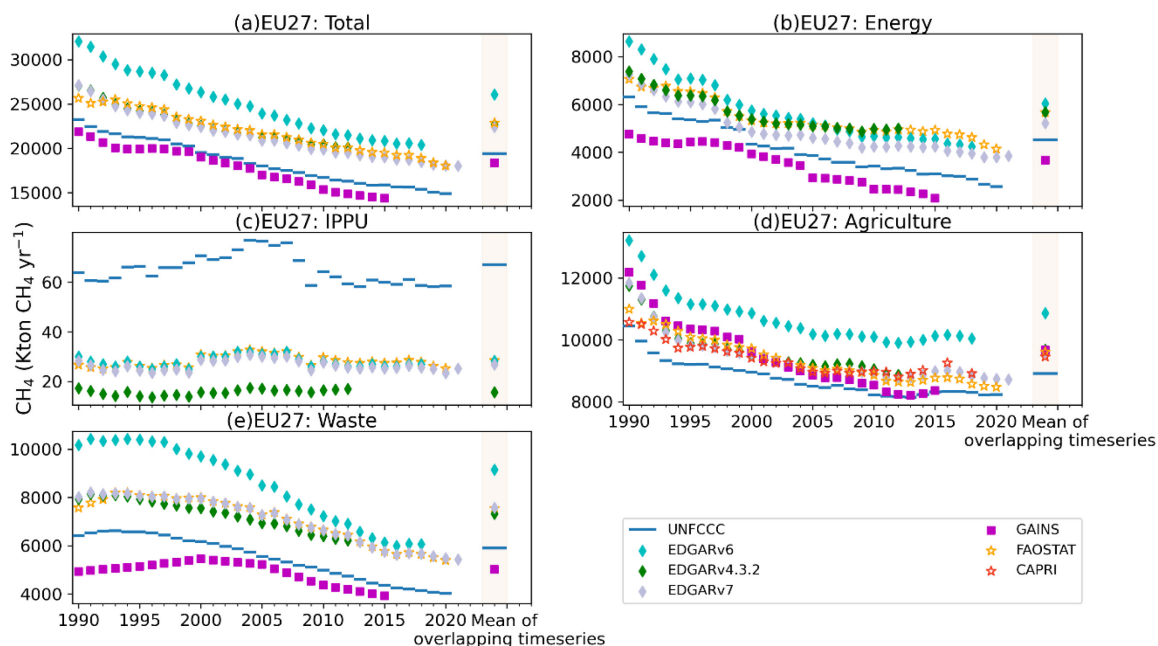


Figure 18: EU27 total anthropogenic sectoral emissions as: a) total, b) Energy, c) Industry and Products in Use (IPPU), d) Agriculture and e) Waste from UNFCCC (2022) submissions and all sectors excl. LULUCF (EDGAR v4.3.2, v6.0 and v7.0, GAINS and FAOSTAT) and CAPRI for Agriculture only. The means represent the common overlapping period 1990-2015. Last reported year in this study refers to 2020 (UNFCCC and FAOSTAT), 2015 (GAINS), 2012 (EDGARv4.3.2), 2018 (EDGARv6.0) and 2021 (EDGARv7.0).

Since 2022, FAOSTAT includes estimates for all IPCC economic sectors: Energy, IPPU, Waste and Other. These data are sourced from the PRIMAP-hist v2.4 dataset (Gütschow et al., 2022). Emissions totals from agrifood domain are computed following the Tier 1 methods of the Intergovernmental Panel on Climate Change (IPCC) Guidelines for National greenhouse gas (GHG) Inventories. Emissions from other economic sectors as defined by the IPCC are also disseminated in the domain for completeness. Emissions are calculated based on data from the UN Statistical Division (UNSD), the International Energy Agency (IEA) and other third-party. Overall, the bottom-up inventories for EU27 do a good job in capturing magnitudes and trends, particularly for Agriculture. IPPU remains the sector which is underestimated by all three EDGAR versions and we hypothesize this has to do with the mapping of activities in EDGAR compared to the UNFCCC reporting guidelines.

5.1.2 Australia

For Australia, most discrepancies are between GAINS and the other data sources, and mainly for Energy and Waste. For Waste emissions, GAINS has an increasing trend, as opposed to EDGAR and UNFCCC, and this is since GAINS is modelled taking into account the socio-economic status of the countries (e.g., the drivers used to project future municipal solid waste generation are GDP per capita and urbanization rate (Gómez-Sanabria *et al* 2018)) which are high in Australia.

EDGAR data is in fair agreement with UNFCCC during the last decade, in particular for Waste and Agriculture while for Energy we see a better match with UNFCCC starting 2013. This is caused by a drop in the solid, gas and oil use, and it reflects in the decline of the implied EFs for underground coal mines which decreased after 2012 (<https://unfccc.int/documents/273478>, Vol.1) while for oil wells the trend coincides with the closure of offshore and onshore wells after 2012. Perhaps a smaller contribution to the

decrease is the split of oil and gas emissions reported for flaring after 2009. Prior to 2009, the Australian Petroleum Production & Exploration Association (APPEA) data did not provide splits for flaring between oil and gas sources and, therefore, flaring emissions were reported in the oil/gas combined category. With the introduction of the National Greenhouse and Energy Reporting scheme (NGER) for the inventory year 2009, separate emissions data has been available for the individual oil and gas flaring categories and therefore the flaring emissions have been reported for 2009 onwards in those respective categories (<https://unfccc.int/documents/273478>, Vol.1). GAINS Energy estimates are going upwards and we hypothesize that GAINS continues to take into account the emissions coming from the open holes of the abandoned mines, while the other inventories do not account for it.

For agriculture, FAO reports very fluctuating emissions showing a clear seasonal pattern. We found that this is due to FAO's inclusion of savannah fires into their Agriculture emissions. The other two BU inventories do not report savannah fires as part of their agricultural emissions but into LULUCF (4A Forest land and 4C Grassland) which is not included in this figure.

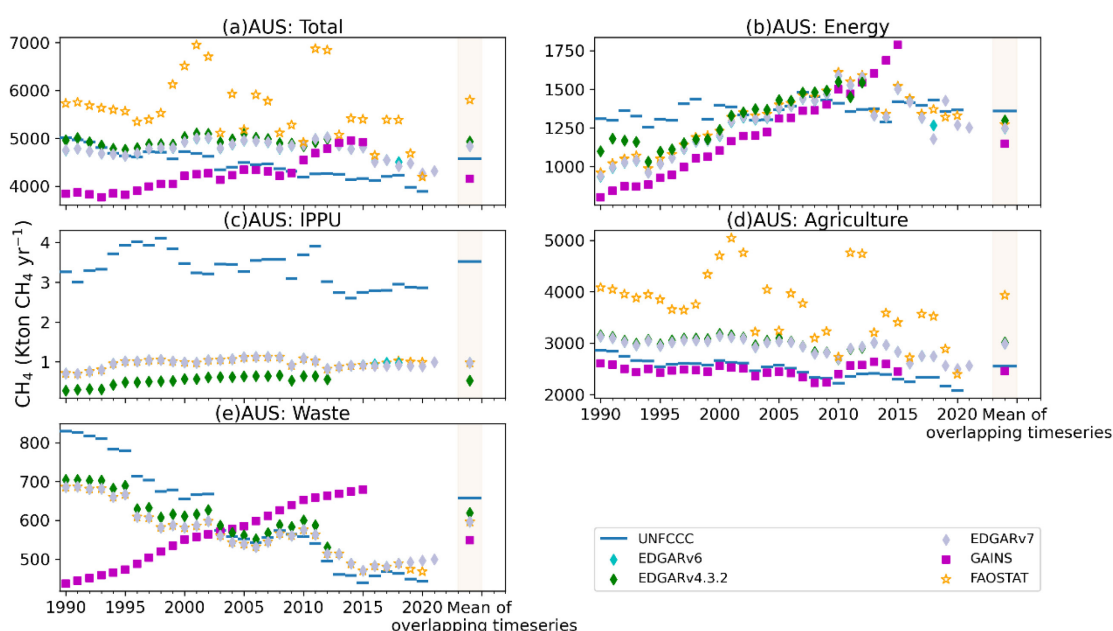


Figure 19: Australia total anthropogenic sectoral emissions as: a) total, b) Energy and Products in Use (IPPU), d) Agriculture and e) Waste from UNFCCC (2022) submissions and all sectors excl. LULUCF (EDGAR v4.3.2, v6.0 and v7.0, GAINS and FAOSTAT). The means represent the common overlapping period 1990-2015. Last reported year in this study refers to 2020 (UNFCCC and FAOSTAT), 2015 (GAINS), 2012 (EDGARv4.3.2), 2018 (EDGARv6.0) and 2021 (EDGARv7.0).

5.1.3 Nordic countries

Across the Nordics countries, there are also large variations in CH₄ (and N₂O) between the UNFCCC NGHGs and different EDGAR estimates (v6 and v7), Figure 20. Methane emissions reported by EDGAR for Sweden, Norway and Finland are significantly higher than official reporting. For some sectors, EDGAR uses the same method for all countries. For example, fugitive emissions of methane in the oil and gas sector are estimated based on the level of production of oil and gas. EDGAR's methane emissions estimates for Norway (solid blue line) follow the pattern of its total production of oil and gas, not its reported emissions of methane. For Sweden, the differences lie in the waste sector. For Finland, the differences lie in both oil and gas and the waste sector. These differences can be up to an order of magnitude at the sector level.

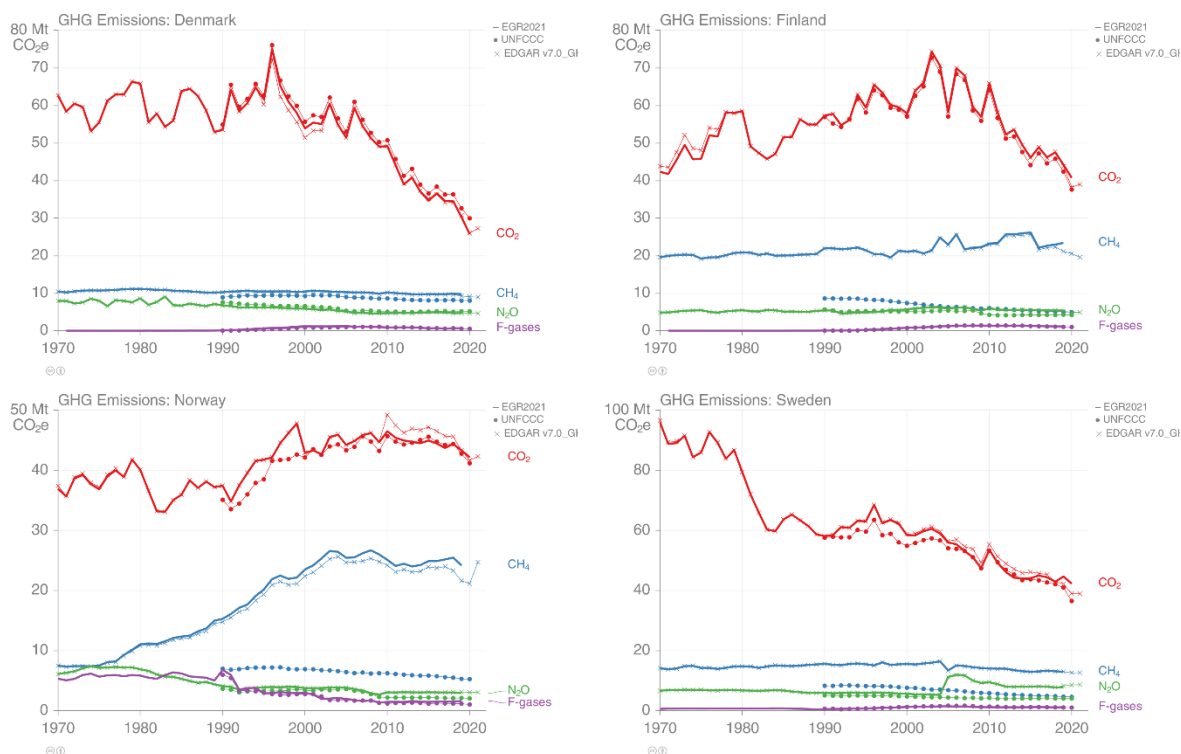


Figure 20: A comparison of CO₂, CH₄, and N₂O in the Nordic countries for UNFCCC, EDGARv6 (shown as EGR2021), and EDGARv7. For CH₄ the differences are significant.

5.2 Atmospheric inversions

For total anthropogenic CH₄ emissions from inversions we updated the data presented in the first version of this deliverable (D8.1) and we compare time series from 2000 to last available reported year from UNFCCC CRFs and BURs, emission data sets (EDGARv4.3.2, EDGARv6.0, EDGARv7.0 and GAINS) against global atmospheric CH₄ inversions from Deng et al. (2022) separated in those based on the assimilation of surface data (SURF) and those assimilating GOSAT satellite column CH₄ data.

5.2.1 USA

The USA atmospheric inversion estimates, given the uncertain inventory estimates, compare well, and confirm a stabilising trend in emissions. However, for the CH₄ emissions from oil and natural gas production regions in the USA, some inversions using remote sensing data from TROPOMI (Shen et al., 2022) on the Sentinel-5P satellite are estimated 45% to 60% higher emissions than reported by US EPA (Schneising et al., 2020; Weller et al., 2020; Zhang et al., 2020) and those will probably match better the GAINS estimates. However, TROPOMI results are not taken up in the figure, because of the relative short time frame of the TROPOMI observations.

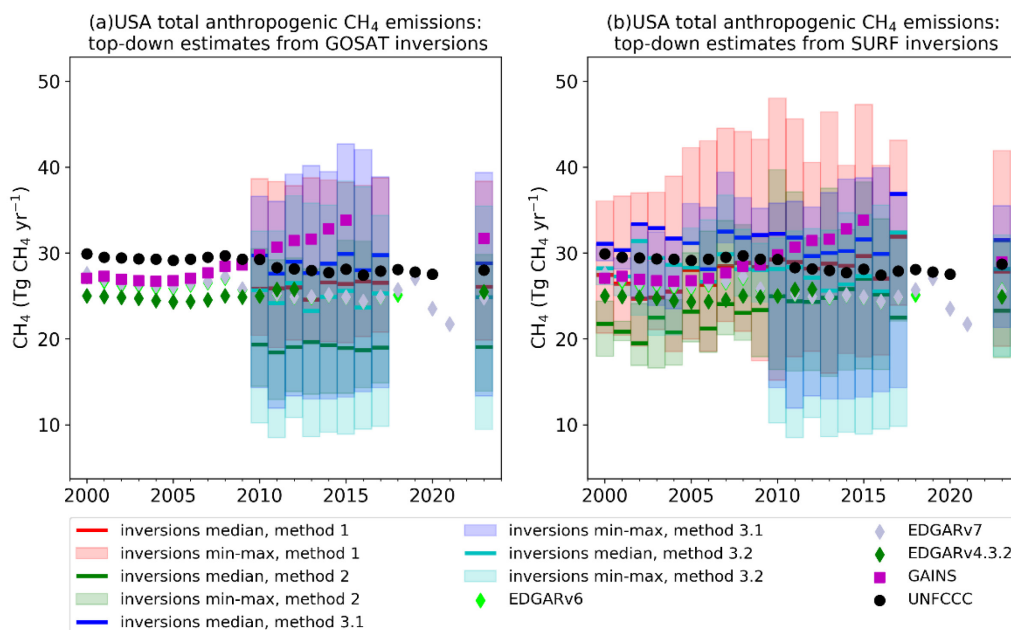


Figure 21: Total anthropogenic CH₄ emissions (Tg CH₄ yr⁻¹) for USA from inventories (EDGARv4.3.2, v6, v7 and GAINS) plotted against UNFCCC national reports (CRFs and BURs) and global inversion ensembles a) CH₄ emissions based on satellite concentration observations (GOSAT) and b) from global model surface stations (SURF). The inversion ensembles are presented for the 4 methods (1, 2, 3.1 and 3.2) as described in section 1.4 of Deng et al. (2022).

5.2.2 EU27

For EU27 we present next to reported data to UNFCCC (2022), anthropogenic CH₄ emissions from regional top-down observation-based inversions as provided to the VERIFY project such as: CTE VERIFY (inclusive (S4) and core(S5)), CIF intercomparison (FFELXPART-CIF), FLEXkF_VERIFY and CAMS v19r and v21r respectively. We show both results based on GOSAT (Figure 22) and on in-situ observation SURF (Figure 23). The total CH₄ inverse fluxes were further corrected for the natural fluxes which were subtracted from the inversions total flux. The natural emissions were those used in the latest VERIFY synthesis and are presented in Fig. 4b of Petrescu et al. (2022). Deng et al., 2022 applies its own methodologies to extract the anthropogenic flux from the total flux.

EU27: Comparison of anthropogenic CH₄ emissions from TD observation-based GOSAT estimates

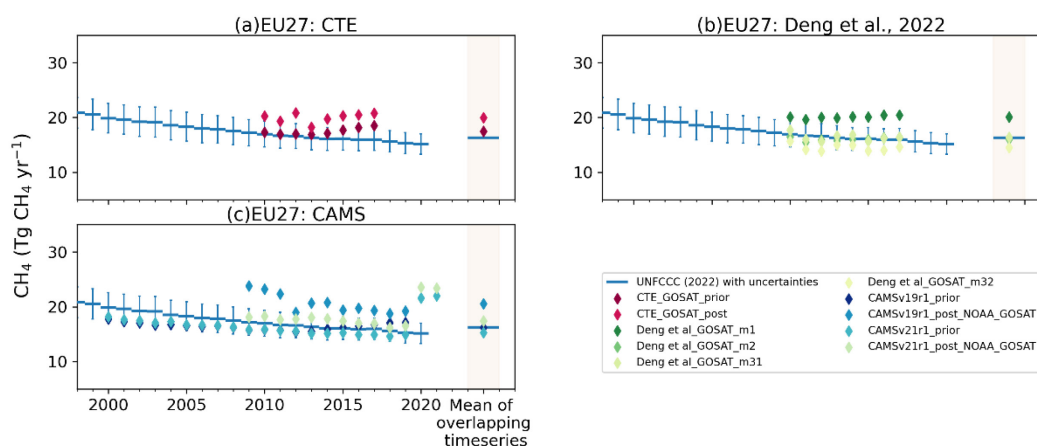


Figure 22: Total anthropogenic CH₄ emissions (Tg CH₄ yr⁻¹) for EU27 from UNFCCC national reports (CRFs) compared to GOSAT obs-based global and regional inversion ensembles from a) CTE-CH₄ b) Deng et al. (2022) methods (m1, m2, m3.1 and m3.2), and c) CAMSv19 and v21.

Each inversion provided both prior and posterior fluxes. As presented in Table 7 most inverse systems use priors of anthropogenic emissions from EDGARv6.0 or v4.3.2. One difference in the results could be attributed to the spatial resolution which differs between inverse systems (CTE 1x1 degree, CAMS 3x2 degree) and the transport models used for allocating emissions to sources. Also, in CAMS, if a 3x2 grid cell included both ocean and countries, then the ocean part of the cell has been assigned to the included countries according to their ratio of presence in that cell. In the final version of this deliverable (D8.3), we plan to analyse prior and posterior data and their uncertainties and to complete the figures for all top emitters with TD results, including prior dataset vs posterior estimated fluxes, for both natural and anthropogenic fluxes.

EU27: Comparison of anthropogenic CH₄ emissions from TD observation-based SURF estimates

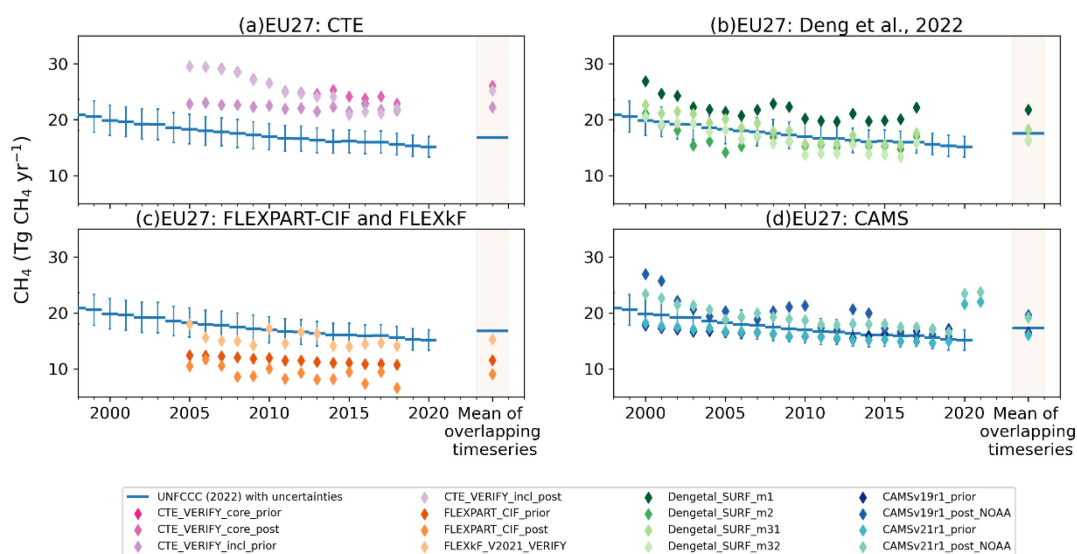


Figure 23: Total anthropogenic CH₄ emissions (Tg CH₄ yr⁻¹) for EU27 from UNFCCC national reports (CRFs) compared to VERIFY simulations (CIF) and SURF observation-based global and regional inversion ensembles from a) CTE-CH₄ b) Deng et al. (2022) methods (m1, m2, m3.1 and m3.2), c) FLEXPART-CIF and FLEXkF and d) CAMSv19r and v21r.

For both GOSAT and SURF based estimates, Deng et al (2022) compares best with the UNFCCC reported values due to methodologies used to separate CH₄ anthropogenic emissions from inversions to compare them with national inventories. The calculations of anthropogenic emissions by each method were performed separately for GOSAT inversions and in situ (SURF) inversions.

Four Once data on global natural CH₄ fluxes (wetlands, fire, geological and inland waters) will be available, we will update and assess their importance in correcting the inverse results, for a valid comparison with UNFCCC NGHGs. The CTE system provided us with runs from the IG3IS project and GCP2021, which will be processed for the next D8.3 report.

For reference, the UNFCCC reported uncertainties are in the range of 11.4% - 14.6%.

5.3 Uncertainties from inverse systems

CTE-CH₄ inversion system referenced by Tsuruta et al. (2017) provided prior and posterior fluxes and uncertainties (standard deviation) from surface inversions for 2005-2018 (those used by Thompson et al. (2022)). There are two sets of inversions: "VERIFY_inclusive" (or S4 run in VERIFY) which uses as many available stations as possible, and "VERIFY_core" (or S5 run in VERIFY) which only uses stations covering a sufficiently long period. The degrees of freedom in the state vector of the system was low, and therefore, the uncertainty estimates may not differ much between the two. Below we present three examples of uncertainty reduction maps, produced with data from the CTE system and which exemplifies how

important the increase in the number of observation stations (2006-2018) is in reducing uncertainties in flux estimates.

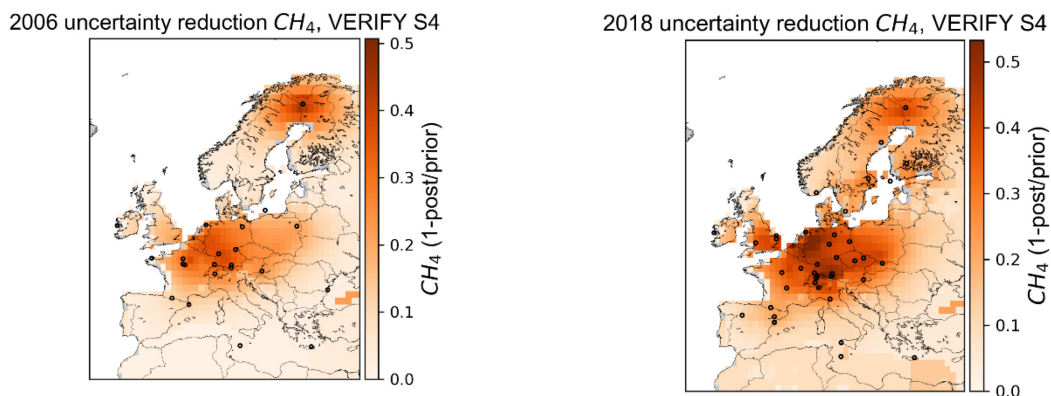


Figure 24: VERIFY_inclusive (S4) inversion run, uncertainty reduction maps computed as $(1 - \Delta_{\text{post}}/\Delta_{\text{prior}})$ for 2006 and 2018 with different sets of observation stations.

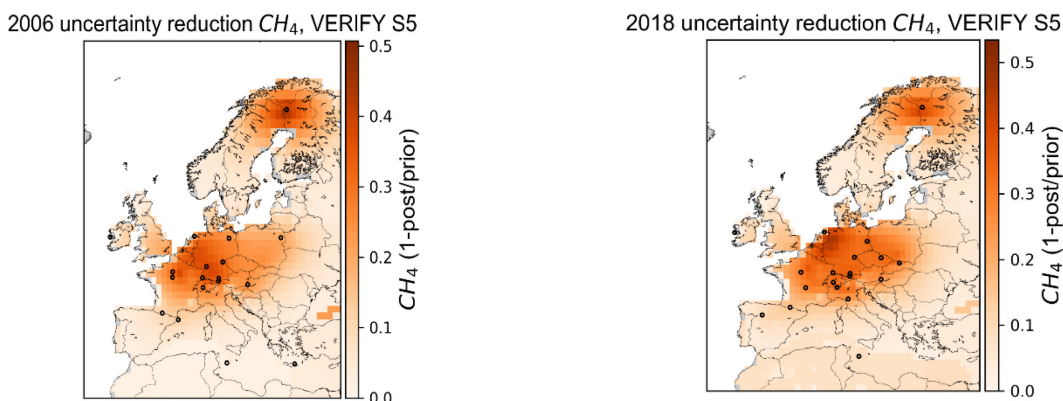


Figure 25: VERIFY_core (S5) inversion run, uncertainty reduction maps computed as $(1 - \Delta_{\text{post}}/\Delta_{\text{prior}})$ for 2006 and 2018 with different sets of observation stations.

From the two VERIFY results, the S4 run with all stations (Figure 24) shows higher uncertainty reductions in 2018 compared to 2006 because of more measurements available. Most reductions are observed in Central Europe (the Netherlands, Germany and Switzerland). For S5 with core stations (Figure 25) the reductions are smaller, and observed in E Poland, N Italy and Spain.

The differences between the two years shown in the uncertainty maps are mostly due to the assimilated observation network sites. Some sites show weaker or stronger effects on the reduction of uncertainty. For those showing less effect, the main reasons are i) uncertainty assigned to the observations (i.e. how much weight/trust we put on it), ii) differences between prior/observations are large (i.e. 'wrong' magnitude or distribution of prior emissions, or bad transport modeling), and iii) prior emissions around the sites are simply very small, and therefore the inversion does not change fluxes much (i.e. prior flux uncertainty is small). For the sites that have a higher effect on uncertainty reduction, these reasons are important to be included in the inversion.

CTE-CH4 also provided us with GOSAT assimilated fluxes, for 2010-2017. In Figure 26 we present the uncertainty reduction maps between 2010 and 2017. Because the covariance structure is not the same as the latest surface inversion and Europe is optimized on 1x1 grid,

but with long spatial correlation (100 km vs 500 km), it is not possible to examine the effect of the satellite information by comparing to the CTE-CH₄ surface inversions presented here. However, it is interesting to note how satellite data assimilation infers changes on a regional scale. Unlike surface stations, satellite data have more power to constrain northern emissions than central Europe.

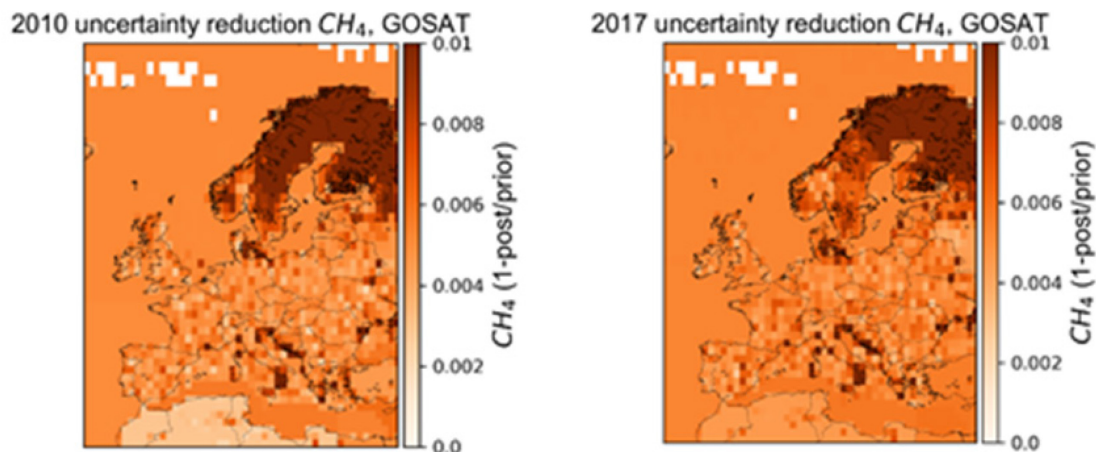


Figure 26: CTE-CH₄ GOSAT inversion run, uncertainty reduction maps computed as $(1 - \Delta_{\text{post}}/\Delta_{\text{prior}})$ for 2010 and 2017.

Because the covariance structure is not the same as the latest surface inversion and Europe is optimized on 1x1 grid, but with long spatial correlation (100 km vs 500 km), it is almost impossible to examine the effect of the satellite information by comparing to the CTE-CH₄ surface inversions presented here. However, it is interesting to note how satellite data assimilation infers changes on a regional scale. Unlike surface stations, satellite data have more power to constrain northern emissions than central Europe.

5.4 Priors

One important reason for differences in simulated results are the priors used by inverse models. We subtracted from total prior/posterior fluxes natural emissions from the VERIFY project to be able to quantify the anthropogenic emissions and compare them with the prior emissions.

Some differences between prior emissions and prior simulated fluxes of the same run (CTE-GOSAT) or differences between runs (GOSAT versus VERIFY) can be explained (Figure 27): versions of some products (e.g., EDGAR) might differ so for example CTE-GOSAT used as anthropogenic prior EDGARv4.3.2FT up to 2017 (defined by the GCP protocol) while CTE-VERIFY core and inclusive runs used priors from simulated CH₄ fluxes from the JSBACH-HIMMELI process-based model which used as anthropogenic fluxes EDGARv6.0.

In Table 7 (Annex) we list the models and their priors (anthropogenic and natural) as used by the top-down inversions. A more in detail analysis and disaggregation of these priors is needed to be able to explain differences between model results (e.g., as those of Figure 18, Figure 19, Figure 20, Figure 21, Figure 22, and Figure 23).

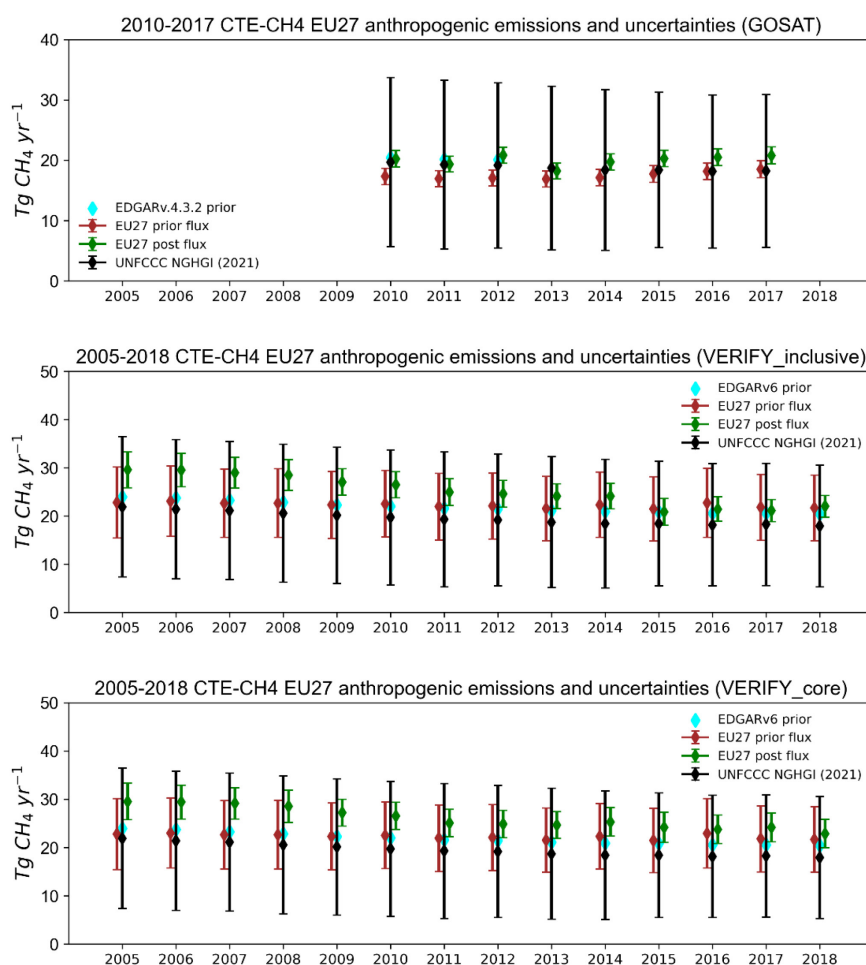


Figure 27: Anthropogenic CH₄ prior and posterior emissions with their uncertainties from CTE-CH₄ - GOSAT, CTE-VERIFY inclusive (S4) and core (S5) runs compared to UNFCCC (2022) inventories and with prior anthropogenic datasets (EDGARv4.3.2 and v6.0)

6 Deviations and counter measures

At the time this report was written, except for CAMS WP6 contribution, we did not receive data/uncertainties from CoCO₂ products. We based most of our analysis on data already processed in the VERIFY project. For the final update of this report (December 2023) we hope to include more CoCO₂ material and more targeted comparisons and analysis.

7 Conclusion

This deliverable presents comparisons of inventory-based and observation-based inventory approaches, building on earlier work in VERIFY (Petrescu et al., 2021a; Petrescu et al., 2021b), and applied here to the largest emitters or countries that can be used to draw out interesting lessons. We highlight the differences and discrepancies between UNFCCC NGHGI, independent inventories, process-based models, and atmospheric inversion estimates. The analysis focused on the fossil CO₂ emissions, net land CO₂ fluxes, and CH₄ total and sectoral anthropogenic emissions.

For fossil CO₂ emissions, figures highlighted the differences between datasets and the importance of harmonising datasets to make more relevant comparisons. We had limited data on CO₂ inversions but showed and discussed inversion results for Europe. The results show a general consistency between inventories and NO₂ based inversions, but without additional analysis of prior and posterior uncertainties it is not possible to assess the consistency

quantitatively. Future work will focus on improved uncertainty analysis, and additionally, expand to cover other key fossil CO₂ emitters.

For net land CO₂ fluxes, a variety of datasets are available to provide country-level estimates: bookkeeping models, process-based models, inversions-based estimates, in addition to inventories. In this version of the report, comparisons were made with inventories in three groups of figures: 1) bookkeeping models, 2) process-based models, 3) inversions. In each case, the issues of system boundaries were discussed. Under some conditions, where key assumptions in different datasets match, it is possible to make meaningful comparisons between datasets. However, in most cases, key assumptions do not align (such as managed land areas, direct versus indirect effects), and this inhibits meaningful comparisons in many cases. In this report, no effort was made to reconcile the bookkeeping models and land surface models comparable with each other, and with UNFCCC inventories. An active area of research is understanding the differences between datasets, to provide sufficient confidence to disseminate more broadly. The inversions also exhibit significant uncertainty, partially reflecting a lack of observations. However, a certain consistency with other studies was found for the larger countries, between some results assimilating surface measurements and others assimilating satellite measurements. The CoCO₂ CAMS inversions now include lateral fluxes and managed land masks, to properly compare with UNFCCC NGHGs.

For CH₄ emissions, we make comparisons with a variety of inventory-based estimates and inversions. CH₄ emissions have increased in the last three decades, but have declined in the USA and EU (regulations) and Russia (dissolution of the Soviet Union). For the inventories, divergences between data sets can generally be attributed to different methodology and tiers used by each of the investigated inventories, when data is available to make comparisons (such as activity data and emission factors). For the inversions, the general magnitudes and trends agree, but uncertainties are too large to be more specific. Uncertainty reduction maps can be used to identify the importance of specific observations, with the location or the time period of observations. The use of a variety of priors across different inversion systems can also inhibit comparability with inventories. For a more robust analysis, more detail is needed on prior and posterior uncertainties, to help identify statistically significant differences between datasets.

8 References

- Andrew, R., 2020. A comparison of estimates of global carbon dioxide emissions from fossil carbon sources. *Earth System Science Data* 12, pp 1437–1465. DOI: 10.5194/essd-12-1437-2020.
- Basu, S., Lehman, S.J., Miller, J.B., Andrews, A.E., Sweeney, C., Gurney, K.R., Xu, X., Southon, J., Tans, P.P., 2020. Estimating US fossil fuel CO₂ emissions from measurements of ¹⁴C in atmospheric CO₂. *Proceedings of the National Academy of Sciences* 117 (24), 13300-13307. DOI: 10.1073/pnas.1919032117.
- Berchet, A., Sollum, E., Thompson, R.L., Pison, I., Thanwerdas, J., Broquet, G., Chevallier, F., Aalto, T., Berchet, A., Bergamaschi, P., Brunner, D., Engelen, R., Fortems-Cheiney, A., Gerbig, C., Groot Zwaftink, C.D., Haussaire, J.M., Henne, S., Houweling, S., Karstens, U., Kutsch, W.L., Lujikx, I.T., Monteil, G., Palmer, P.I., van Peet, J.C.A., Peters, W., Peylin, P., Potier, E., Rödenbeck, C., Saunois, M., Scholze, M., Tsuruta, A., Zhao, Y., 2021. The Community Inversion Framework v1.0: a unified system for atmospheric inversion studies. *Geosci. Model Dev.* 14 (8), 5331-5354. DOI: 10.5194/gmd-14-5331-2021. 1991-9603.
- BP, 2022. bp Statistical Review of World Energy 2022. Available at: <https://www.bp.com/en/global/corporate/energy-economics/statistical-review-of-world-energy.html> (accessed 28 June 2022).
- Britz, W., Witzke, P., 2014. CAPRI model documentation 2014. Available at: <https://www.capri-model.org/dokuwiki/doku.php?id=capri:docs> (accessed 20 December 2022).

- Brunner, D., Arnold, T., Henne, S., Manning, A., Thompson, R.L., Maione, M., O'Doherty, S., Reimann, S., 2017. Comparison of four inverse modelling systems applied to the estimation of HFC-125, HFC-134a, and SF₆ emissions over Europe. *Atmos. Chem. Phys.* 17 (17), 10651-10674. DOI: 10.5194/acp-17-10651-2017. 1680-7324.
- Brunner, D., Henne, S., Keller, C.A., Reimann, S., Vollmer, M.K., O'Doherty, S., Maione, M., 2012. An extended Kalman-filter for regional scale inverse emission estimation. *Atmos. Chem. Phys.* 12 (7), 3455-3478. DOI: 10.5194/acp-12-3455-2012. 1680-7324.
- Chevallier, F., 2021. Fluxes of Carbon Dioxide From Managed Ecosystems Estimated by National Inventories Compared to Atmospheric Inverse Modeling. *Geophysical Research Letters* 48 (15), e2021GL093565. DOI: <https://doi.org/10.1029/2021GL093565>. 0094-8276.
- Chevallier, F., Fisher, M., Peylin, P., Serrar, S., Bousquet, P., Bréon, F.-M., Chédin, A., Ciais, P., 2005. Inferring CO₂ sources and sinks from satellite observations: Method and application to TOVS data. *Journal of Geophysical Research: Atmospheres* 110 (D24). DOI: <https://doi.org/10.1029/2005JD006390>. 0148-0227.
- Crippa, M., Guizzardi, D., Banja, M., Solazzo, E., Muntean, M., Schaaf, E., Pagani, F., Monforti-Ferrario, F., Olivier, J.G.J., Quadrelli, R., Riskez Martin, A., Taghavi-Moharamli, P., Grassi, G., Rossi, S., Oom, D., Branco, A., San-Miguel, J., Vignati, E., 2022. CO₂ emissions of all world countries. Publications Office of the European Union, Luxembourg ISBN 1831-9424. Available at: <https://edgar.jrc.ec.europa.eu/> (accessed 20 September 2022).
- Crippa, M., Guizzardi, D., Solazzo, E., Muntean, M., Schaaf, E., Monforti-Ferrario, F., Banja, M., Olivier, J.G.J., Grassi, G., Rossi, S., Vignati, E., 2021. GHG emissions of all world countries - 2021 Report. Publications Office of the European Union, Luxembourg ISBN 978-92-76-41547-3, EUR 30831 EN, JRC126363. Available at: https://edgar.jrc.ec.europa.eu/report_2021 (accessed 6 January 2022).
- Crippa, M., Oreggioni, G., Guizzardi, D., Muntean, M., Schaaf, E., Lo Vullo, E., Solazzo, E., Monforti-Ferrario, F., Olivier, J.G.J., Vignati, E., 2019. Fossil CO₂ and GHG emissions of all world countries: 2019 report. Publications Office of the European Union, Luxembourg EUR 29849 EN, JRC117610, ISBN 978-92-76-11100-9. Available at: <https://edgar.jrc.ec.europa.eu/overview.php?v=booklet2019> (accessed 14 April 2020).
- Deng, Z., Ciais, P., Tzompa-Sosa, Z.A., Saunois, M., Qiu, C., Tan, C., Sun, T., Ke, P., Cui, Y., Tanaka, K., Lin, X., Thompson, R.L., Tian, H., Yao, Y., Huang, Y., Lauerwald, R., Jain, A.K., Xu, X., Bastos, A., Sitch, S., Palmer, P.I., Lauvaux, T., d'Aspremont, A., Giron, C., Benoit, A., Poulter, B., Chang, J., Petrescu, A.M.R., Davis, S.J., Liu, Z., Grassi, G., Albergel, C., Tubiello, F.N., Perugini, L., Peters, W., Chevallier, F., 2022. Comparing national greenhouse gas budgets reported in UNFCCC inventories against atmospheric inversions. *Earth Syst. Sci. Data* 14 (4), 1639-1675. DOI: 10.5194/essd-14-1639-2022. 1866-3516.
- Denier van der Gon, H.A.C., Dellaert, S.N.C., Visschedijk, A.J.H., Kuenen, J., Super, I., 2020. Second High Resolution emission data 2005-2017. VERIFY project (GA 776810) deliverable D2.2. Available at: <https://verify.lsce.ipsl.fr/index.php/repository/public-deliverables/wp2-verification-methods-for-fossil-co2-emissions/d2-2-second-high-resolution-emission-data-2005-2017> (accessed 1 February 2022).
- EIA, *no date*. International Energy Statistics: Table Notes. Energy Information Administration. Available at: https://www.eia.gov/beta/international/data/browser/views/partial/table_notes.html (accessed 2 August 2019).
- FAOSTAT, 2022. Emissions Totals. Food and Agriculture Organization of the United Nations. Available at: <https://www.fao.org/faostat/en/#data/GT> (accessed 17 November 2022).
- Federici, S., Tubiello, F.N., Salvatore, M., Jacobs, H., Schmidhuber, J., 2015. New estimates of CO₂ forest emissions and removals: 1990–2015. *Forest Ecology and Management* 352, 89-98. DOI: <https://doi.org/10.1016/j.foreco.2015.04.022>. 0378-1127.

- Fortems-Cheiney, A., Broquet, G., 2021a. Final re-analysis of the national scale CO₂ anthropogenic emissions over 2005-2015. LSCE/CEA VERIFY project (GA 776810) deliverable D2.12.
- Fortems-Cheiney, A., Broquet, G., 2021b. Second re-analysis of the national scale CO₂ anthropogenic emissions over 2005-2015. LSCE/CEA VERIFY project (GA 776810) deliverable D2.11. Available at: https://projectsworkspace.eu/sites/VERIFY/Deliverables/WP2/VERIFY_D2.11_Second%20Re-analysis%20of%20the%20national%20scale%20CO2%20anthropogenic%20emissions%20over%202005-2015_v1.pdf (accessed 11 February 2022).
- Fortems-Cheiney, A., Broquet, G., Pison, I., Saunois, M., Potier, E., Berchet, A., Dufour, G., Siour, G., Denier van der Gon, H., Dellaert, S.N.C., Boersma, K.F., 2021. Analysis of the Anthropogenic and Biogenic NO_x Emissions Over 2008–2017: Assessment of the Trends in the 30 Most Populated Urban Areas in Europe. *Geophysical Research Letters* 48 (11), e2020GL092206. DOI: <https://doi.org/10.1029/2020GL092206>.
- Friedlingstein, P., Jones, M.W., O'Sullivan, M., Andrew, R.M., Bakker, D.C.E., Hauck, J., Le Quéré, C., Peters, G.P., Peters, W., Pongratz, J., Sitch, S., Canadell, J.G., Ciais, P., Jackson, R.B., Alin, S.R., Anthoni, P., Bates, N.R., Becker, M., Bellouin, N., Bopp, L., Chau, T.T.T., Chevallier, F., Chini, L.P., Cronin, M., Currie, K.I., Decharme, B., Djutouchouang, L., Dou, X., Evans, W., Feely, R.A., Feng, L., Gasser, T., Gilfillan, D., Gkritzalis, T., Grassi, G., Gregor, L., Gruber, N., Gürses, Ö., Harris, I., Houghton, R.A., Hurtt, G.C., Iida, Y., Ilyina, T., Lujikx, I.T., Jain, A.K., Jones, S.D., Kato, E., Kennedy, D., Klein Goldewijk, K., Knauer, J., Korsbakken, J.I., Körtzinger, A., Landschützer, P., Lauvset, S.K., Lefèvre, N., Lienert, S., Liu, J., Marland, G., McGuire, P.C., Melton, J.R., Munro, D.R., Nabel, J.E.M.S., Nakaoka, S.I., Niwa, Y., Ono, T., Pierrot, D., Poulter, B., Rehder, G., Resplandy, L., Robertson, E., Rödenbeck, C., Rosan, T.M., Schwinger, J., Schwingshackl, C., Séférian, R., Sutton, A.J., Sweeney, C., Tanhua, T., Tans, P.P., Tian, H., Tilbrook, B., Tubiello, F., van der Werf, G., Vuichard, N., Wada, C., Wanninkhof, R., Watson, A., Willis, D., Wiltshire, A.J., Yuan, W., Yue, C., Yue, X., Zaehle, S., Zeng, J., 2022a. Global Carbon Budget 2021. *Earth Syst. Sci. Data*.
- Friedlingstein, P., O'Sullivan, M., Jones, M.W., Andrew, R.M., Gregor, L., Hauck, J., Le Quéré, C., Lujikx, I.T., Olsen, A., Peters, G.P., Peters, W., Pongratz, J., Schwingshackl, C., Sitch, S., Canadell, J.G., Ciais, P., Jackson, R.B., Alin, S.R., Alkama, R., Arneeth, A., Arora, V.K., Bates, N.R., Becker, M., Bellouin, N., Bittig, H.C., Bopp, L., Chevallier, F., Chini, L.P., Cronin, M., Evans, W., Falk, S., Feely, R.A., Gasser, T., Gehlen, M., Gkritzalis, T., Gloege, L., Grassi, G., Gruber, N., Gürses, Ö., Harris, I., Hefner, M., Houghton, R.A., Hurtt, G.C., Iida, Y., Ilyina, T., Jain, A.K., Jersild, A., Kadono, K., Kato, E., Kennedy, D., Klein Goldewijk, K., Knauer, J., Korsbakken, J.I., Landschützer, P., Lefèvre, N., Lindsay, K., Liu, J., Liu, Z., Marland, G., Mayot, N., McGrath, M.J., Metzl, N., Monacci, N.M., Munro, D.R., Nakaoka, S.I., Niwa, Y., O'Brien, K., Ono, T., Palmer, P.I., Pan, N., Pierrot, D., Pockock, K., Poulter, B., Resplandy, L., Robertson, E., Rödenbeck, C., Rodriguez, C., Rosan, T.M., Schwinger, J., Séférian, R., Shutler, J.D., Skjelvan, I., Steinhoff, T., Sun, Q., Sutton, A.J., Sweeney, C., Takao, S., Tanhua, T., Tans, P.P., Tian, X., Tian, H., Tilbrook, B., Tsujino, H., Tubiello, F., van der Werf, G.R., Walker, A.P., Wanninkhof, R., Whitehead, C., Willstrand Wranne, A., Wright, R., Yuan, W., Yue, C., Yue, X., Zaehle, S., Zeng, J., Zheng, B., 2022b. Global Carbon Budget 2022. *Earth System Science Data* 14 (11), 4811-4900. DOI: 10.5194/essd-14-4811-2022. 1866-3516.
- Gasser, T., Crepin, L., Quilcaille, Y., Houghton, R.A., Ciais, P., Obersteiner, M., 2020. Historical CO₂ emissions from land use and land cover change and their uncertainty. *Biogeosciences* 17 (15), 4075-4101. DOI: 10.5194/bg-17-4075-2020. 1726-4189.
- Gilfillan, D., Marland, G., 2021. CDIAC-FF: global and national CO₂ emissions from fossil fuel combustion and cement manufacture: 1751–2017. *Earth Syst. Sci. Data* 13 (4), 1667-1680. DOI: 10.5194/essd-13-1667-2021. 1866-3516.

- Gómez-Sanabria, A., Höglund-Isaksson, L., Rafaj, P., Schöpp, W., 2018. Carbon in global waste and wastewater flows – its potential as energy source under alternative future waste management regimes. *Adv. Geosci.* 45, 105-113. DOI: 10.5194/adgeo-45-105-2018. 1680-7359.
- Grassi, G., Conchedda, G., Federici, S., Abad Viñas, R., Korosuo, A., Melo, J., Rossi, S., Sandker, M., Somogyi, Z., Vizzarri, M., Tubiello, F.N., 2022a. Carbon fluxes from land 2000–2020: bringing clarity to countries' reporting. *Earth Syst. Sci. Data* 14 (10), 4643-4666. DOI: 10.5194/essd-14-4643-2022. 1866-3516.
- Grassi, G., House, J., Kurz, W.A., Cescatti, A., Houghton, R.A., Peters, G.P., Sanz, M.J., Viñas, R.A., Alkama, R., Arneth, A., Bondeau, A., Dentener, F., Fader, M., Federici, S., Friedlingstein, P., Jain, A.K., Kato, E., Koven, C.D., Lee, D., Nabel, J.E.M.S., Nassikas, A.A., Perugini, L., Rossi, S., Sitch, S., Viovy, N., Wiltshire, A., Zaehle, S., 2018. Reconciling global-model estimates and country reporting of anthropogenic forest CO₂ sinks. *Nature Climate Change* 8 (10), 914-920. DOI: 10.1038/s41558-018-0283-x. 1758-6798.
- Grassi, G., Schwingshackl, C., Gasser, T., Houghton, R.A., Sitch, S., Canadell, J.G., Cescatti, A., Ciais, P., Federici, S., Friedlingstein, P., Kurz, W.A., Sanz Sanchez, M.J., Abad Viñas, R., Alkama, R., Ceccherini, G., Kato, E., Kennedy, D., Knauer, J., Korosuo, A., McGrath, M.J., Nabel, J., Poulter, B., Rossi, S., Walker, A.P., Yuan, W., Yue, X., Pongratz, J., 2022b. Mapping land-use fluxes for 2001-2020 from global models to national inventories. *Earth Syst. Sci. Data Discuss.* 2022, 1-42. DOI: 10.5194/essd-2022-245. 1866-3591.
- Grassi, G., Stehfest, E., Rogelj, J., van Vuuren, D., Cescatti, A., House, J., Nabuurs, G.-J., Rossi, S., Alkama, R., Viñas, R.A., Calvin, K., Ceccherini, G., Federici, S., Fujimori, S., Gusti, M., Hasegawa, T., Havlik, P., Humpenöder, F., Korosuo, A., Perugini, L., Tubiello, F.N., Popp, A., 2021. Critical adjustment of land mitigation pathways for assessing countries' climate progress. *Nature Climate Change* 11 (5), 425-434. DOI: 10.1038/s41558-021-01033-6. 1758-6798.
- Gütschow, J., Pflüger, M., 2022. The PRIMAP-hist national historical emissions time series (1750-2021) v2.4 [Data set], Zenodo. Available at: <https://zenodo.org/record/7179775> (accessed 17 October 2022).
- Hansis, E., Davis, S.J., Pongratz, J., 2015. Relevance of methodological choices for accounting of land use change carbon fluxes. *Global Biogeochemical Cycles*, 2014GB004997. DOI: 10.1002/2014GB004997. 1944-9224.
- Höglund-Isaksson, L., 2012. Global anthropogenic methane emissions 2005–2030: technical mitigation potentials and costs. *Atmos. Chem. Phys.* 12 (19), 9079-9096. DOI: 10.5194/acp-12-9079-2012. 1680-7324.
- Höglund-Isaksson, L., 2017. Bottom-up simulations of methane and ethane emissions from global oil and gas systems 1980 to 2012. *Environmental Research Letters* 12 (2), 024007. DOI: 10.1088/1748-9326/aa583e. 1748-9326.
- Höglund-Isaksson, L., Gómez-Sanabria, A., Klimont, Z., Rafaj, P., Schöpp, W., 2020. Technical potentials and costs for reducing global anthropogenic methane emissions in the 2050 timeframe –results from the GAINS model. *Environmental Research Communications* 2 (2), 025004. DOI: 10.1088/2515-7620/ab7457. 2515-7620.
- Houghton, R.A., Nassikas, A.A., 2017. Global and regional fluxes of carbon from land use and land cover change 1850–2015. *Global Biogeochemical Cycles* 31 (3), 456-472. DOI: <https://doi.org/10.1002/2016GB005546>. 0886-6236.
- IEA, 2022. Greenhouse Gas Emissions from Energy. Available at: <https://www.iea.org/data-and-statistics/data-product/greenhouse-gas-emissions-from-energy>.
- IPCC, 2006. 2006 IPCC Guidelines for National Greenhouse Gas Inventories, Prepared by the National Greenhouse Gas Inventories Programme, Eggleston H.S., Buendia L., Miwa K., Ngara T. and Tanabe K. (eds). IGES, Japan. Available at: <https://www.ipcc-nggip.iges.or.jp/public/2006gl/> (accessed 8 April 2019).
- Janssens-Maenhout, G., Crippa, M., Guizzardi, D., Muntean, M., Schaaf, E., Dentener, F., Bergamaschi, P., Pagliari, V., Olivier, J., Peters, J., van Aardenne, J., Monni, S.,

- Doering, U., Petrescu, R., Solazzo, E., Oreggioni, G., 2019. EDGAR v4.3.2 Global Atlas of the three major Greenhouse Gas Emissions for the period 1970-2012. *Earth System Science Data* 2019, 959-1002. DOI: 10.5194/essd-11-959-2019.
- Janssens-Maenhout, G., Petrescu, A.M.R., Solazzo, E., Peylin, P., Ciais, P., Qiu, C., McGrath, M., Andrew, R., Peters, G., 2021. Report (fact sheet) on the observation-based GHG budgets and inventory to USA. Available at: [https://projectsworkspace.eu/sites/VERIFY/Deliverables/WP6/VERIFY_D6.3_Report_%20\(fact%20sheet\)%20on%20the%20observation-based%20GHG%20budgets%20and%20inventory%20to%20USA_v2.pdf](https://projectsworkspace.eu/sites/VERIFY/Deliverables/WP6/VERIFY_D6.3_Report_%20(fact%20sheet)%20on%20the%20observation-based%20GHG%20budgets%20and%20inventory%20to%20USA_v2.pdf) (accessed 4 February 2022).
- Konovalov, I.B., Lvova, D.A., 2018. Estimation of CO₂ emissions from fossil fuel burning in Europe. Federal Research Center Institute of Applied Physics of the Russian Academy of Sciences, Nizhny Novgorod Russia.
- Maksyutov, S., Brunner, D., Manning, A., Fraser, P., Tarasova, O., Volosciuk, C., 2019. From Atmospheric Observations and Analysis of Greenhouse Gases to Emission Estimates: a Scientific Adventure. *WMO Bulletin* 68 (2).
- Menut, L., Bessagnet, B., Khvorostyanov, D., Beekmann, M., Blond, N., Colette, A., Coll, I., Curci, G., Foret, G., Hodzic, A., Mailler, S., Meleux, F., Monge, J.L., Pison, I., Siour, G., Turquety, S., Valari, M., Vautard, R., Vivanco, M.G., 2013. CHIMERE 2013: a model for regional atmospheric composition modelling. *Geosci. Model Dev.* 6 (4), 981-1028. DOI: 10.5194/gmd-6-981-2013. 1991-9603.
- Minx, J.C., Lamb, W.F., Andrew, R.M., Canadell, J.G., Crippa, M., Döbbeling, N., Forster, P.M., Guizzardi, D., Olivier, J., Peters, G.P., Pongratz, J., Reisinger, A., Rigby, M., Saunio, M., Smith, S.J., Solazzo, E., Tian, H., 2021. A comprehensive dataset for global, regional and national greenhouse gas emissions by sector 1970-2019. *Earth Systems Science Data* 13, 5213–5252.
- O'Rourke, P.R., Smith, S.J., Mott, A., Ahsan, H., McDuffie, E.E., Crippa, M., Klimont, Z., McDonald, B., Wang, S., Nicholson, M.B., Feng, L., Hoesly, R.M., 2021. CEDS v_2021_04_21 Release Emission Data (v_2021_02_05) [Data set], Zenodo. Available at: <https://doi.org/10.5281/zenodo.4741285> (accessed 10 May 2021).
- Petrescu, A.M.R., McGrath, M.J., Andrew, R.M., Peylin, P., Petres, G.P., Ciais, P., Broquet, G., Tubiello, F.N., Gerbig, C., Pongratz, J., Janssens-Maenhout, G., Grassi, G., Nabuurs, G.-J., Regnier, P., Lauerwald, R., Kuhnert, M., Balcovič, J., Schelhaas, M.-J., Denier van der Gon, H.A.C., Solazzo, E., Qiu, C., Pilli, R., Konovalov, I.B., Houghton, R., Günther, D., Perugini, L., Crippa, M., Ganzenmüller, R., Luijkx, I., Smith, P., Munassar, S., Thompson, R.L., Conchedda, G., Monteil, G., Scholze, M., Karstens, U., Brokmann, P., Dolman, H., 2021a. The consolidated European synthesis of CO₂ emissions and removals for EU27 and UK: 1990-2018. *Earth System Science Data* 13, 2363–2406. DOI: 10.5194/essd-13-2363-2021.
- Petrescu, A.M.R., Peters, G.P., Janssens-Maenhout, G., Ciais, P., Tubiello, F.N., Grassi, G., Nabuurs, G.J., Leip, A., Carmona-Garcia, G., Winiwarter, W., Höglund-Isaksson, L., Günther, D., Solazzo, E., Kiesow, A., Bastos, A., Pongratz, J., Nabel, J.E.M.S., Conchedda, G., Pilli, R., Andrew, R.M., Schelhaas, M.J., Dolman, H., 2020. European anthropogenic AFOLU emissions and their uncertainties: a review and benchmark data. *Earth Syst. Sci. Data* 12, 961-1001. DOI: 10.5194/essd-12-961-2020.
- Petrescu, A.M.R., Qiu, C., Ciais, P., Thompson, R.L., Peylin, P., McGrath, M.J., Solazzo, E., Janssens-Maenhout, G., Tubiello, F.N., Bergamaschi, P., Brunner, D., Peters, G.P., Höglund-Isaksson, L., Regnier, P., Lauerwald, R., Bastviken, D., Tsuruta, A., Winiwarter, W., Patra, P.K., Kuhnert, M., Oreggioni, G.D., Crippa, M., Saunio, M., Perugini, L., Markkanen, T., Aalto, T., Groot Zwaafink, C.D., Tian, H., Yao, Y., Wilson, C., Conchedda, G., Günther, D., Leip, A., Smith, P., Haussaire, J.M., Leppänen, A., Manning, A.J., McNorton, J., Brockmann, P., Dolman, A.J., 2021b. The consolidated European synthesis of CH₄ and N₂O emissions for the European Union and United Kingdom: 1990–2017. *Earth Syst. Sci. Data* 13 (5), 2307-2362. DOI: 10.5194/essd-13-2307-2021. 1866-3516.

- Petrescu, A.M.R., Qiu, C., McGrath, M.J., Peylin, P., Peters, G.P., Ciais, P., Thompson, R.L., Tsuruta, A., Brunner, D., Kuhnert, M., Matthews, B., Palmer, P.I., Tarasova, O., Regnier, P., Lauerwald, R., Bastviken, D., Höglund-Isaksson, L., Winiwarer, W., Etiope, G., Aalto, T., Balsamo, G., Bastrikov, V., Berchet, A., Brockmann, P., Ciotoli, G., Conchedda, G., Crippa, M., Dentener, F., Groot Zwaaftink, C.D., Guizzardi, D., Günther, D., Haussaire, J.M., Houweling, S., Janssens-Maenhout, G., Kouyate, M., Leip, A., Leppänen, A., Lugato, E., Maisonnier, M., Manning, A.J., Markkanen, T., McNorton, J., Muntean, M., Oreggioni, G.D., Patra, P.K., Perugini, L., Pison, I., Raivonen, M.T., Saunio, M., Segers, A.J., Smith, P., Solazzo, E., Tian, H., Tubiello, F.N., Vesala, T., Wilson, C., Zaehle, S., 2022. The consolidated European synthesis of CH₄ and N₂O emissions for EU27 and UK: 1990-2020. *Earth Syst. Sci. Data Discuss.* 2022, 1-97. DOI: 10.5194/essd-2022-287. 1866-3591.
- Pinty, B., Ciais, P., Dee, D., Dolman, H., Dowell, M., Engelen, R., Holmlund, K., Janssens-Maenhout, G., Meijer, Y., Palmer, P., Scholze, M., Gon, H.D.v.d., Heimann, M., Juvyns, O., Kentarchos, A., Zunker, H., 2019. An Operational Anthropogenic CO₂ Emissions Monitoring & Verification Support Capacity – Needs and high level requirements for in situ measurements. European Commission Joint Research Centre EUR 29817 EN. Available at: <https://ec.europa.eu/jrc/en/science-update/measuring-man-made-carbon-dioxide-co-emissions-support-paris-agreement> (accessed 29 January 2021).
- Rodgers, C.D., 2000. *Inverse Methods for Atmospheric Sounding: Theory and Practice*. World Scientific, ISBN: ISBN 981-02-2740-X. Available at: https://library.wmo.int/doc_num.php?explnum_id=1654.
- Saunio, M., Stavert, A.R., Poulter, B., Bousquet, P., Canadell, J.G., Jackson, R.B., Raymond, P.A., Dlugokencky, E.J., Houweling, S., Patra, P.K., Ciais, P., Arora, V.K., Bastviken, D., Bergamaschi, P., Blake, D.R., Brailsford, G., Bruhwiler, L., Carlson, K.M., Carrol, M., Castaldi, S., Chandra, N., Crevoisier, C., Crill, P.M., Covey, K., Curry, C.L., Etiope, G., Frankenberg, C., Gedney, N., Hegglin, M.I., Höglund-Isaksson, L., Hugelius, G., Ishizawa, M., Ito, A., Janssens-Maenhout, G., Jensen, K.M., Joos, F., Kleinen, T., Krummel, P.B., Langenfelds, R.L., Laruelle, G.G., Liu, L., Machida, T., Maksyutov, S., McDonald, K.C., McNorton, J., Miller, P.A., Melton, J.R., Morino, I., Müller, J., Murguía-Flores, F., Naik, V., Niwa, Y., Noce, S., O'Doherty, S., Parker, R.J., Peng, C., Peng, S., Peters, G.P., Prigent, C., Prinn, R., Ramonet, M., Regnier, P., Riley, W.J., Rosentretter, J.A., Segers, A., Simpson, I.J., Shi, H., Smith, S.J., Steele, L.P., Thornton, B.F., Tian, H., Tohjima, Y., Tubiello, F.N., Tsuruta, A., Viovy, N., Voulgarakis, A., Weber, T.S., van Weele, M., van der Werf, G.R., Weiss, R.F., Worthy, D., Wunch, D., Yin, Y., Yoshida, Y., Zhang, W., Zhang, Z., Zhao, Y., Zheng, B., Zhu, Q., Zhu, Q., Zhuang, Q., 2020. The Global Methane Budget 2000–2017. *Earth System Science Data* 12 (3), 1561-1623. DOI: 10.5194/essd-12-1561-2020.
- Schneising, O., Buchwitz, M., Reuter, M., Vanselow, S., Bovensmann, H., Burrows, J.P., 2020. Remote sensing of methane leakage from natural gas and petroleum systems revisited. *Atmos. Chem. Phys.* 20 (15), 9169-9182. DOI: 10.5194/acp-20-9169-2020. 1680-7324.
- Shen, L., Gautam, R., Omara, M., Zavala-Araiza, D., Maasackers, J.D., Scarpelli, T.R., Lorente, A., Lyon, D., Sheng, J., Varon, D.J., Nesser, H., Qu, Z., Lu, X., Sulprizio, M.P., Hamburg, S.P., Jacob, D.J., 2022. Satellite quantification of oil and natural gas methane emissions in the US and Canada including contributions from individual basins. *Atmos. Chem. Phys.* 22 (17), 11203-11215. DOI: 10.5194/acp-22-11203-2022. 1680-7324.
- Solazzo, E., Crippa, M., Guizzardi, D., Muntean, M., Choulga, M., Janssens-Maenhout, G., 2021. Uncertainties in the Emissions Database for Global Atmospheric Research (EDGAR) emission inventory of greenhouse gases. *Atmos. Chem. Phys.* 21 (7), 5655-5683. DOI: 10.5194/acp-21-5655-2021. 1680-7324.
- Thompson, R.L., Chevallier, F., Maksyutov, S., Patra, P.K., Bowman, K., 2022. Chapter 4 - Top-down approaches, in: Poulter, B., Canadell, J.G., Hayes, D.J., Thompson, R.L.

- (Eds.), *Balancing Greenhouse Gas Budgets*. Elsevier, ISBN: 978-0-12-814952-2, pp. 87-155. Available at: <https://www.sciencedirect.com/science/article/pii/B9780128149522000083>.
- Tsuruta, A., Aalto, T., Backman, L., Hakkarainen, J., van der Laan-Luijkx, I.T., Krol, M.C., Spahni, R., Houweling, S., Laine, M., Dlugokencky, E., Gomez-Pelaez, A.J., van der Schoot, M., Langenfelds, R., Ellul, R., Arduini, J., Apadula, F., Gerbig, C., Feist, D.G., Kivi, R., Yoshida, Y., Peters, W., 2017. Global methane emission estimates for 2000–2012 from CarbonTracker Europe-CH₄ v1.0. *Geosci. Model Dev.* 10 (3), 1261-1289. DOI: 10.5194/gmd-10-1261-2017. 1991-9603.
- Tubiello, F.N., 2019. Greenhouse Gas Emissions Due to Agriculture, in: Ferranti, P., Berry, E.M., Anderson, J.R. (Eds.), *Encyclopedia of Food Security and Sustainability*. Elsevier, Oxford, ISBN: 978-0-12-812688-2, pp. 196-205. Available at: <https://www.sciencedirect.com/science/article/pii/B9780081005965219963>.
- Tubiello, F.N., Conchedda, G., Wannier, N., Federici, S., Rossi, S., Grassi, G., 2021. Carbon emissions and removals from forests: new estimates, 1990–2020. *Earth Syst. Sci. Data* 13 (4), 1681-1691. DOI: 10.5194/essd-13-1681-2021. 1866-3516.
- UNFCCC, 2022. National Inventory Submissions 2022. United Nations Framework Convention on Climate Change. Available at: <https://unfccc.int/ghg-inventories-annex-i-parties/2022> (accessed 14 June 2022).
- UNFCCC, n.d.-a. Biennial Update Report submissions from Non-Annex I Parties. Available at: <https://unfccc.int/BURs> (accessed 4 February 2022).
- UNFCCC, n.d.-b. National Communication submissions from Non-Annex I Parties. Available at: <https://unfccc.int/non-annex-I-NCs> (accessed 4 February 2022).
- Weber, T., Wiseman, N.A., Kock, A., 2019. Global ocean methane emissions dominated by shallow coastal waters. *Nature Communications* 10 (1), 4584. DOI: 10.1038/s41467-019-12541-7.
- Weiss, F., Leip, A., 2012. Greenhouse gas emissions from the EU livestock sector: A life cycle assessment carried out with the CAPRI model. *Agriculture, Ecosystems & Environment* 149, 124-134. DOI: <https://doi.org/10.1016/j.agee.2011.12.015>. 0167-8809.
- Weller, Z.D., Hamburg, S.P., von Fischer, J.C., 2020. A National Estimate of Methane Leakage from Pipeline Mains in Natural Gas Local Distribution Systems. *Environmental Science & Technology* 54 (14), 8958-8967. DOI: 10.1021/acs.est.0c00437. 0013-936X.
- Zhang, Y., Gautam, R., Pandey, S., Omara, M., Maasackers, J.D., Sadavarte, P., Lyon, D., Nesser, H., Sulprizio, M.P., Varon, D.J., Zhang, R., Houweling, S., Zavala-Araiza, D., Alvarez, R.A., Lorente, A., Hamburg, S.P., Aben, I., Jacob, D.J., 2020. Quantifying methane emissions from the largest oil-producing basin in the United States from space. *Science Advances* 6 (17), eaaz5120. DOI: doi:10.1126/sciadv.aaz5120.

Document History

Version	Author(s)	Date	Changes
V1	VU Amsterdam, CICERO, LSCE	04/02/2022	
V2	VU Amsterdam, CICERO, LSCE	23/12/2022	Includes reviewer comments in track changes
V3	VU Amsterdam, CICERO, LSCE		Included review comments

Internal Review History

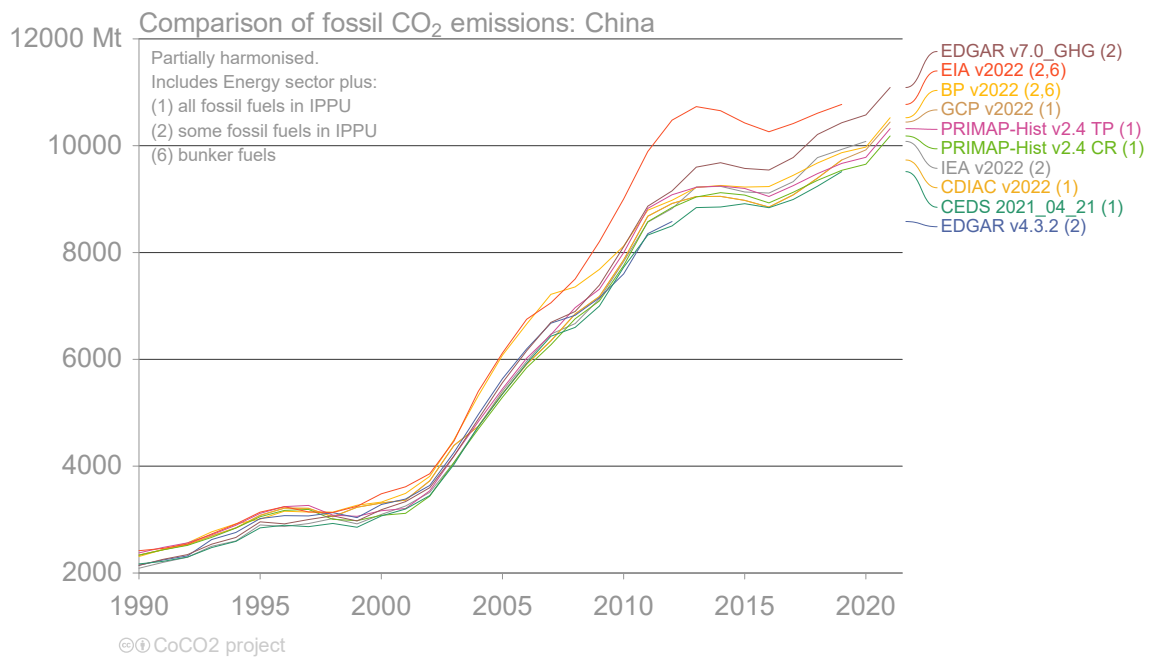
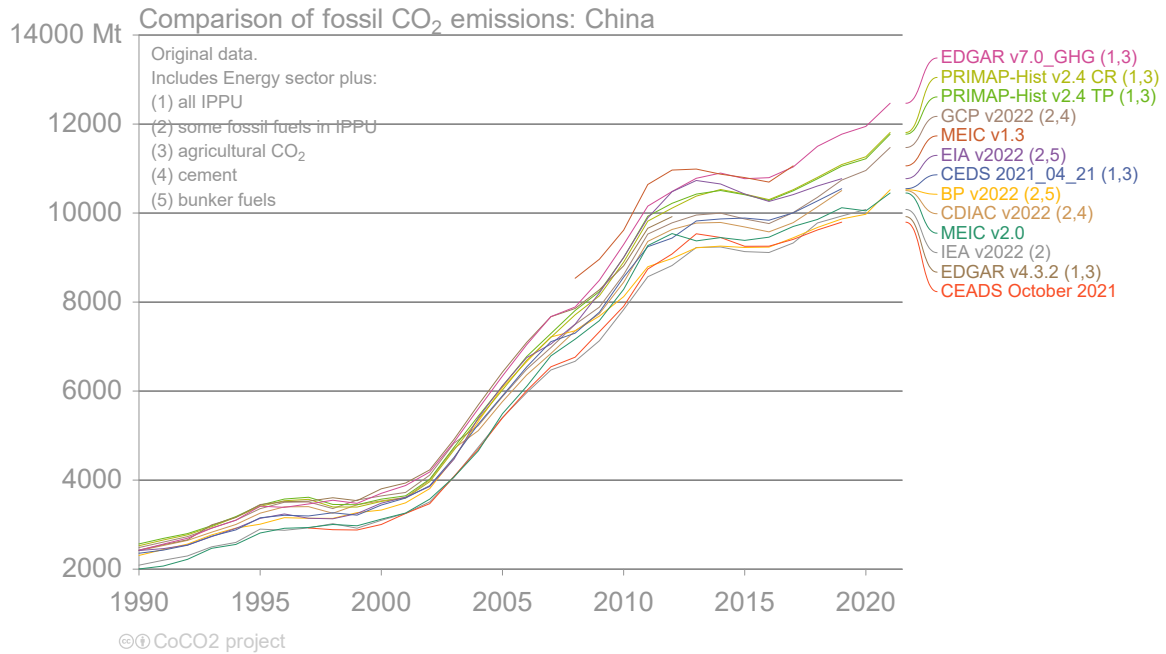
Internal Reviewers	Date	Comments
Claire Granier (LAERO)	30/01/2023	All comments addressed in the final version
Andrea Kaiser-Weiss (DWD)	30/01/2023	All comments addressed in the final version

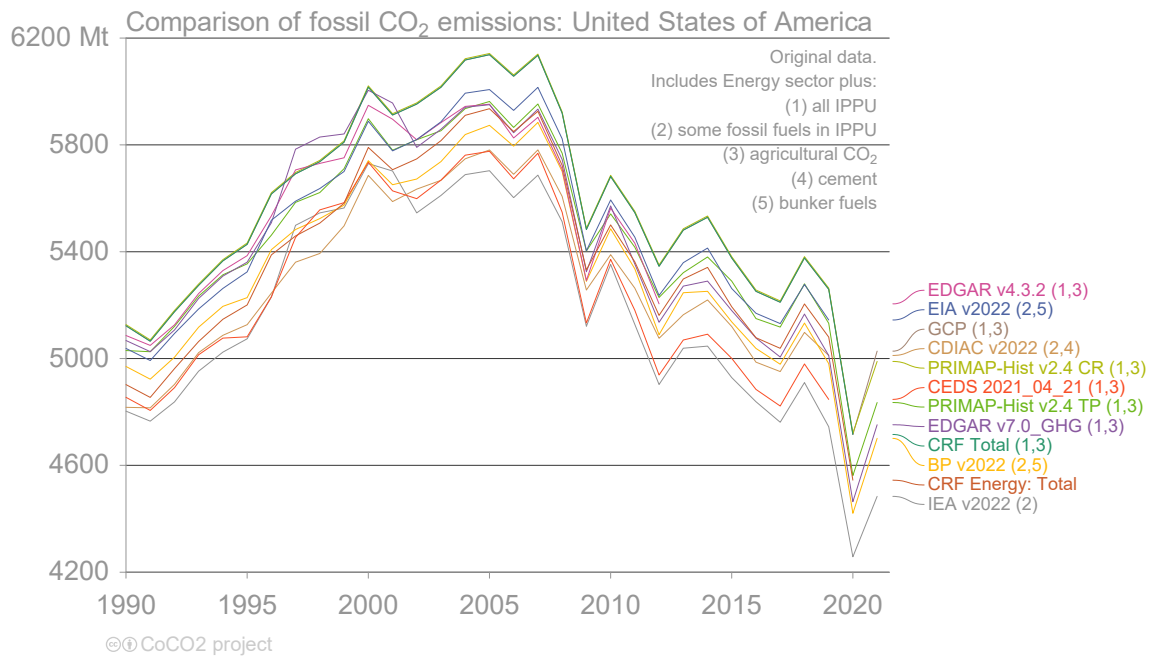
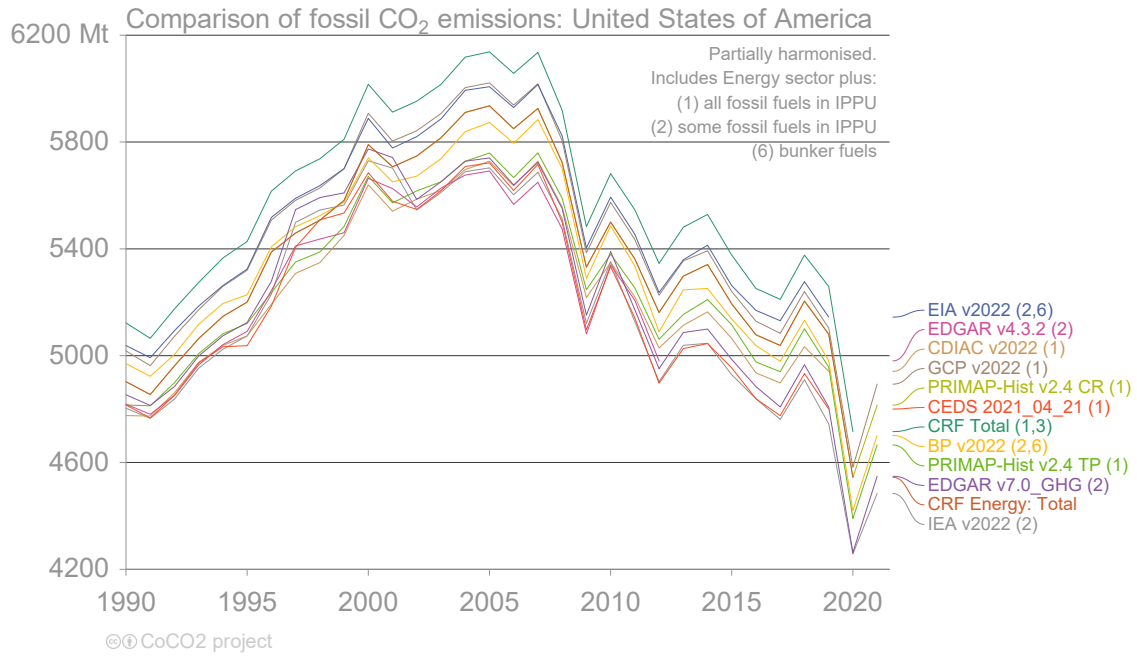
Estimated Effort Contribution per Partner

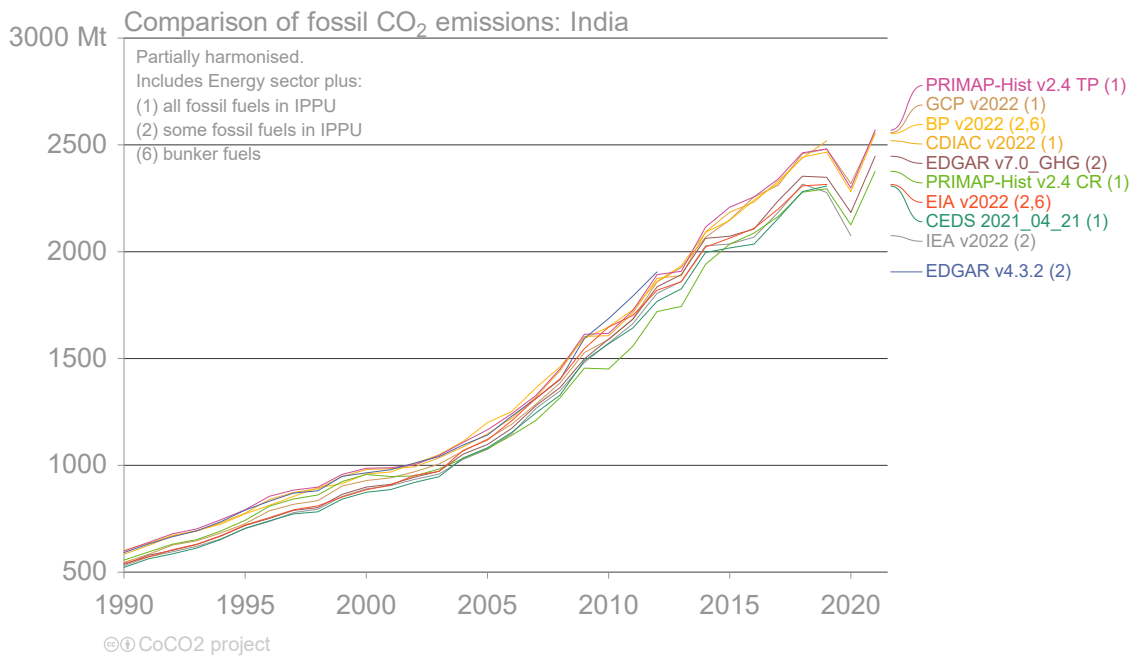
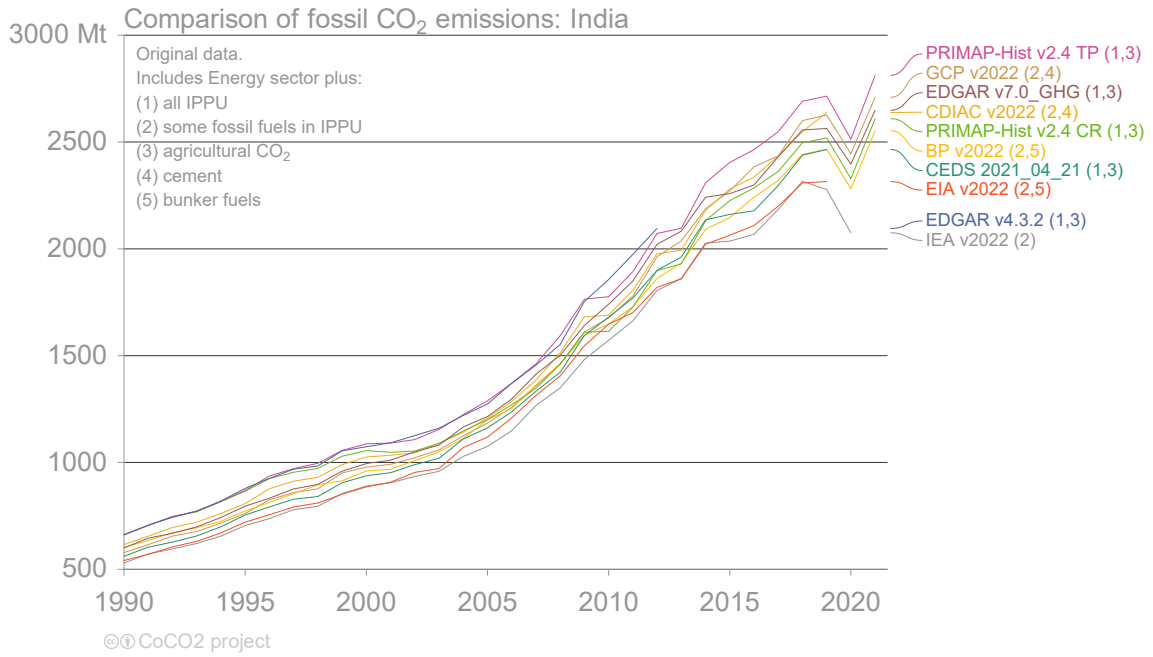
Partner	Effort
VU Amsterdam	2
CICERO	2
LSCE	2
Total	6

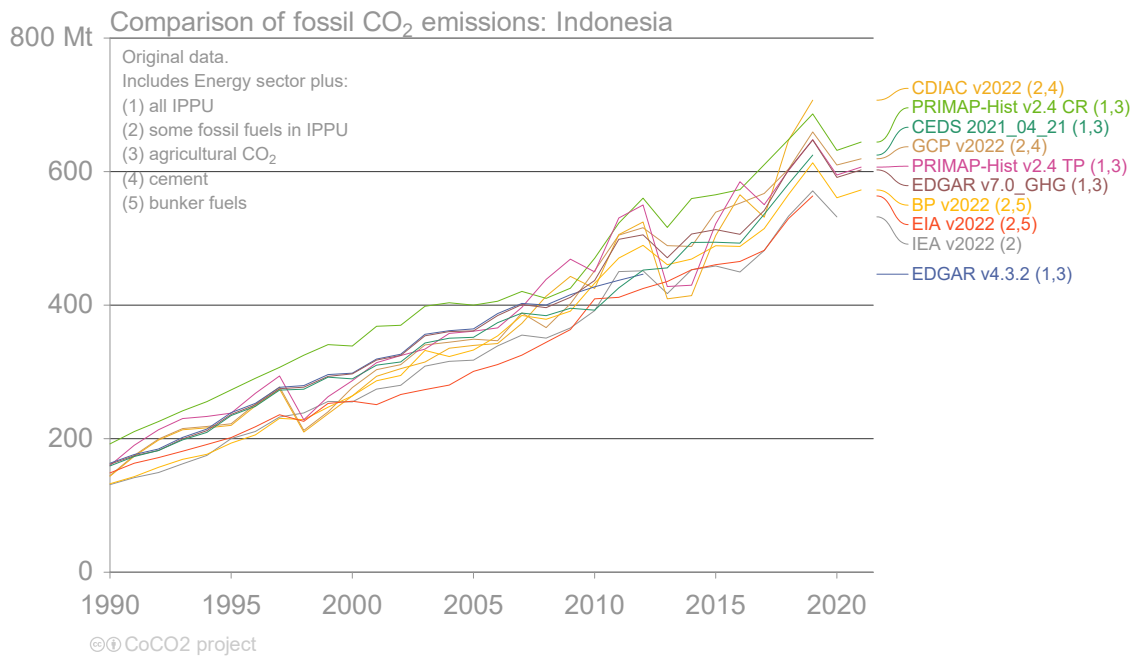
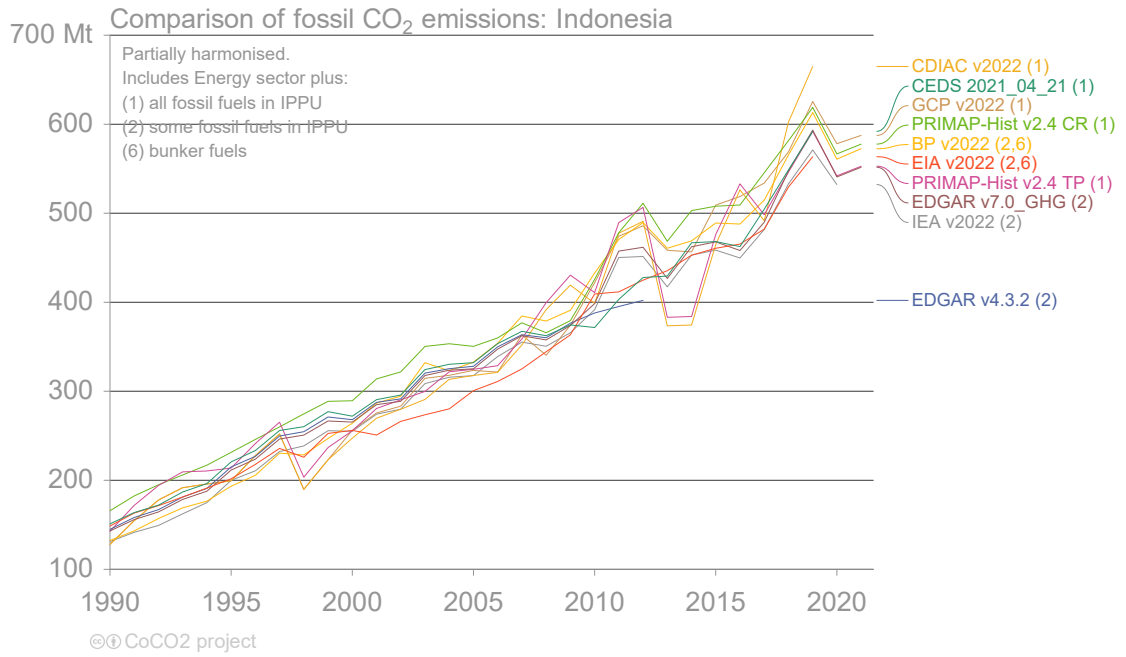
9 Annex 1: Fossil CO₂ figures

This Annex presents additional figures comparing fossil CO₂ estimates from inventory sources for the top-ten emitters globally.

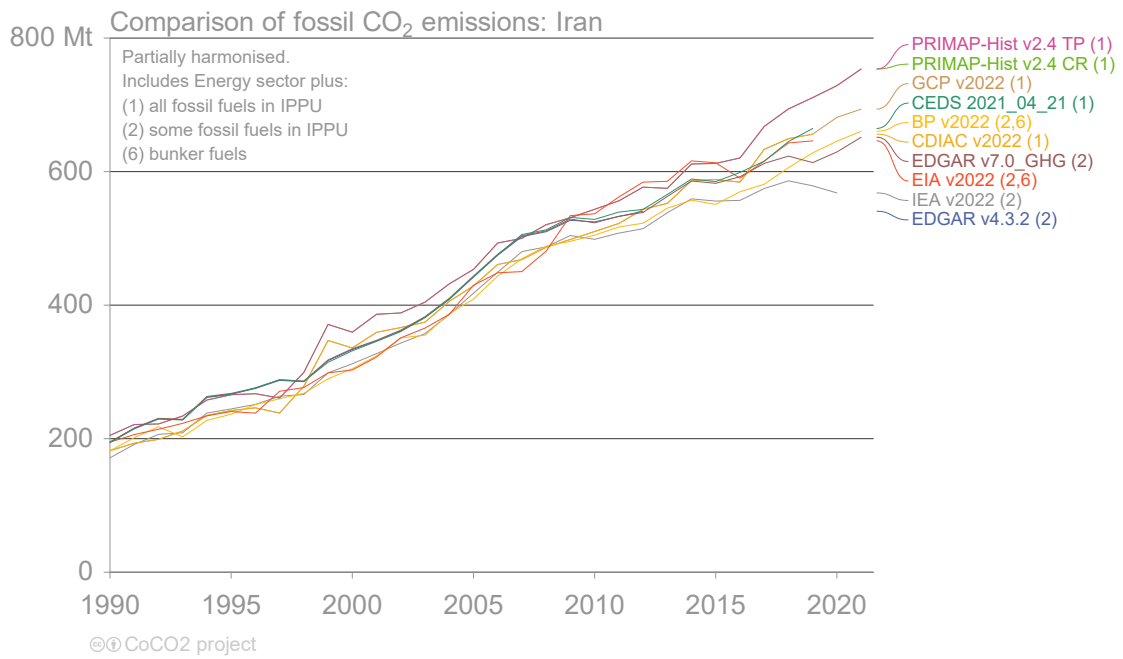
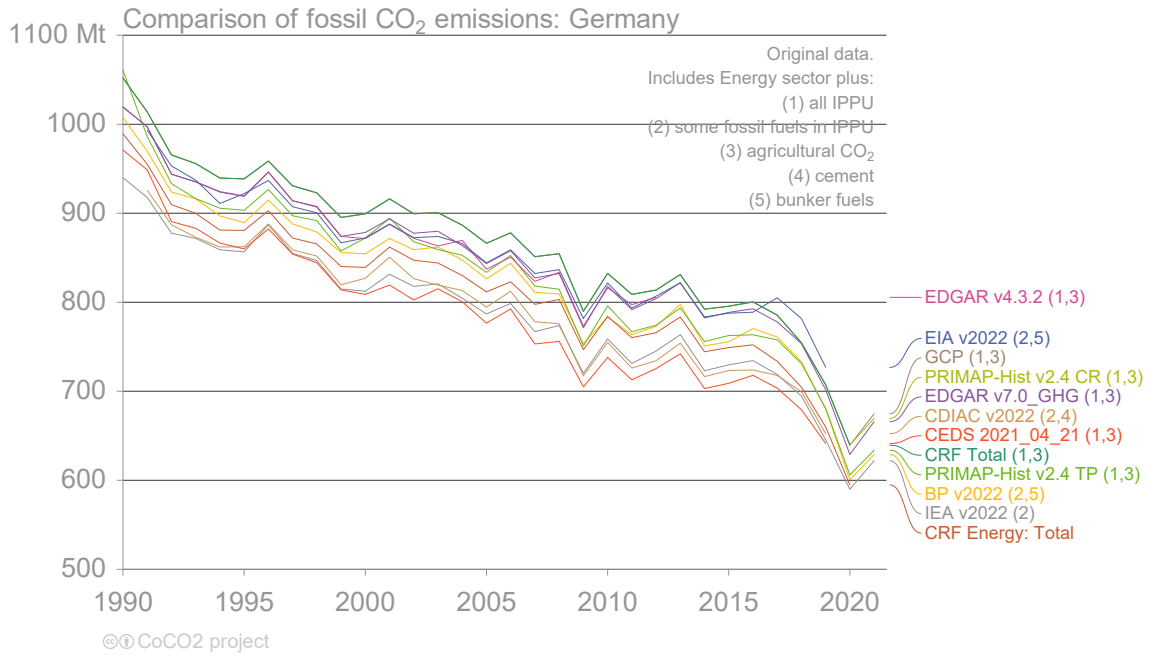


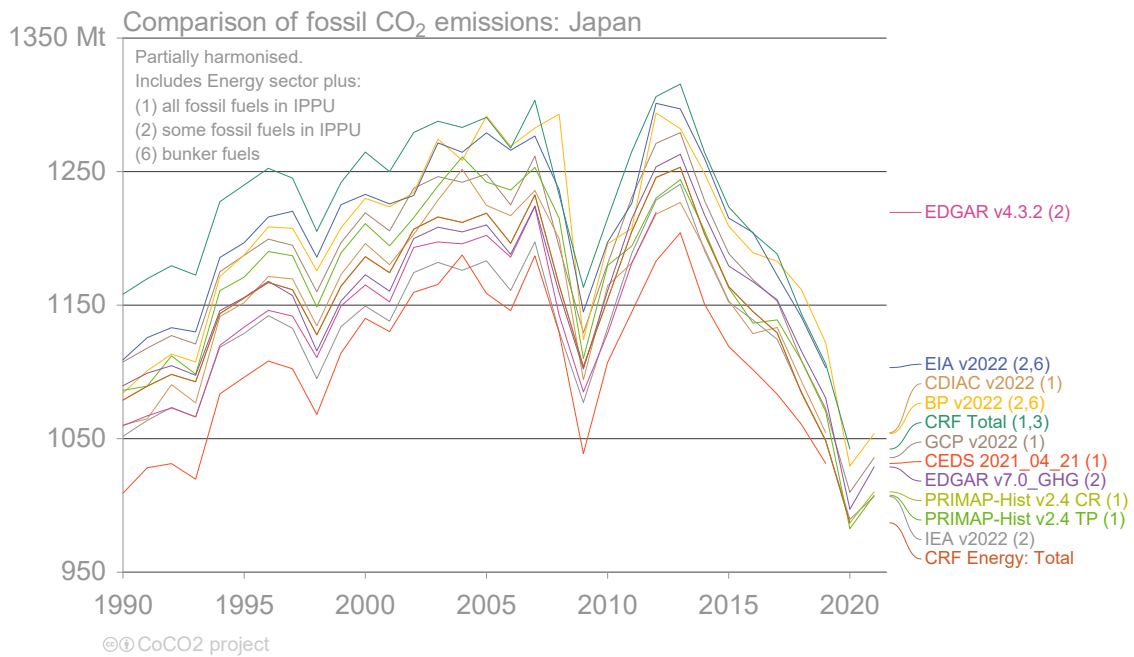
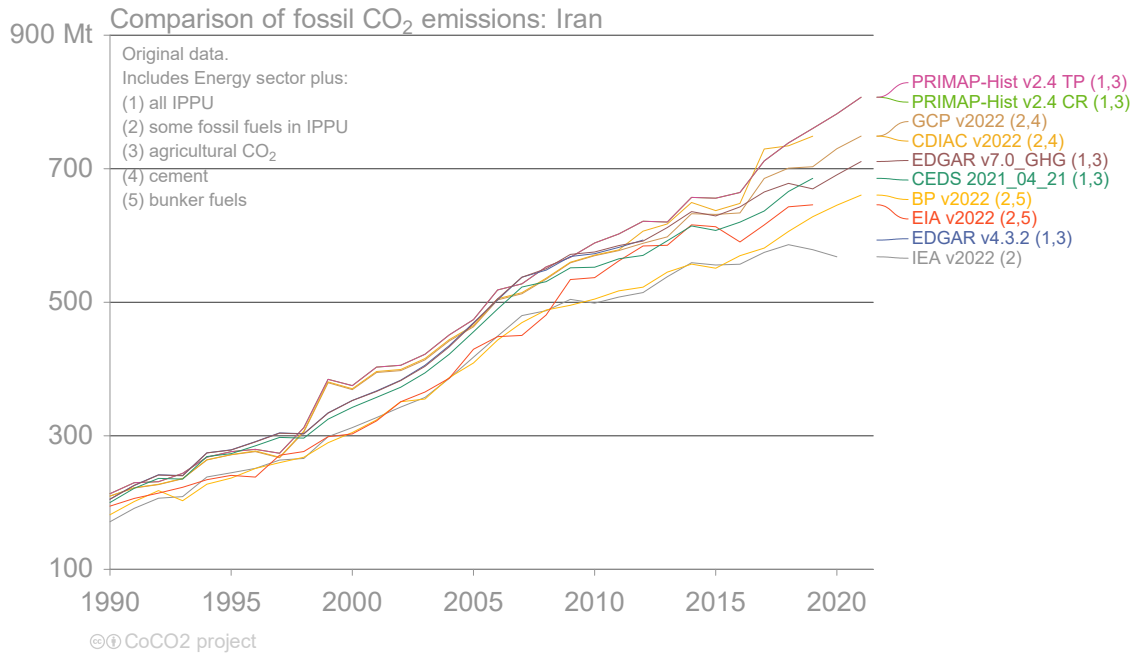


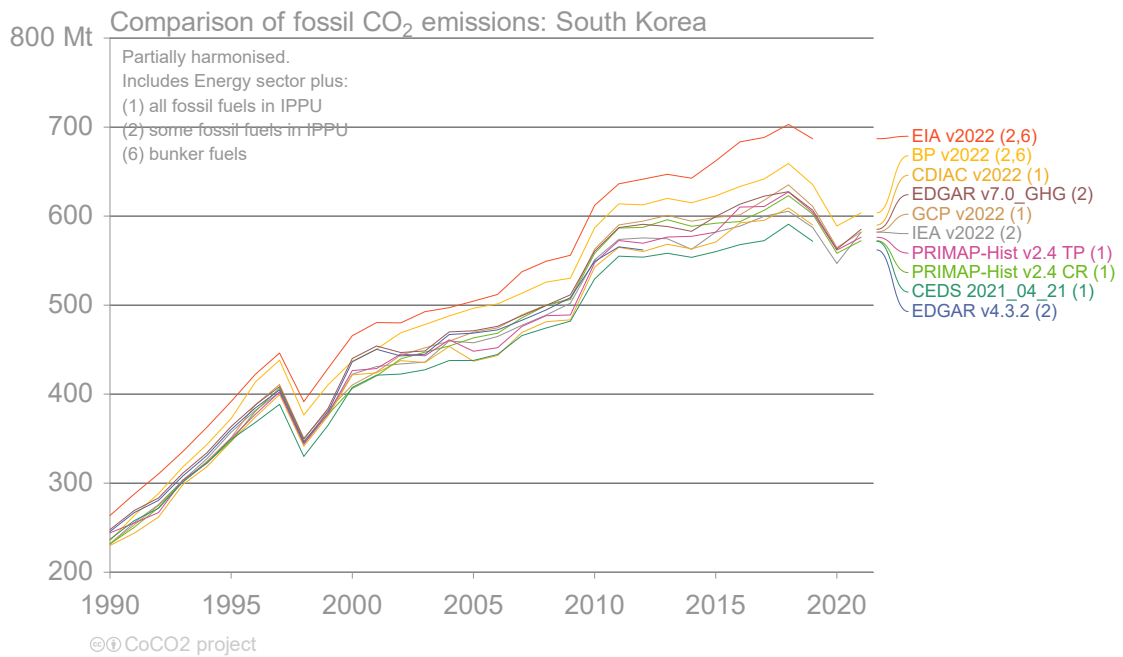
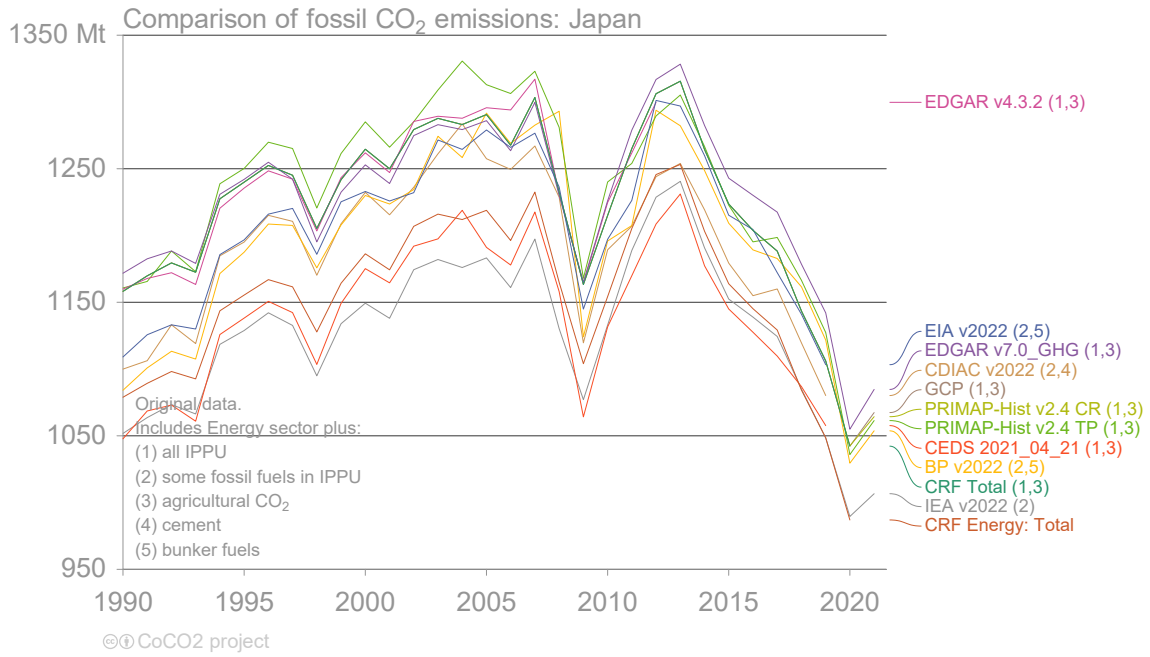


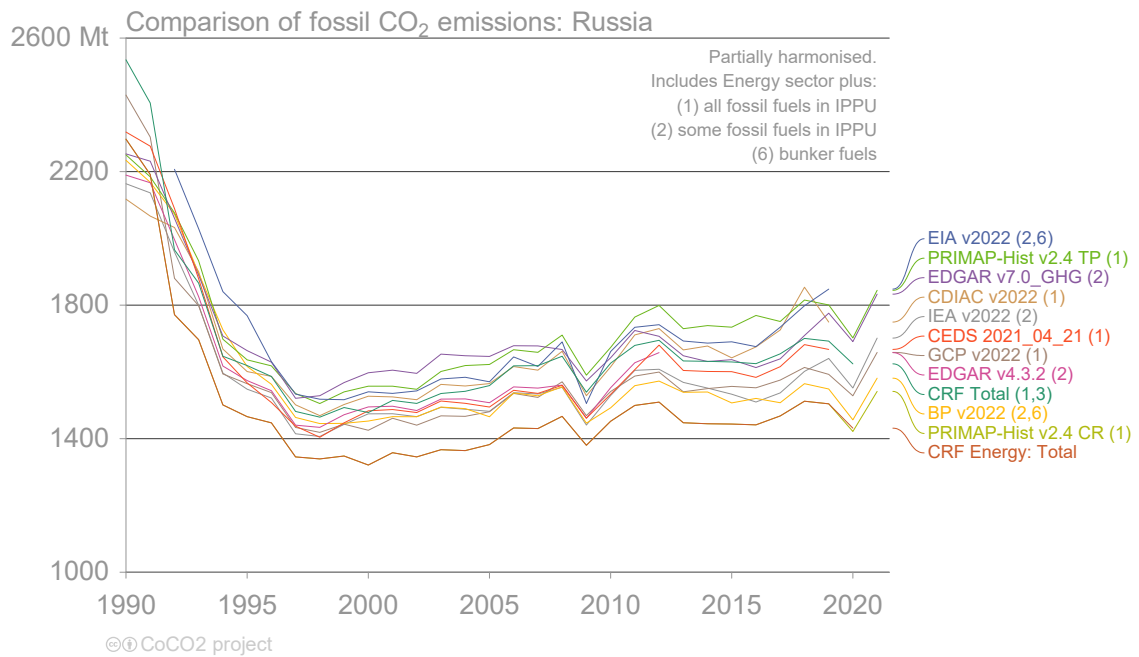
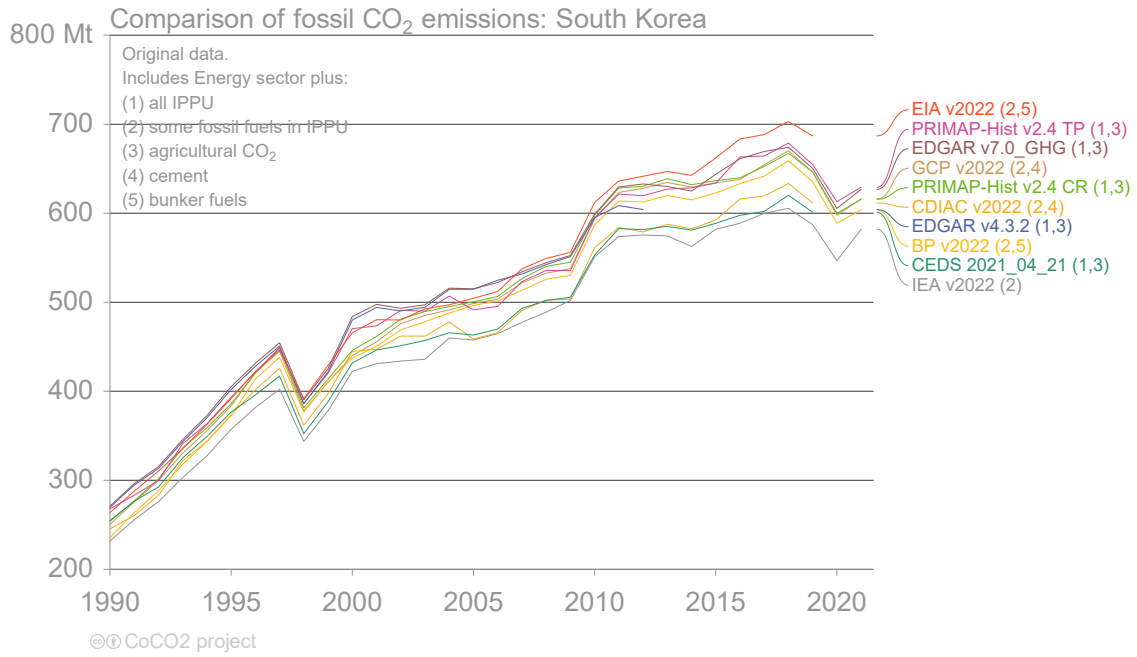


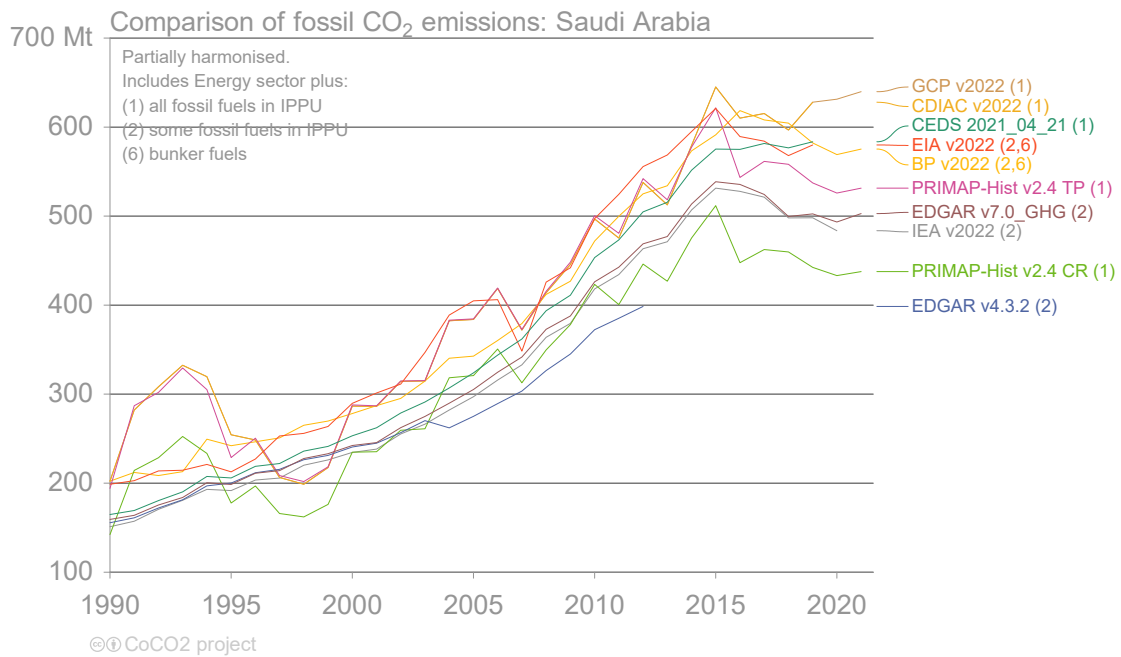
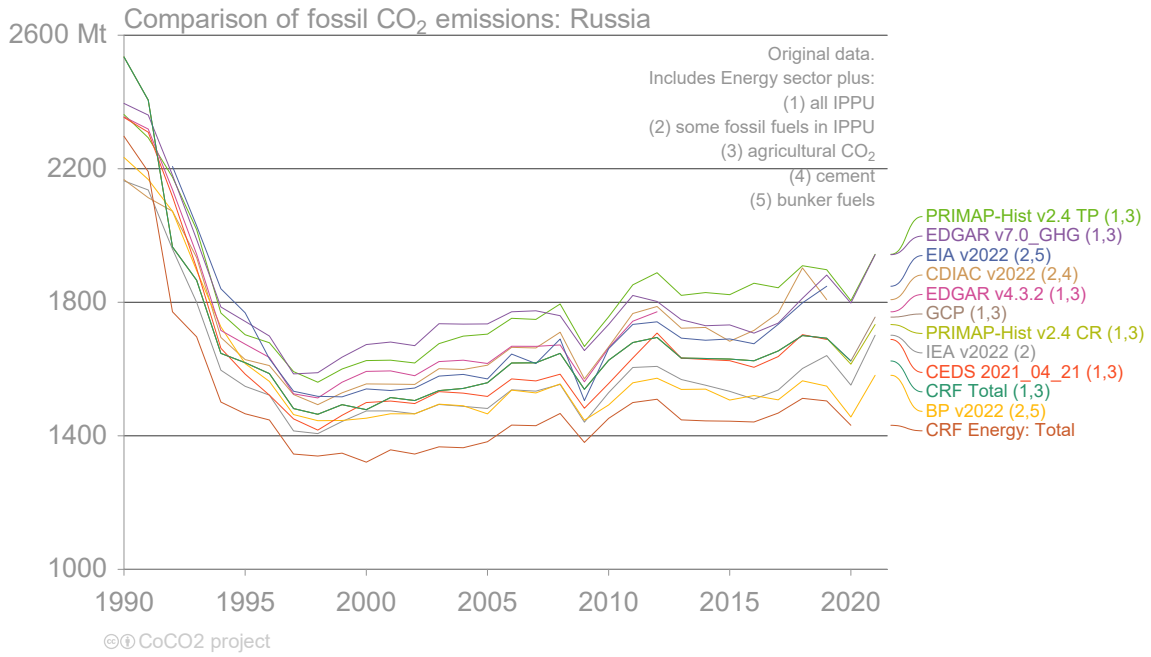
CoCO₂

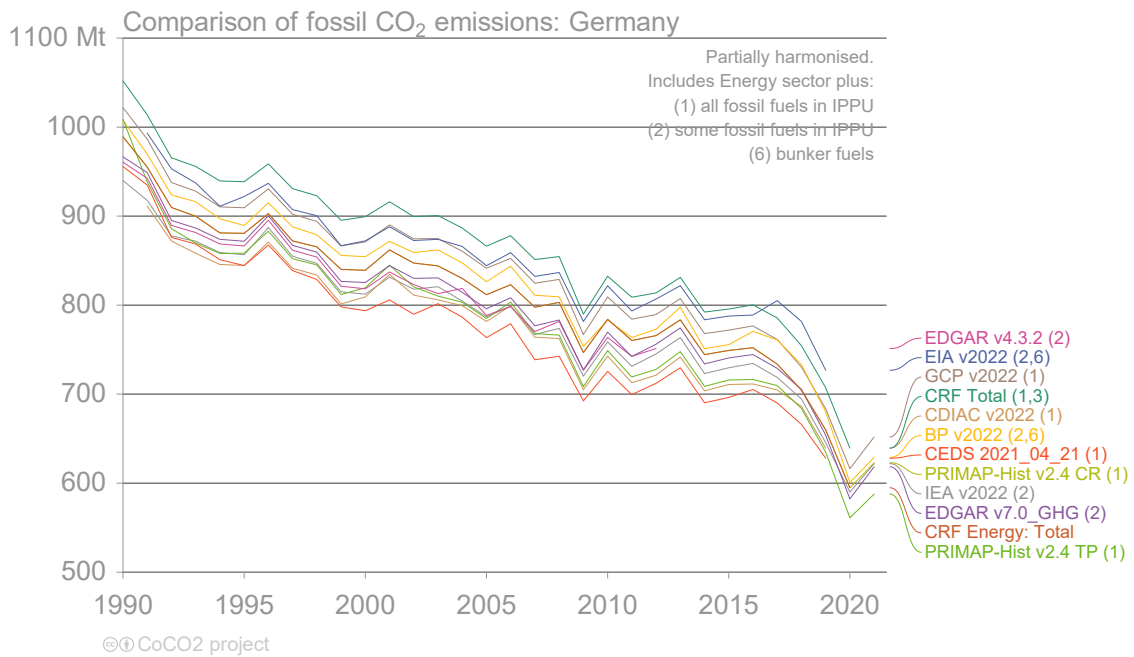
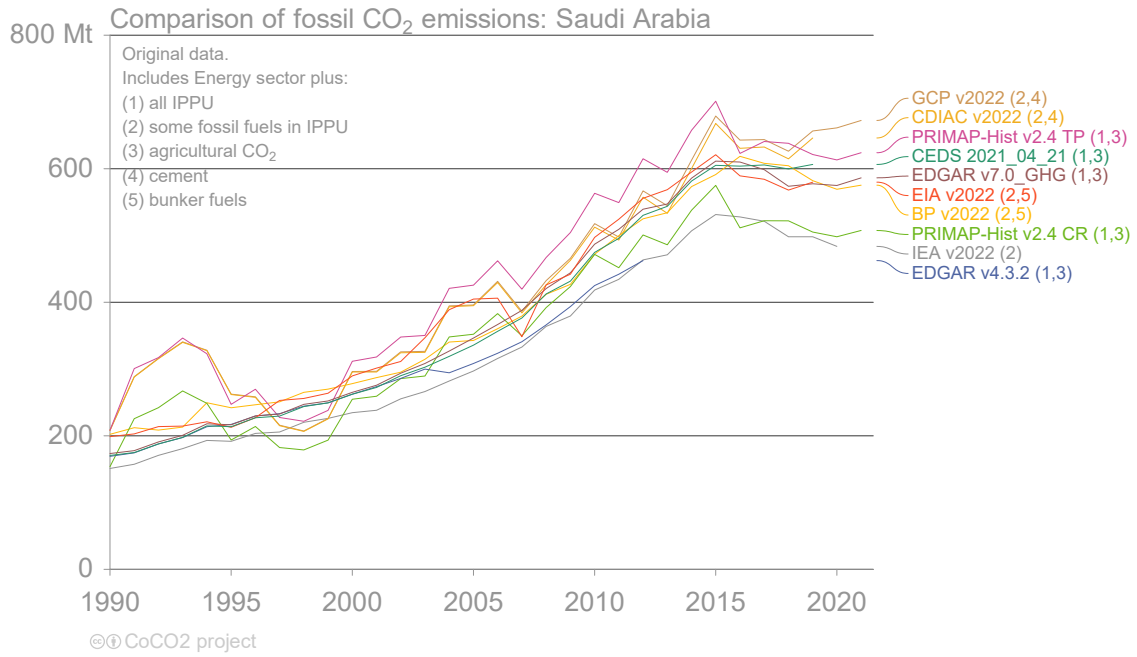












10 Annex 2: Additional fossil CO₂ inversion figure

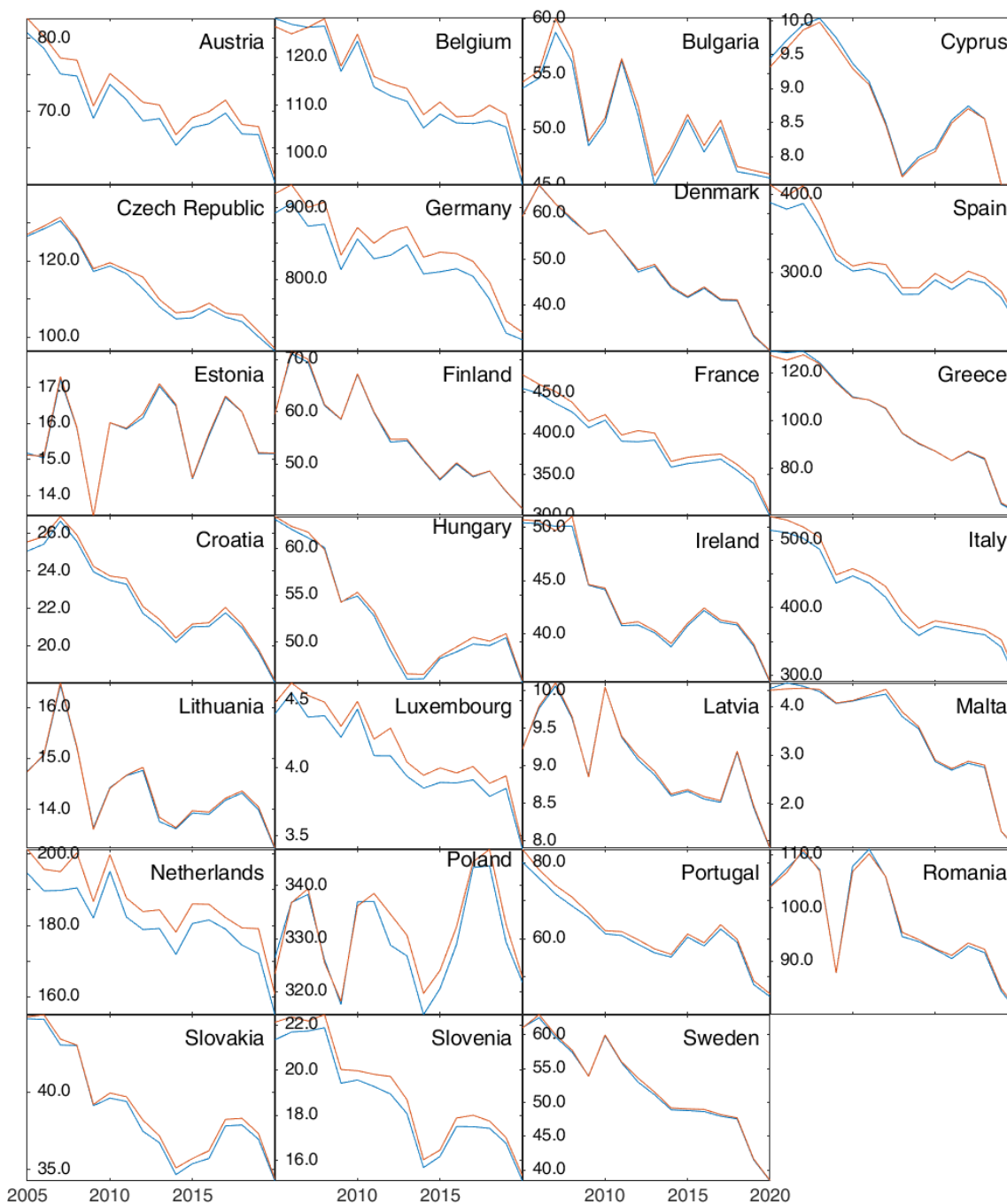


Figure 28: Comparison of inversion results (red lines) for each EU country with FFCO₂ prior emissions estimated by the TNO-GHGco-v3 inventory (blue lines), Mt CO₂ (Fortems-Cheiney and Broquet, 2021b). Note that the proximity of the inversion results to the prior estimates is not a direct indicator of verification, without additional information on the prior and posterior uncertainty and supporting statistical analysis (see discussion in the text).

11 Annex 3: Net land CO₂ fluxes figures

Additional net land CO₂ flux figures available on request (too many to include in this Annex)

12 Annex 4: Methane figures

This Annex presents additional figures comparing CH₄ estimates from inventories and inversions sources for the top emitters globally.

Table 5: Contribution from BU and TD of top 10 emitters (Tg CH₄) to the global anthropogenic budget (average of 2010-last available year).

Total anthropogenic, inventories (Tg CH ₄ yr-1)					Inversions estimates (Tg CH ₄ yr-1)							
					Deng et al., 2022 method 1		Deng et al., 2022 method 2		Deng et al., 2022 method 3.1		Deng et al., 2022 method 3.2	
UNFCCC	EDGARv6	EDGARv7	FAOSTAT	GAINS	SURF	GOSAT	SURF	GOSAT	SURF	GOSAT	SURF	GOSAT
55	64	66	57	53	44	53	46	51	51	54	47	50
27	25	24	25	30	29	26	25	19	32	29	28	25
20	28	31	28	30	32	28	30	28	38	30	34	26
16	21	19	19	18	20	20	16	16	16	16	14	15
16	21	21	20	16	22	23	22	23	30	38	21	29
12	15	16	15	30	19	18	17	16	23	19	23	19
8	12	13	12	10	12	11	12	9	7	11	8	11
6	6	7	6	5	5	5	5	4	4	3	5	4
4	5	6	5	5	5	5	4	4	2	3	4	4
4	5	5	5	5	4	5	4	4	3	4	6	6
avg 2010-2020	avg 2010-2018	avg 2010-2021	avg 2010-2020	avg 2010-2015								

Table 6: Uncertainties estimated for CH₄ sources at the global scale: based on ensembles of inventories and inversion estimates, national reports, and specific uncertainty assessments of EDGAR. Note that this table provides uncertainty estimates from some of the key literature based on different methodological approaches. It is not intended to be an exhaustive treatment of the literature.

	Estimated uncertainty in USA inventories ^a	Janssens-Maenhout et al. (2019) EDGARv4.3.2 uncertainty at 2 σ	Solazzo et al. (2021) EDGARv5 uncertainty at 2 σ	Global inventories uncertainty range ^b	Saunio et al. (2020) BU uncertainty range ^c	Saunio et al. (2020) TD uncertainty range ^c
Total global anthropogenic sources (incl. Biomass burning)					±6 %	±6 %
Total global anthropogenic sources (excl. Biomass burning)		±47 %	-33 % to +46 %	±8 %	±5 %	
Agriculture and Waste					±8 %	±8 %
Rice		±60 %	31 %–38 %	±22 %	±20 %	
Enteric fermentation	±10 to 20 %			±5 %	±8 %	
Manure management	±20 % and up to ±65 %					
Landfills and Waste	±10 % but likely much larger	±91 %	78 %–79 %	±17 %	±7 %	
Fossil fuel production & use					±20 %	±25 %
Coal	-15 % to +20 %	±75 %	65 %	±40 %	±28 %	
Oil and gas	-20 % to +150 %		93 %	±19 %	±15 %	
Other		±100 %	±100 %	±64 %	±130 %*	
Biomass and biofuel burning					±25 %	±25 %
Biomass burning					±35 %	
Biofuel burning		Included in "Other"	147 %	±24 %	±17 %	

^a Based on (NASEM, 2018)

^b Uncertainty calculated as ((min-max)/2)/mean*100 from the estimates of year 2017 of the six inventories plotted in Figure 1. This does not consider uncertainty on each individual estimate.

^c Uncertainty calculated as ((min-max)/2)/mean*100 from individual estimates for the 2008-2017 decade. This does not consider uncertainty on each individual estimate, which is probably larger than the range presented here.

* Mainly due to difficulties in attributing emissions to small specific emission sector.

Table 7: A description of the priors used in different inversions

Project	Model/ensemble	Prior CO ₂ anthropogenic							
VERIFY	EUROCOM	Fossil: EDGAR v4.3 (Janssens-Maenhout et al., 2019), BP statistics, and TNO datasets							
VERIFY	CIF-CHIMERE	Fossil: EDGAR v4.3 (Janssens-Maenhout et al., 2019), BP statistics, and TNO datasets							
VERIFY	CarboScopeRegional	Fossil: EDGAR v4.3 (Janssens-Maenhout et al., 2019), BP statistics, and TNO datasets							
VERIFY	LUMIA	Fossil: EDGAR v4.3 (Janssens-Maenhout et al., 2019), BP statistics, and TNO datasets							
GCP 2021 Friedlingstein et al., 2021	All	GridFEDv2021 and v2022, are also based on EDGARv4.3.2 (Janssens-Maenhout et al., 2019).							
Project	Model	Prior CH ₄ anthropogenic	Prior CH ₄ natural						
			Wetlands/mineral soils	Geological	Fire	Termites	Soil sink	Ocean/Lakes	Wild animals
VERIFY	CTE-CH4_FMI	Fossil, agriculture and waste: EDGAR v6.0	JSBACH-HIMMELI	GCP_CH4 Etiope et al., 2019	RCO plus GFED4s.1	Castaldi as GCP_CH4	LPX-Bern DYPTOP (Stocker et al., 2014)	Weber (in prep) for oceans and ULB for lakes in Europe, 0 for the rest of the world	
VERIFY	FLEXKF-CAMSv19r)_EMPA		JSBACH-HIMMELI			GCP	Ridgwell /GCP	GCP/ULB	
VERIFY	FLEXINVERT		LPX-Bern DYPTOP (Stocker et al., 2014)		GFED4s	Ito and Inatomi, 2012	LPX-Bern DYPTOP (Stocker et al., 2014)	(Tsuruta et al., 2017)	

VERIFY	TM5_4DVAR JRC		GCP_CH4_2019	GCP_CH4_2019 (global total: 15 Tg CH ₄ yr ⁻¹)		GCP_CH4_2019	GCP_CH4_2019	GCP_CH4_2019	
CAMsv19r Segers et al., 2020		EDGAR v4.3.2	LPJ-wsl		ACCMIP- MACCity and GFAS	Sanderson /GCP	Ridgwell /GCP	Lambert /GCP	Osolson climatology
VERIFY-CIF	FLEXPART- CIF NILU	EDGARv6	JSBACH- HIMMELI	Etiopie,2019	EDGAR-v6 (biofuel) and GFED-v41s (biomass)	Castaldi as GCP_CH4		(Weber et al., 2019) ULB inland waters	
GCP Saunois et al., 2020	GELCA- SURF_NIES		VISIT (Ito and Inatomi, 2012)	n/a	GFEDv3.1 then GFAS v1.2 after 2011	Sanderson (TransCom-CH ₄ / GCP)	VISIT (Ito and Inatomi, 2012)	n/a	
GCP Saunois et al., 2020	MIROCv4- SURF_JAMAST EC		VISIT (Ito and Inatomi, 2012) (global total range : 173-197 Tg CH ₄ yr ⁻¹)	Etiopie and Milkov, 2004 (global total: 7.5 Tg CH ₄ yr ⁻¹)	GFEDv4s (global total range : 14-35 Tg CH ₄ yr ⁻¹)	Sanderson (TransCom-CH ₄) (global total: 20.5 Tg CH ₄ yr ⁻¹)	VISIT (Ito and Inatomi, 2012)	Lambert/Houweling (TransCom-CH ₄) (global total: 18.5 Tg CH ₄ yr ⁻¹)	
GCP Saunois et al., 2020	NICAM- SURF_NIES		VISIT (Ito and Inatomi, 2012)	GCP based on Etiopie 2015	GFEDv4s / GCP	Sanderson (TransCom-CH ₄ / GCP)	VISIT (Ito and Inatomi, 2012)	Lambert/Houweling (TransCom-CH ₄ / GCP)	
GCP Saunois et al., 2020	TOMCAT- SURF_ECMWF		JULES emissions from Mc Norton 2016a	Tomcat 2006	GFED V4	Matthews and Fung 2006	Patra et al. 2011	Tomcat 2006 Matthews and Fung 1987 - all emissions total rescaled to Schwietzke et al. 2016	

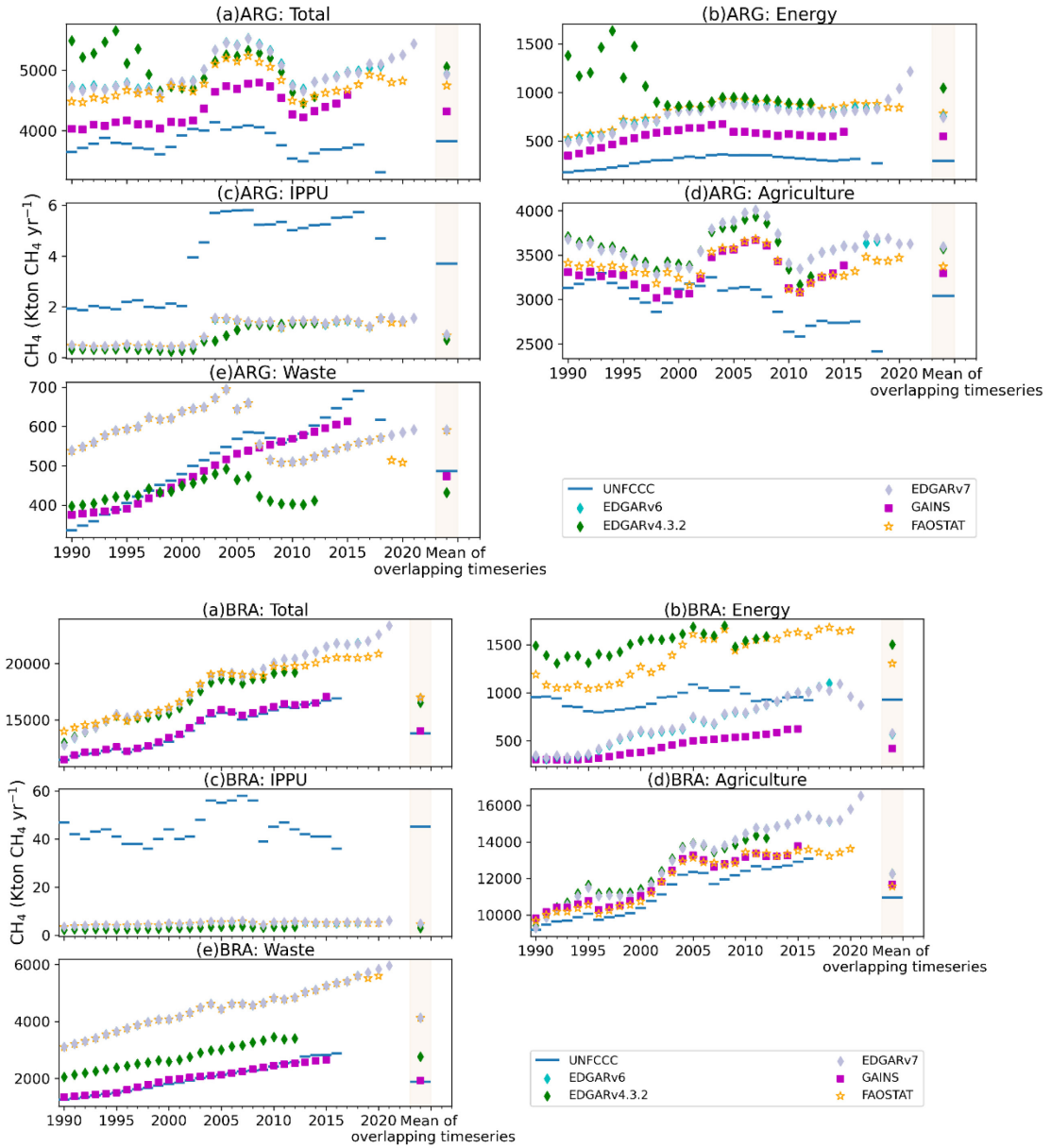
GCP Saunois et al., 2020	NTFVAR- GOSAT_NIES		VISIT (Ito and Inatomi, 2012)	Etiopie and Milkov, 2004	GFAS v1.2	Ito and Inatomi 2012	VISIT (Ito and Inatomi, 2012)	TransCom-CH4	
GCP Saunois et al., 2020	NTFVAR- SURF_NIES		VISIT (Ito and Inatomi, 2012)	Etiopie and Milkov, 2004	GFAS v1.2	Ito and Inatomi 2012	VISIT (Ito and Inatomi, 2012)	TransCom-CH4	
GCP Saunois et al., 2020	LMDZ- GOSAT1_LSCE		Bloom 2017	n/a	GFED V41s	Sanderson /GCP	Ridgwell /GCP	Lambert /GCP	
GCP Saunois et al., 2020	LMDZ- GOSAT2_LSCE		GCP - ensemble mean ESSD Saunois et al . 2016	GCP based on Etiopie 2015	GFED V41s	Sanderson /GCP	Ridgwell /GCP	Lambert /GCP	
GCP Saunois et al., 2020	LMDZ- GOSAT3_ CALTEC H LMDZ- GOSAT4_ CALTEC H LMDZ- GOSAT5_ CALTEC H LMDZ- GOSAT6_ CALTEC H		Kaplan 2002 rescaled by Bergamaschi 2007	n/a	GFED V41	Sanderson 1996 /GCP	Ridgwell /GCP	Lambert and Schmidt 1993	

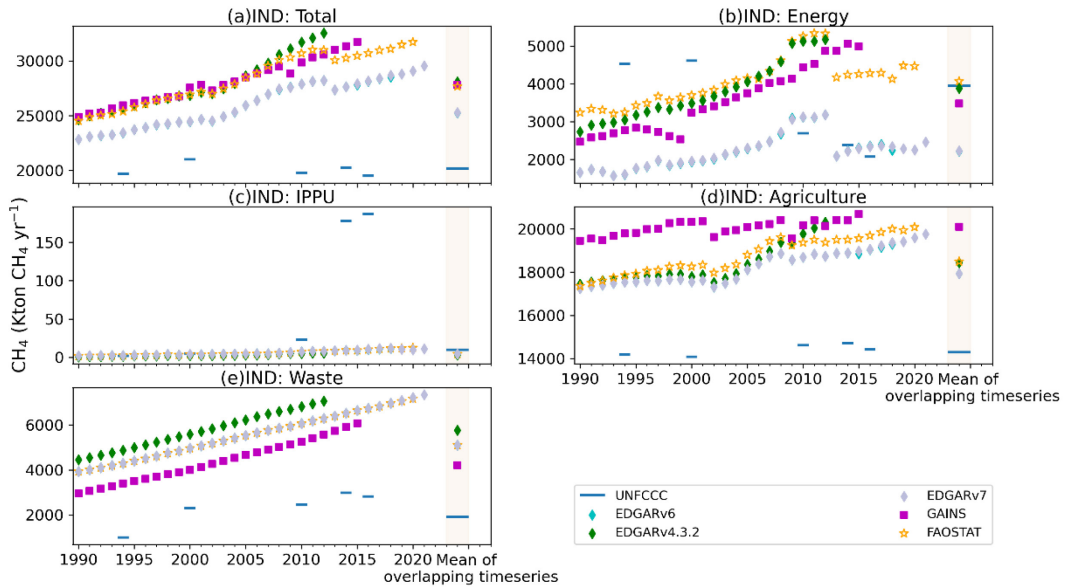
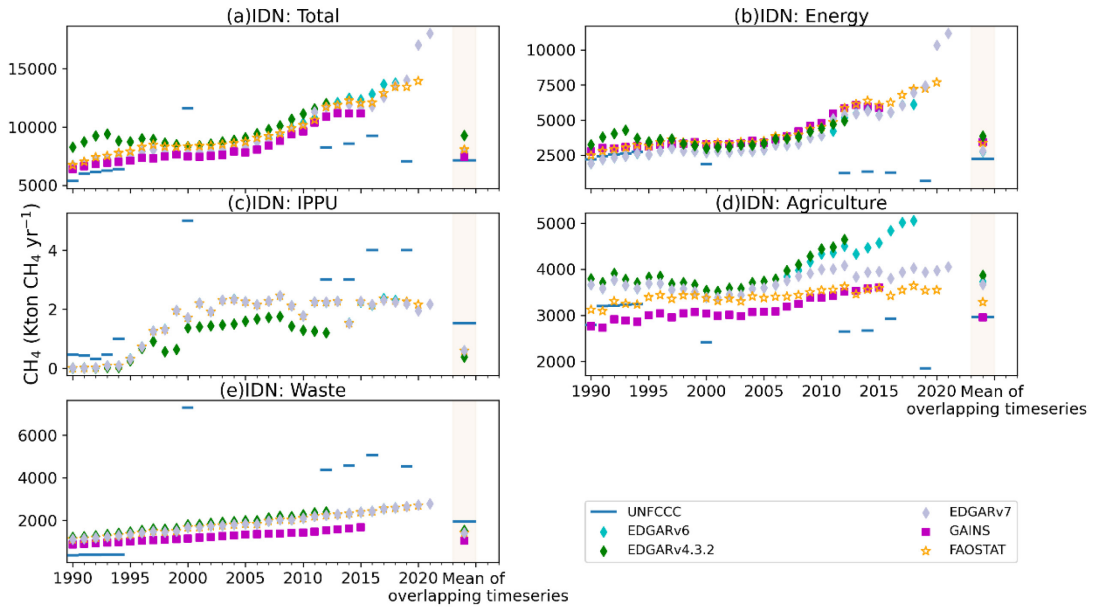
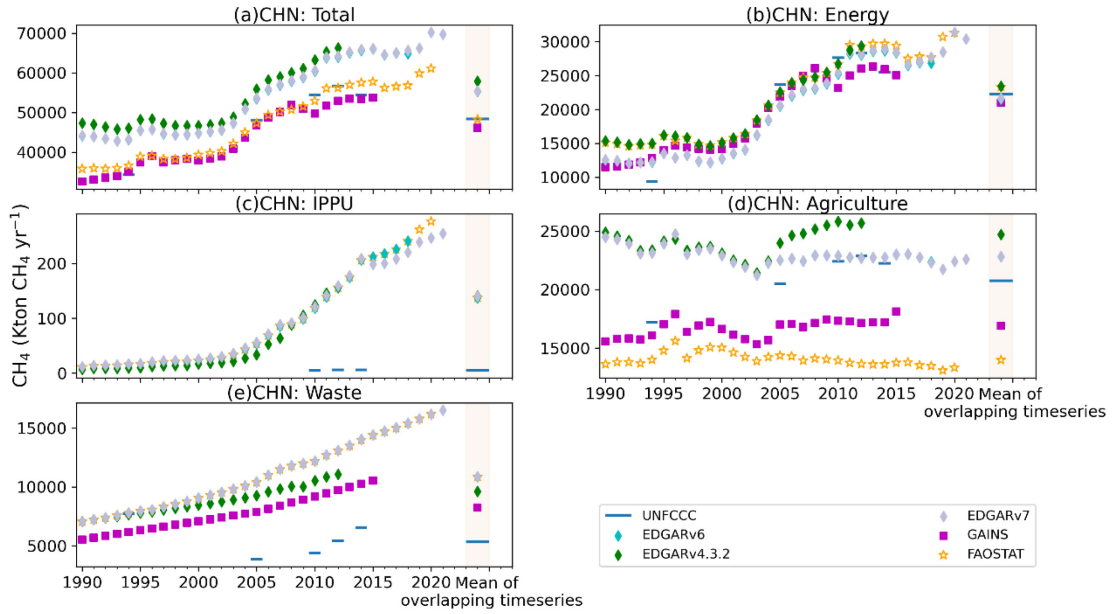
	LMDZ-SURF1_C ALTECH								
	LMDZ-SURF2_C ALTECH								
GCP Saunois et al., 2020	TM5-CAMS-GOSAT_TNO		Kaplan climatology	n/a	GFED V31 climatology after 2011	Sanderson /GCP	Ridgwell /GCP	Lambert /GCP	Osolson climatology
GCP Saunois et al., 2020	TM5-GOSAT1_EC		WETCHIMP ensemble mean;	GCP_CH ₄ 2019 (global total: 15 Tg CH ₄ yr ⁻¹)		Sanderson /GCP	Ridgwell /GCP	Lambert /GCP	Osolson climatology
GCP Saunois et al., 2020	TM5-GOSAT2_EC		GCP_CH ₄ _2019	GCP_CH ₄ 2019 (global total: 15 Tg CH ₄ yr ⁻¹)	GCP_CH ₄ _2019	GCP_CH ₄ _2019	GCP_CH ₄ _2019	GCP_CH ₄ _2019	
GCP Saunois et al., 2020	TM5-SURF1_EC		WETCHIMP ensemble mean;	GCP_CH ₄ 2019 (global total: 15 Tg CH ₄ yr ⁻¹)		Sanderson /GCP	Ridgwell /GCP	Lambert /GCP	Osolson climatology
GCP Saunois et al., 2020	TM5-SURF2_EC		GCP_CH ₄ _2019	GCP_CH ₄ 2019 (global total: 15 Tg CH ₄ yr ⁻¹)	GCP_CH ₄ _2019	GCP_CH ₄ _2019	GCP_CH ₄ _2019	GCP_CH ₄ _2019	
GCP Saunois et al., 2020	CTE-GOSAT_FMI		GCP_CH ₄ _2019	Etiopie 2015	GCP_CH ₄ _2019 (=GFED4s)	GCP_CH ₄ _2019	GCP_CH ₄ _2019	GCP_CH ₄ _2019	
GCP	CTE-SURF_FMI		GCP_CH ₄ _2019	Etiopie 2015	GCP_CH ₄ _2019 (=GFED4s)	GCP_CH ₄ _2019	GCP_CH ₄ _2019	GCP_CH ₄ _2019	

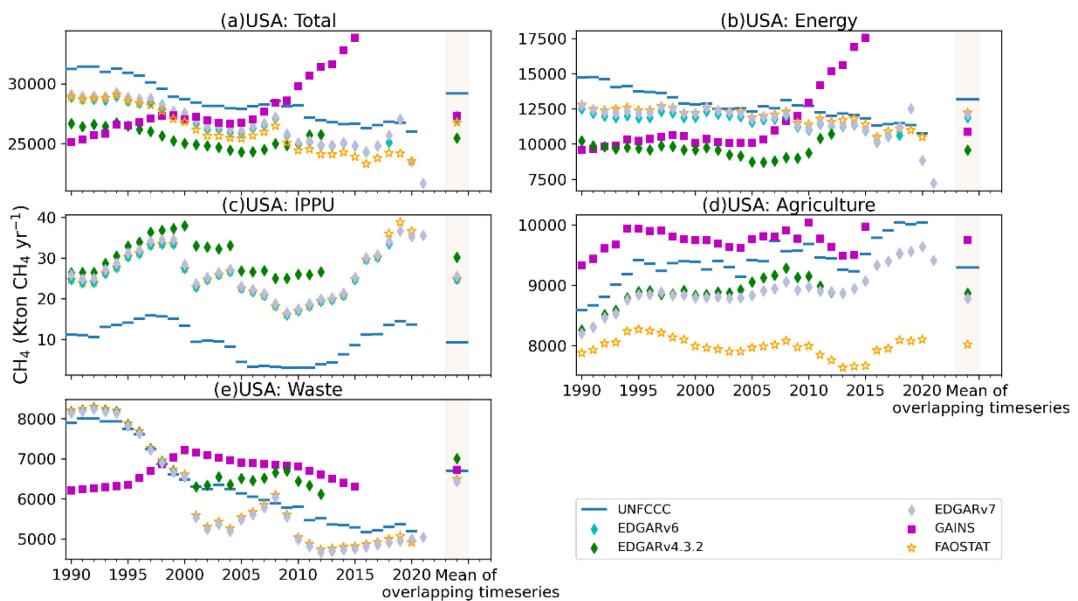
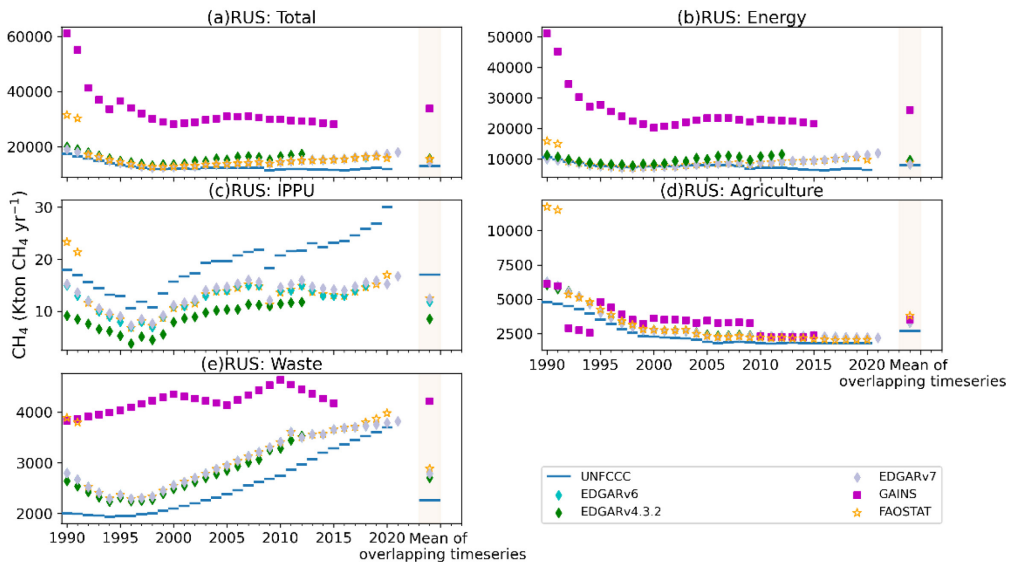
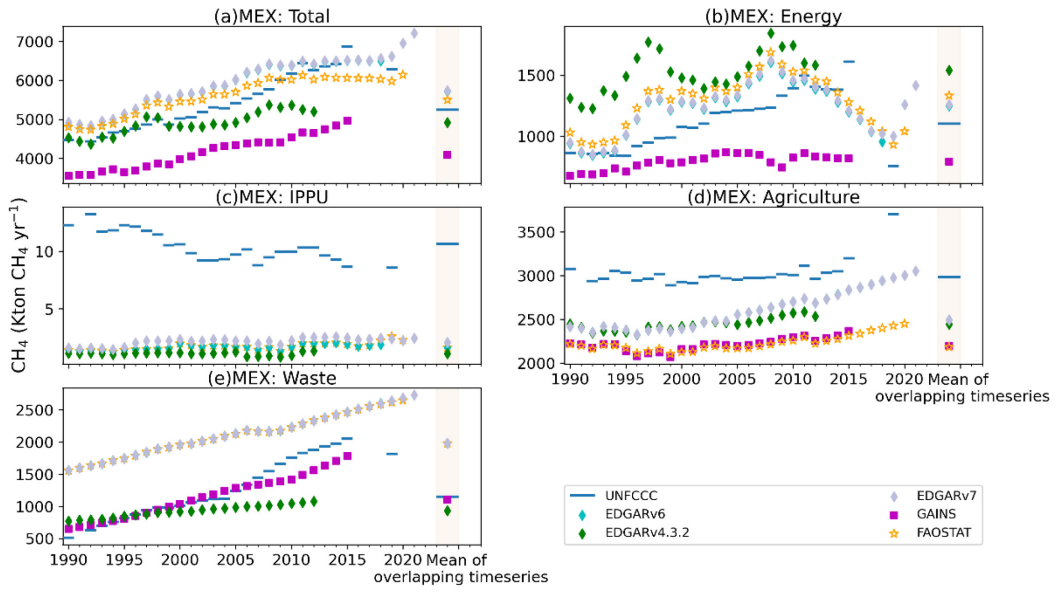
CoCO₂

Saunois et al., 2020									
-------------------------	--	--	--	--	--	--	--	--	--

Figures with total and sectoral CH₄ anthropogenic emissions from inventory estimates (Tg CH₄ yr⁻¹), for the top emitter countries:







Figures with total anthropogenic CH₄ emissions from inventories vs inversions estimates (Tg CH₄ yr⁻¹), for the top emitter countries.

